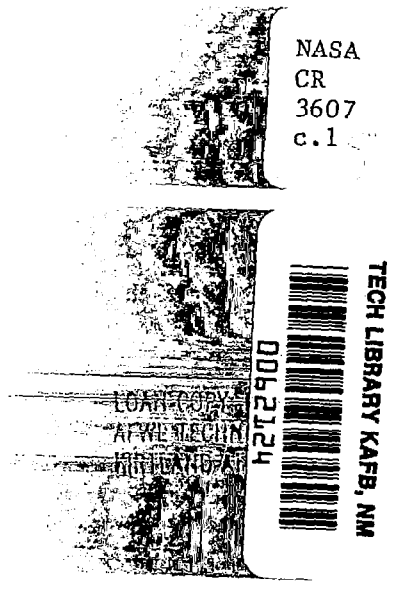

NASA Contractor Report 3607

Effects of Fiber/Matrix Interactions on the Properties of Graphite/Epoxy Composites

Paul E. McMahon and Lincoln Ying

CONTRACT NAS1-15749
SEPTEMBER 1982

NASA

NASA Contractor Report 3607

Effects of Fiber/Matrix Interactions on the Properties of Graphite/Epoxy Composites

Paul E. McMahon and Lincoln Ying
Celanese Corporation
Summit, New Jersey

Prepared for
Langley Research Center
under Contract NAS1-15749

National Aeronautics
and Space Administration

Scientific and Technical
Information Branch

1982

TABLE OF CONTENTS

TABLE OF CONTENTS
(continued)

APPENDIXES

LIST OF FIGURES

LIST OF FIGURES

LIST OF FIGURES

LIST OF TABLES

SUMMARY

An extensive literature review on the effect of interface/interphase on composite properties was followed by experiments which illustrate the significance of interphase in composite performance.

The review covered adhesion theory, wetting characteristics of carbon fiber, load transfer mechanisms in a fibrous composite, test methods to measure and evaluate fiber-matrix interfacial bond strengths, effect of moisture at the interface and properties of the interface/interphase, including impact toughness, on composite performance. A critical discussion of the literature is presented along with appropriate citations and references.

In contrast to adhesion in glass fiber/epoxy composites, carbon fiber/epoxy adhesion is not simply promoted by "coupling agents" but rather it results from physical and/or chemical interactions with the matrix. Much work has been done to characterize the surface energetics of carbon fiber but no correlation has been identified between wetting behavior and interfacial bond strength. Many techniques have been developed to study fiber/matrix interfacial bond strength but few are applicable to carbon fiber. Preliminary data have shown that single filament critical length determination is applicable to evaluate carbon fiber - epoxy bond strength. This technique was adapted in this study to evaluate finish variants on carbon fiber in epoxy composites.

Moisture at the interface of carbon fiber/epoxy composites has been shown to have little effect on composite properties. The decrease in composite properties in humid environments is primarily due to plasticization of the matrix by water.

Improvement of impact toughness of carbon fiber/epoxy composites can be achieved by modification at the fiber/matrix interface. However, this is usually associated with a significant decrease in mechanical properties. This is because weak interfacial bonds allow more impact energy to be absorbed, thereby increasing the impact toughness. A few workers have suggested that "tailoring" interphase properties can improve toughness without lowering the mechanical properties, but, this concept has not yet been demonstrated experimentally.

In this study, experimental results were obtained which show the effect of interphase on composite performance and illustrate its significance. Various finish variants were formulated, based on different chemical and mechanical properties, and applied to Celion® 6000 carbon fiber. Wetting behavior, studied by the Wilhelmy wetting force technique, and interfacial bond strength, evaluated by single filament critical length determination were characterized for these fibers. Composite properties at room and elevated temperatures and impact toughness were also measured.

It is concluded that good wetting is essential to provide good adhesion but better wetting properties do not necessarily translate to better bond strength. Also, it is shown that with a weak interfacial bond strength, impact toughness is improved. But, most significantly, a 30% increase in impact toughness was measured without loss of room temperature and elevated temperature composite mechanical properties by "tailoring" the interphase properties.

INTRODUCTION

In the last decade, much attention has been focused on fiber-reinforced polymeric matrix composites. These composite materials are both versatile and complex. Their versatility stems from a wide choice of constituent materials available and from the variety of ways in which composites can be fabricated to provide a combination of desired properties. These tailor-made properties are frequently not available and cannot be achieved in conventional isotropic materials. On the other hand, they are complex by virtue of their chemical and mechanical nature and thus should not be regarded as a single material, but as a material system. Inherent in this multi-phase material system is the fiber/matrix interface which is the critical link that provides the structural integrity for the fibrous composites.

Conventionally, the interface is regarded as the bond between fiber and matrix. This interfacial bond is considered to have zero thickness and to result from the interaction between the fiber surface and the matrix material. The interphase region of a fibrous composite is the area immediately adjacent to and including the interface and extends a finite distance into the bulk matrix material. This concept is illustrated in Figure 1.

An extensive review of the literature indicates that much work has been done on fiber/matrix interface characterization. These include the evaluation of fiber surface energetics via wetting force measurement; surface elemental analysis via ESCA, AUGER, XPS, etc. and surface topography/morphology studies via SEM. However, little effort has been spent to correlate this information with composite performance. In short, the role of the interface in determining composite properties is not known. Furthermore, little attention has been given to the understanding of the nature of the interphase and how it affects composite properties. In particular, the load transfer mechanism in the interphase region is not clear. This report is intended to clarify these areas of uncertainty and to illustrate the influence of the interphase region on composite performance.

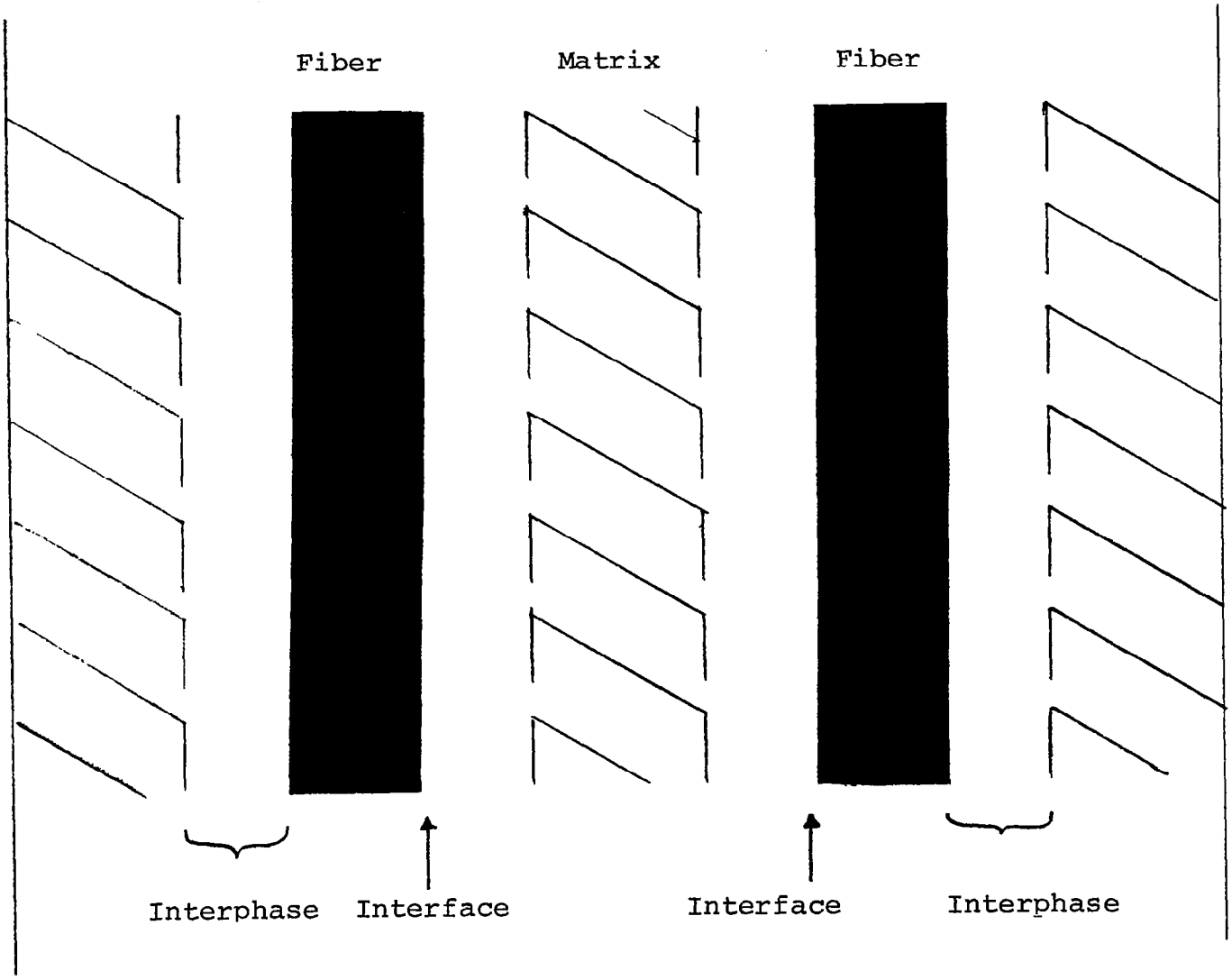

FIGURE 1. FIBER-MATRIX INTERFACE/INTERPHASE IN FIBROUS COMPOSITE MATERIAL

BACKGROUND AND LITERATURE REVIEW

ROLE OF THE INTERFACE IN COMPOSITE MATERIALS

Among many factors that govern the characteristics of a fibrous composite, it is clear that the adhesion at the fiber/matrix interface plays an important role in structural integrity of these two-phase materials. Since there are a limited number of ways to directly study adhesion at the interface, composite failure mode and shear strength are commonly employed to assess interfacial bond strengths.

Two extreme cases generally occur in interfacial failure mode studies. For weak interfacial bonding, fiber "pull out" is responsible for the rupture. This is because the fibers are not bonded by the matrix and they slide in their cavities. Therefore, load cannot be transferred in such a discontinuous medium. In this case, the composite fails in a shear mode and the shear strength is usually low. On the other hand, if the interfacial bonding is strong, then the matrix will transfer the load to the fibers until it reaches the breaking strength of the fibers. In this case, the failure is sudden and catastrophic. A higher shear strength is associated with this kind of tensile failure.

Virgin carbon fibers exhibit lower bondability with polymer matrixes (e.g., epoxy, polyester) and surface treatments are employed to increase the interfacial bond strength. All commercially available carbon fibers are surface treated. These surface treatments are generally oxidative in nature and provide functional groups on the fiber surface which increase wettability and/or bondability. Much of the early work has emphasized increases of composite shear strength.

Goan et al[1] studied a sodium chlorate/sulfuric acid oxidation process which doubled composite short beam shear strength. However, this process degraded the fiber tensile strengths. A 4% loss in fiber strength (impregnated strand tensile test) was observed. Druin et al[2] studied gas phase oxidation processes where similar results were obtained.

Carbon fiber strength is surface flaw sensitive. Extensive oxidation/etching can increase surface flaws which leads to a reduction in properties. Ehrburger et al,[3] Molleyre and Bastick,[4] Fitzer et al[5] and Duffy[6] studied various types of oxidation processes to optimize the incorporation of functional groups onto the fiber surface and reduce the possibility of extensive oxidation/etching.

Ehrburger et al[7,8] found that, by the insertion of weak acidic groups, interlaminar shear strength (ILSS) could be enhanced just as much as with the incorporation of strong acidic groups on AC (type II), ex-acrylic carbon fiber surfaces. However, the mode of failure was different. A shearing mode of fracture was

observed with weak acidic groups while tensile failure was observed with strong acidic groups. A possible explanation suggested by the author for this observation was that the weak acidic groups increased the surface energetics of the fibers and resulted in better wetting and good adsorption which enhanced the coupling. The strong acidic groups - mainly carboxylic or phenolic groups - are coupled with the matrix via tighter and stronger primary bonds at the interface which create a brittle composite.

Although little is known about the adhesion mechanisms involved in a fibrous composite material, it is clear that the role of the interface in a composite material is significant.

References to the Role of the Interface in Composite Materials

(1) J. C. Goan, L. A. Joo and G. E. Sharpe, "Surface Treatment for Graphite Fibers," Proc. 27th Ann. Tech. Conf. of SPI, 21-E (1972).

(2) M. L. Druin, G. R. Ferment and V. N. P. Rao, "Enhancement of the Surface Characterization of Carbon Fibers," US Patent 3,754,957, Aug. 28 (1973).

(3) P. Ehrburger, J. J. Herque and J. B. Donnet, "Electrochemical Treatment of Carbon and Graphite Fibers," 4th London Inter. Carbon and Graphite Conf., Soc. of Chem. Ind. (1976), 201.

(4) F. Molleyre and M. Bostick, "Modification of the Texture of Carbon Fibers Through Gaseous Oxidization Agents," 4th London Inter. Carbon and Graphite Conf., Soc. of Chem. Ind. (1976), 190.

(5) E. Fitzer, K. H. Geigl and L. M. Manocha, "Surface Chemistry of Carbon Fibers and Its Influence on Mechanical Properties of Phenolic Based Composites," 5th London Inter. Carbon and Graphite Conf., Soc. of Chem. Ind. (1978), 405.

(6) J. V. Duffy, "Carbonized Polymer Coatings as Surface Treatments for Carbon Fibers," Naval Ordnance Lab A320-5203/292-2WF00-544-201, NTIS AD-766782.

(7) P. Ehrburger, J. J. Herque and J. B. Donnet, "Interface Properties of Carbon Fiber Composites," 5th London Inter. Carbon and Graphite Conference, 1, Soc. of Chem. Ind. (1978), 398.

(8) P. Ehrburger and J. B. Donnet, "Interface in Composite Materials," Phil. Trans. R. Soc. London, A294 (1980), 495-505.

EFFECT OF INTERPHASE PROPERTIES ON COMPOSITE PERFORMANCE

Commercially available carbon fibers are usually sized with an epoxy compatible finish to enhance handling characteristics. Epoxy-based systems are generally used since epoxy resins are commonly used as components of the matrix materials and such materials can be easily applied to the fibers. These sizes also act as lubricants as well as "loose" binders which prevent fiber damage and minimize fiber fuzz. The loose binder should not hinder the spreading of the fibers during the prepregging process, but should allow the resin to penetrate bundles and wet individual fibers to eliminate dry spots or voids.

Sizing can be accomplished by passing tows of fibers through a bath containing a dilute solution of the finish material. Following such a coating, the fibers must be dried to remove solvent. Better adhesion properties were observed by Drzal et al[1] and Goan et al[2] with commercial epoxy-sized fibers. This phenomenon can be explained on the basis that the fibers were sized with a low viscosity fluid, thus enhancing wetting. Furthermore, the spontaneous spreading of the sizing solution minimizes trapped air pockets at the interface between fiber and finish.

The overall effect of size materials on composite properties is not fully understood. This is partly because the size materials are applied onto the fiber in very thin layers, normally 1.5% by weight of the fiber, which is equivalent to an approximately 800 Å thick coating (Appendix A).

Few analytical techniques can be applied to study the interphase of a carbon fiber epoxy composite because of its small dimension. Furthermore, the fiber geometry, and the low atomic number elements on the surface further limit the applicable analytical techniques. These add to the difficulties in understanding the role of the interphase in composite properties. However, some of the effects of interphase can be observed in mechanical tests.

Arai et al[3] showed an increase in both interlaminar shear strength (ILSS) and flexural strength of a carbon fiber epoxy composite by electrolytic polymerization of vinyl monomers onto the carbon fibers. Pinchin and Woodhams[4] pyrolyzed graphite onto carbon fiber surfaces and increased the surface energetics. This was reflected in an increase in shear (ILSS) and flexural strengths. Furthermore, a slight improvement on impact toughness was also measured. An hypothesis, based upon this phenomenon, is that the pyrolytic graphite deposit forms a sheath around the fiber which creates an additional interface. During the debonding and/or crack propagating processes, this additional interface absorbs more energy by exposing additional free surfaces.

Broutman and Agarwal[6,7] did a theoretical study on composite properties with an interphase layer. Assuming both phases behave

elastically with perfect bonding at the interface, it was shown that composite strength reached a maximum when the interphase modulus reached a value of 69 MPa (10^4 psi). It should be noted that Broutman used the term interface modulus but, according to the definitions of interface and interphase described earlier, interphase modulus is more appropriate because interface is regarded as zero thickness. Further increases in the interphase modulus do not change the composite strength. This is shown in Figure 2. However, composite modulus continues to increase with increasing interphase modulus (Figure 3). This further increase in modulus without composite strength changing further, indicates that composite elongation can be maximized at this critical interphase modulus (Figure 4).

Although Broutman's theoretical study was not supported by experimental data, the critical interphase modulus determined in his study was significantly lower than the modulus of the matrix. This is similar to the flexible interlayer concept discussed by Benedetto and Nicolais[5]. This concept attributes the effectiveness of finishes to stress relief in the interphase region. Since there is a difference in thermal expansion coefficient of the fiber and the matrix, significant residual stress will accumulate at the interface due to elevated temperature curing as well as shrinkage of the matrix during polymerization. However, by incorporation of a flexible interlayer, residual stresses can be relieved. Although these two concepts are different in approach, they both conclude that the properties of the composite can be improved through selective tailoring of the interphase.

Marom and Arridge[12] studied the stress patterns of soft interlayers on stainless steel inclusions. Reduction of stress concentration at the interface was observed and an improvement in the ultimate tensile strength was measured. However, Marom stated that optimization of this soft interlayer is necessary to prevent poor transverse properties. This effect was reported by Gatward and Hull,[13] when they coated a flexibilized polyvinyl butyral polymer onto glass fiber and a decrease in transverse tensile properties was measured.

Taniguchi et al[9] incorporated a flexibilized epoxy at the interphase of a carbon fiber/epoxy composite and preliminary data showed improvement in flexural and shear strength. Kardoes et al[10,11] and Lavengood et al[14] coated boron fibers and glass fibers with a low cross-linking density epoxy system to a thick, flexible interlayer. Increase in mechanical properties, both moisture conditioned and unconditioned, were measured. A 1000% increase in torsional fatigue life was measured and Figure 5 shows the improvement of transverse properties of glass fiber/epoxy composites by incorporation of a soft interphase.

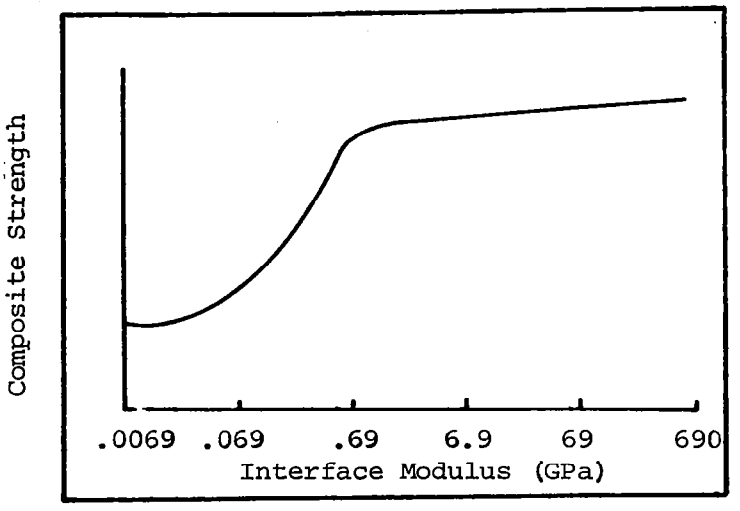

FIGURE 2. COMPOSITE STRENGTH AS A FUNCTION OF INTERFACE MODULUS*

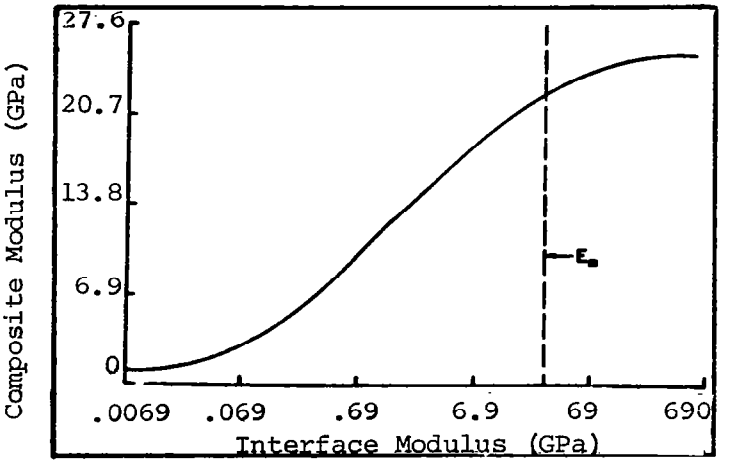

FIGURE 3. COMPOSITE MODULUS AS A FUNCTION OF INTERFACE MODULUS*

*From Broutman and Agarwal (Ref. 7)
Reproduced by permission.

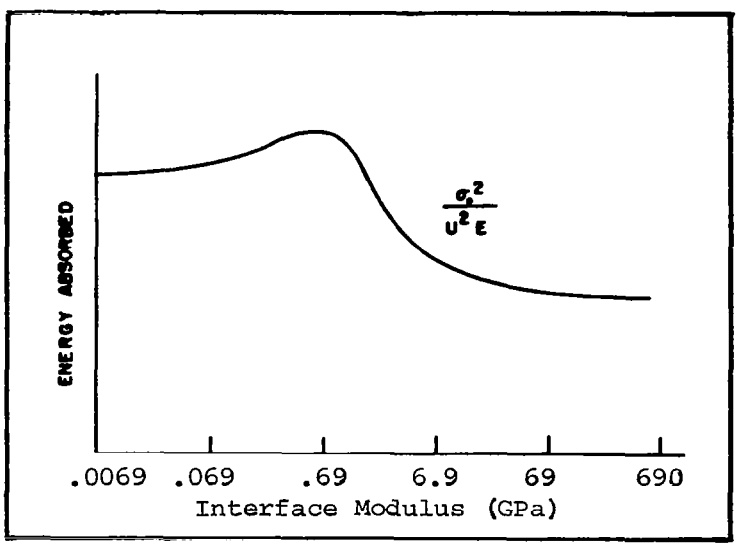

FIGURE 4. COMPOSITE STRAIN ENERGY ABSORBED AS A FUNCTION OF INTERFACE MODULUS*

*From Broutman and Agarwal (Ref. 7). Reproduced by permission.

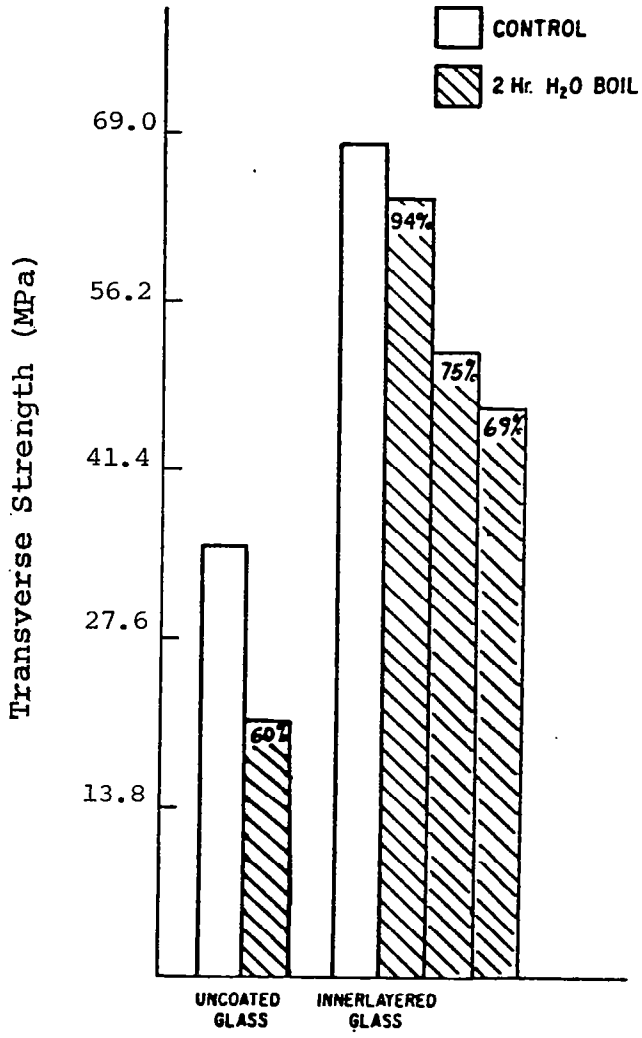

FIGURE 5. TRANSVERSE STRENGTH OF GLASS FIBER REINFORCED COMPOSITES BEFORE AND AFTER TWO HOURS IN BOILING WATER*

*From Lavengood and Micheno (Ref. 14). Reproduced by permission.

Riess et al[8] developed an interphase material with poly-[isoprene-b-(styrene-alt-maleic anhydride)] block copolymer:

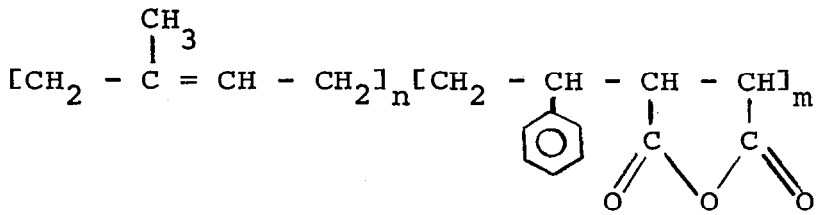

(Isoprene) (SAM)

According to the compatibility of the polymers, the polyisoprene will agglomerate to form micellar structures at the interphase while the SAM block is mixed with the matrix resin to form a continuous phase. This inclusion of a second, elastomeric phase, is to relieve residual stress and to damp the elastic energy as discussed earlier. A proposed interphase structure is shown in Figure 6.

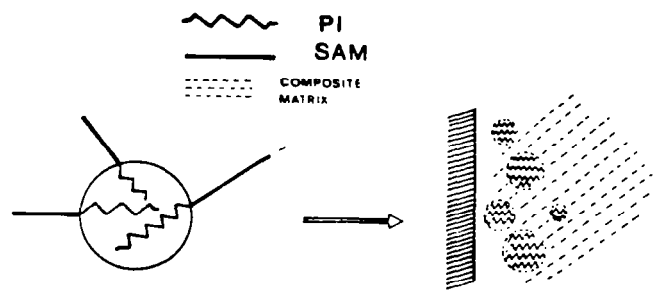

FIGURE 6. MICELLE STRUCTURE OF THE COPOLYMER MICELLAR ADSORPTION*

*From Riess et al (Ref. 8). Reproduced by permission

This PI-SAM interphase material can couple to the carbon fiber surface through the dipole-dipole interaction sketched in Figure 7.

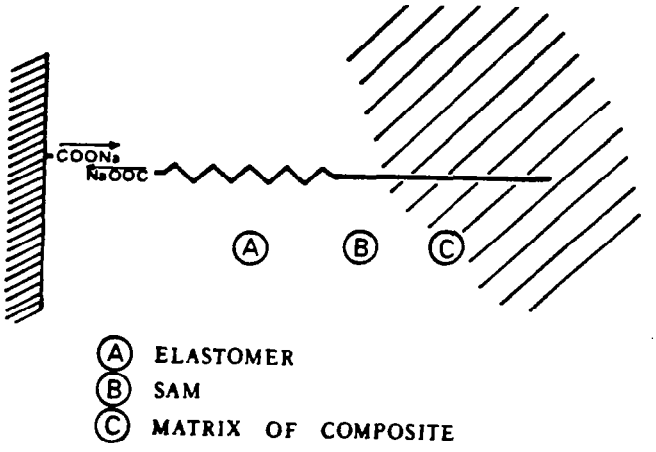

FIGURE 7. FIXATION OF BLOCK COPOLYMERS ON CARBON FIBRES BY DIPOLE-DIPOLE BONDING*

The introduction of this "soft" interphase not only increased the shear strength of the composite, both unconditioned and conditioned in water at 50°C, but also improved the impact toughness. Some of these results are shown in Figures 8 and 9.

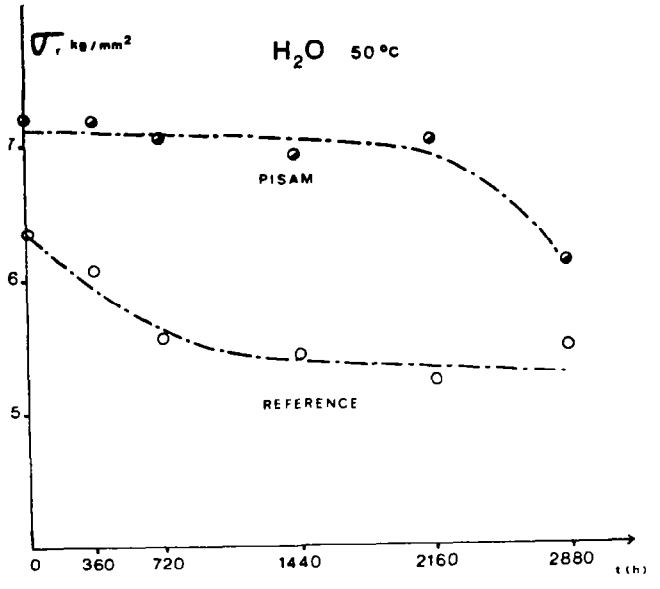

FIGURE 8. SHEAR STRENGTH OF COMPOSITES AFTER WATER TREATMENT AT 50°C*

① RESIN
② RESIN + FIBRES
③ RESIN + GRAFTED FIBRES

*From Riess et al. (Ref. 8).
Reproduced by permission.

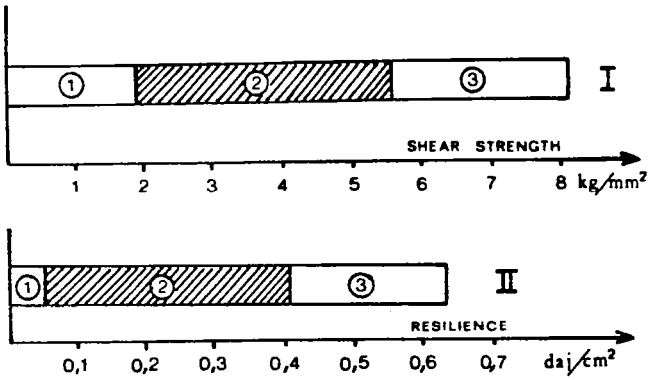

FIGURE 9. SHEAR STRENGTH AND RESILIENCE OF:
RESIN (EPOXY)
RESIN + UNTREATED FIBRES
RESIN + GRAFTED FIBRES*

*From Riess et al (Ref. 8).
Reproduced by permission.

In reviewing the theoretical concepts together with the limited experimental data, a soft interphase between fiber and matrix clearly improves some of the composite properties. The objective of this report is to provide further understanding of the role of interphase in composite properties and to define guidelines and principles for the selection of optimal interphase materials to improve overall performance.

References to the Effect of Interphase Properties on Composite Performance

(1) L. T. Drzal, M. J. Rich, D. L. Hall, "Structure-Property Relationships at the Composite Interphase," 15th Biennial Conf. on Carbon, Amer. Carbon Soc., June (1981).

(2) J. C. Goan, L. A. Joo and G. E. Sharpe, "Surface Treatment for Graphite Fibers," Proc. 27th Ann. Tech. Conf. of SPI, Sec. 21-E (1972).

(3) Kojiro Arai, Okayama; Noriaki Sugai, Fukuoka; "Treatment of Carbon Fibers," US Patent 4,130,465, Dec. 19 (1978).

(4) D. J. Pinchin, R. T. Woodhams, "Pyrolytic Surface Treatment of Graphite Fibers," J. of Mat'l. Sci., 9 (1974), 300-306.

(5) A. T. DiBenedetto and L. Nicolais, "Interfaces in Composites," Adv. in Comp. Mat'ls., G. Piatti, editor, Ch. 8, 153, Applied Sci. Publ., Ltd. (1978).

(6) L. J. Broutman and B. D. Agarwal, "A Theoretical Study of the Effect of an Interfacial Layer on the Properties of Composites," Polym. Eng. & Sci., 14, 8, 581 (Aug. 1974).

(7) L. J. Broutman and B. D. Agarwal, "A Theoretical Study of the Effect of the Interface on Composite Toughness," Proc. 28th Ann. Tech. Conf. SPI, 5-B (1973).

(8) G. Riess and M. Bourdeaux, M. Brie and G. Jouquet, "Surface Treatment of Carbon Fibers with Alternating and Block Copolymers," Proc. 2nd Carbon Fibers Conf., The Plastics Institute, 52 (1974).

(9) Itsuki Taniguchi, Ryuichi Hoh, Toshihiro Iwatsuki and Shiggehiro Ohuchi, "Resinous Composition for Surface-Treating Reinforcing Fibers and Surface Treating Process," US Patent 4,167,538, Sept. (1979).

(10) L. D. Tryson and J. L. Kardos, "The Use of Ductile Inner-layers in Glass Fiber Reinforced Epoxies," Proc. 36th Ann. Tech. Conf., Reinforced Plastics/Composites Institute, SPI, 2-E (1981).

(11) J. L. Kardos, "Composite Properties Enhancement via a Ductile Innerlayer, " Critical Link Interface Symposium at NY Polytech. Inst. (1980).

(12) G. Marom and R. G. C. Arridge, "Stress Concentrations and Transverse Modes of Failure in Composites With a Soft Fiber Matrix Interlayer," Mat'l. Sci. and Eng., 23 (1976) 23-32.

(13) C. Gatward and D. Hull, "Effect of Flexible Interface on Transverse Properties of Polyester-Glass Composite Materials," Proc. of the Reinforced Plastic Group Meeting on Interfaces in Composite Materials (Ref. C283), Plastics and Rubber Institute (1981).

(14) R. E. Lavengood and M. J. Michno, Jr., "The Effects of Thick Innerlayers on the Mechanical Performance of Fiber Reinforced Composites," SPE-EPS Division Tech. Conf., Additives--Their Effect on Process Parameters and Product Performance, Oct. 7-8, (1975).

ROLE OF INTERFACE/INTERPHASE IN COMPOSITE TOUGHNESS

Toughness in composite materials is not a well defined property. This is due in part to the difficulties in designing test methods to study the toughness of a multi-phased anisotropic material. In general, toughness is measured by the resistance of the material to crack growth and propagation. However, for multi-phase anisotropic materials, this is not totally representative.

An increasingly common method in toughness measurement is instrumented impact. This method utilizes a load cell mounted onto an impacter. The load cell is capable of recording load during impact in microseconds. A microprocessor then outputs a load deflection curve together with the energy absorption profile during the course of impact. The maximum force on the load deflection curve is taken as the required load for penetration.

Due to the multi-phase characteristic of a composite, its toughness can be improved in several ways. A toughened matrix and/or a higher strain fiber are both capable of increasing the toughness of a composite. Although little is known about the interface and interphase, it has the potential to significantly influence the toughness of composites.

The interface can affect the toughness of a composite by providing various energy absorbing mechanisms like debonding, fiber stress relaxation and fiber pullout during fracture. In the case of weak interfacial bonds, debonding takes place in advance of the crack tip. The degree of debonding, as well as the energy absorbed due to the debonding process, depends largely upon the interfacial bond strength. In the opposite case of strong interfacial bonds, fibers will break prior to debonding and energy is absorbed due to stress relaxation at the ends of the broken fibers. Furthermore, energy is also absorbed due to some fiber pullout which is related to the strength of interfacial bonds. When all of these energies are accounted for, it is expected that the weak interfacial bond will provide very high fracture toughness in composites. This phenomenon has been observed by many workers.[1-4]

However, by tailoring the interphase properties, a significant improvement in composite toughness can be obtained without a severe loss of mechanical properties due to weak interfacial bond strength. Broutman et al[5-7] have analytically demonstrated that interphase properties can be tailored to obtain both toughness and strength. In general, a softer material at the interphase is preferred.

Plueddemann[8] incorporated a rubber interphase in glass/epoxy composites. Improved toughness together with relatively good adhesion strength was obtained. Hancox and Wells[9] coated different amounts of silicone rubber at the surface of carbon

fibers. A 107% increase in work of fracture without measurable decrease in flexural strength was determined with 1% by weight silicone rubber at the interphase of a carbon fiber/epoxy composite. Williams[10] polymerized polyvinylalcohol and polysulfone onto carbon fiber and enhancement in shear strength, notched fracture toughness and low-velocity impact toughness were achieved. Subramanian and Jakubowski[11] coated carbon fibers with various kinds of polymers by electropolymerization and demonstrated that impact toughness and shear strength can simultaneously increase when optimum interphase properties were incorporated.

In addition to the mechanical properties of the interphase, the physical thickness of the interphase is another critical parameter that needs to be optimized in order to achieve the ultimate properties of composite materials. As discussed by Hancox and Wells,[9] when silicone rubber exceeded the 1% by weight level, a dramatic decrease in flexural strength was observed. Similar observations were also reported by Cavano and Winters[12] and Peiffer.[13]

Another approach was taken by Atkins[14] where intermittent bonding along the fiber surface was suggested. The weakly bonded sections allow debonding and fiber pullout during fracture while the strongly bonded areas enable load transfer. The combination of these could then simultaneously provide high fracture toughness and good tensile strength. Furthermore, Reiss et al[15] incorporated a two-phase block copolymer, polyisoprene-polystyrene-maleic anhydride, at the interphase. Where the polyisoprene is providing the energy absorbing characteristic and the stryene-maleic anhydride block (SAM) is enhancing the compatibility and joint strength of the fiber with the matrix, increases in shear strength and toughness were both measured. In addition, this tailored interphase enhanced the moisture-conditioned shear strength.

In view of the results discussed above, composite toughness can be increased without accompanying degradation of the remaining mechanical properties. This can be achieved by proper selection of interphase properties, such as transition temperature, modulus, strength, etc. and the physical characteristics such as the quantity and thickness of this interphase.

References to the Role of Interface/Interphase in Composite Toughness

(1) P. K. Mallick and L. J. Broutman, "The Influence on the Fracture Toughness of Low Aspect Ratio Fiber Composites," Proc. 29th Ann. Tech. Conf. of SPI, Sec. 13-B (1974).

(2) M. G. Bader, J. E. Bailey and I. Bell, "The Effect of Fiber-Matrix Interface Strength on the Impact and Fracture Properties of Carbon-Fiber-Reinforced Epoxy Resin Composites," J. Phys. D: Appl. Phys., 6 (1973), 572.

(3) D. G. Pires, C. E. Fong, J. F. Mandell and F. J. McGarry, "Fiber/Matrix Interaction Effects on Fracture Toughness of Structural Composites," DTIC, AMMRC-CTR-75-15, (1975).

(4) T. Jones, N. P. Suh and N. H. Sung, "A Method of Improving the Fracture Toughness of Fiber Reinforced Composites," MIT Reports, Dept. of Mech. Eng., MIT-Industry Polymer Processing Program.

(5) P. Yeung and L. J. Broutman, "The Effect of Glass-Resin Interface Strength on the Impact Strength of Fiber Reinforced Plastics," Proc. 32nd Ann. Tech. Conf. of SPI, 9-B (1977).

(6) L. J. Broutman and B. D. Agarwal, "A Theoretical Study of the Effect of an Interfacial Layer on the Properties of Composites," Polym. Eng & Sci., 14, 8 Aug. (1974), 581.

(7) L. J. Broutman and B. D. Agarwal, "A Theoretical Study of the Effect of the Interface on Composite Toughness," Proc. 28th Ann. Tech. Conf. of SPI, 5-B (1973).

(8) E. P. Plueddeman, "Bonding Rigid Polymers to Mineral Surfaces Through a Rubbery Interface," Proc. 29th Ann. Tech. Conf. of SPI, 24-A (1974).

(9) N. L. Hancox and H. Wells, "The Effects of Fiber Surface Coatings on the Mechanical Properties of CFRP," Fiber Sci. and Tech., 10 (1977), 9.

(10) J. H. Williams, Jr., "Improvement of Composite Fracture Toughness by Fusible Fibers and Coatings," NTIS N77-71276 (1976).

(11) R. V. Subramanian and J. J. Jakubowski, "Electropolymerization on Carbon Fibers--Effect on Composite Properties," Polym. Research Sec. Mat'l. Sci. and Eng. Dept., Washington State Univ. Research Report.

(12) P. J. Cavano and W. E. Winters,"Composite Impact Strength Improvement Through a Fiber/Matrix Interphase," NTIS N76-13221, 1975.

(13) D. G. Peiffer, "Impact Strength of Thick-Interlayer Composites," J. of Appl. Polym. Sci., 24 (1979), 1451-5.

(14) A. G. Atkins, "Intermittent Bonding for High Toughness/High Strength Composites," J. of Mat'l. Sci., 10 (1975), 819-832.

(15) G. Reiss, M. Bourdeaux, M. Brie and G. Joupuet, "Surface Treatment of Carbon Fibers with Alternating and Block Copolymers," Proc. 2nd Carbon Fibers Conf., The Plastics Institute (1974), 52.

EFFECT OF MOISTURE ON THE CARBON FIBER/EPOXY INTERFACE AND INTERPHASE

Moisture is usually found on all solid surfaces and water molecules are usually the inhibitors/contaminants for adhesive bonding. Water is generally attracted and adsorbed onto the surface of solids through hydrogen bonding to the surface hydroxyl groups. The water molecules are normally one or two monolayers deep on the solid surface but this is enough to induce stress corrosion and assist crack propagation.

Evidence of adsorbed water molecules at glass fiber/epoxy interfaces has been shown and its detrimental effect on composite properties were discussed by Bascom.[1] According to Bascom, water molecules are attracted by the highly concentrated surface hydroxyl groups on the glass fibers and the reduction in composite properties are due to stress corrosion at the interface as well as in the bulk matrix.

Although carbon fibers also contain many functional groups on their surfaces, moisture has a smaller effect on carbon/epoxy composites. According to Gauchel and Nash,[2] only minor reductions in composite properties are observed after long-term exposure to water (12 months). Furthermore, these property reductions were primarily due to the plasticization effect of water on the epoxy matrix. Springer and Loos,[3] and Augl[4,5] showed that by characterizing effects of moisture on epoxy matrix properties, the moisture effect on carbon/epoxy composites performance can be predicted with a high degree of confidence. In other words, composite performance reduction is primarily due to bulk matrix plasticization.

In addition, McKague et al[6] at General Dynamics have studied the moisture effect on carbon/epoxy composites as a function of the sizing materials. McKague concluded that the size variants studied showed no effect on total moisture absorptivity (Figures 10 through 15) or glass transition temperature (Table I), nor did it affect the resistance to thermal cycling between -54°C and 124°C (-65°F and 255°F), (Table II).

In conclusion, for carbon fiber/epoxy composites, the decrease in shear strength after moisture conditioning is primarily due to plasticization of the matrix by water. This is contrary to glass fiber/epoxy composites, wherein irreversible damage has been reported due to moisture degradation of chemical bonds at the interface. This has not been shown for carbon fiber/epoxy composites. Although moisture may have some effect on the interphase region in carbon fiber composites, experimental techniques are not available which can separate the effects of plasticization of the interphase from plasticization of the bulk of the matrix itself. Furthermore, there is no evidence of chemical degradation of the interphase region by moisture at ordinary use temperatures. Therefore, no experimental effort will be devoted in this study to demonstrate the significance of moisture at the interface and interphase.

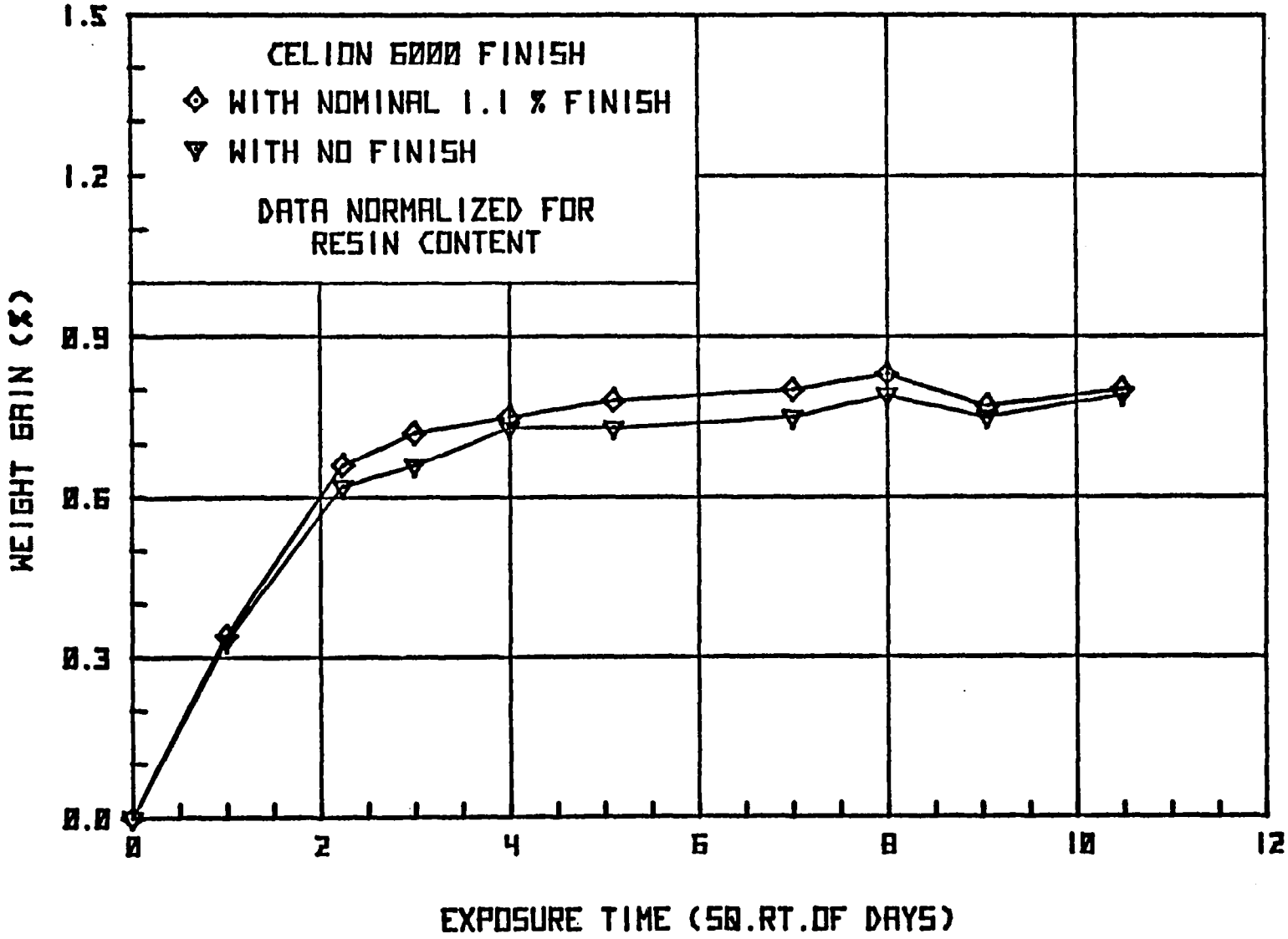

FIGURE 10. MOISTURE ABSORPTION OF CELANESE FURNISHED CELION®6000/5200 LAMINATES WITH AND WITHOUT NOMINAL SIZING FINISH*

*From McKague et al (Ref. 6)
Reproduced by permission.

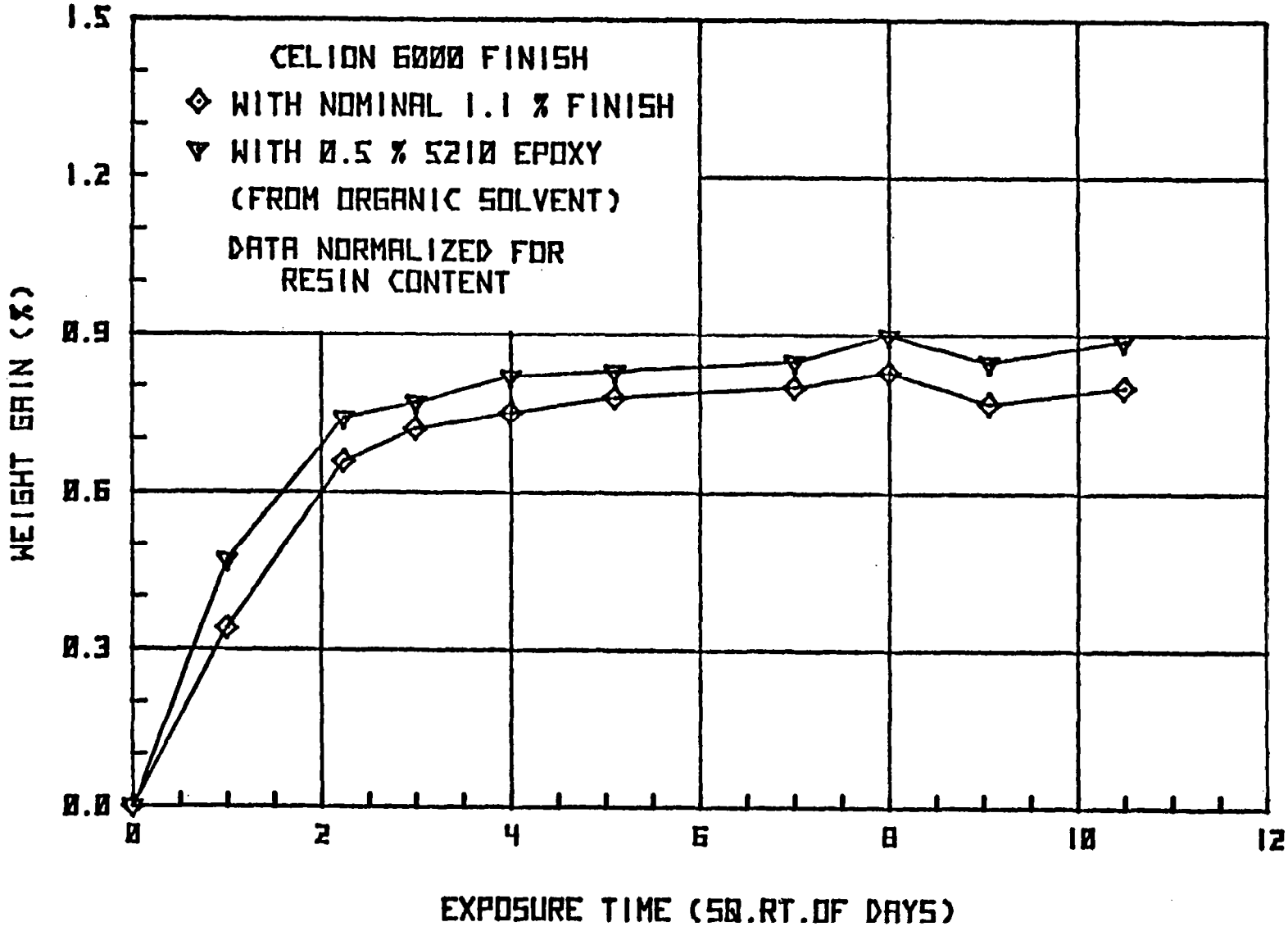

FIGURE 11. MOISTURE ABSORPTION OF CELANESE FURNISHED CELION®6000/5200 LAMINATES--SERIES 743-A AND 115-A SIZING*

*From McKague et al (Ref. 6)
Reproduced by permission.

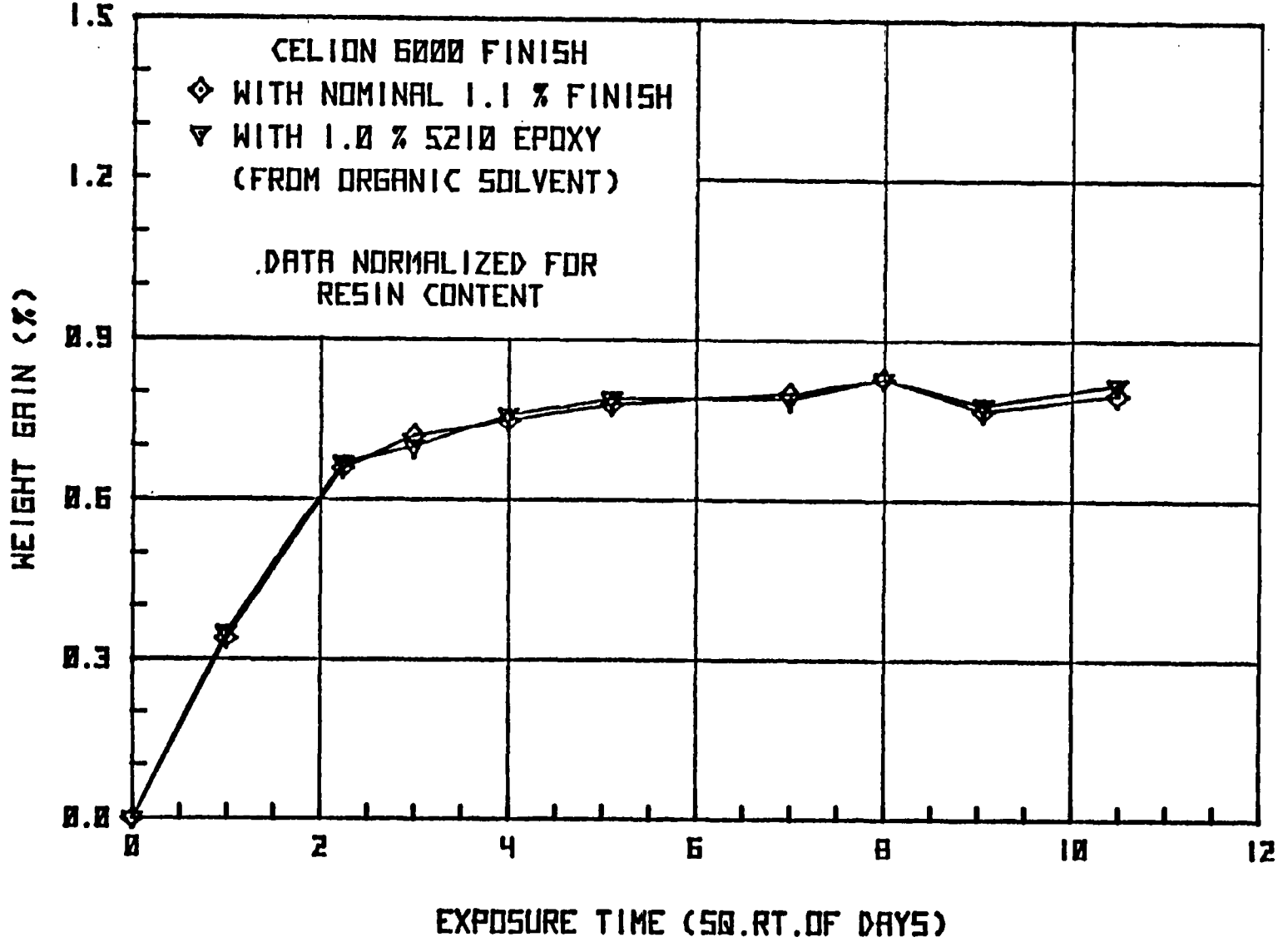

FIGURE 12. MOISTURE ABSORPTION OF CELANESE FURNISHED CELION®6000/5200 LAMINATES--SERIES 743-A AND 101-A SIZING*

*From McKague et al (Ref. 6)
Reproduced by permission.

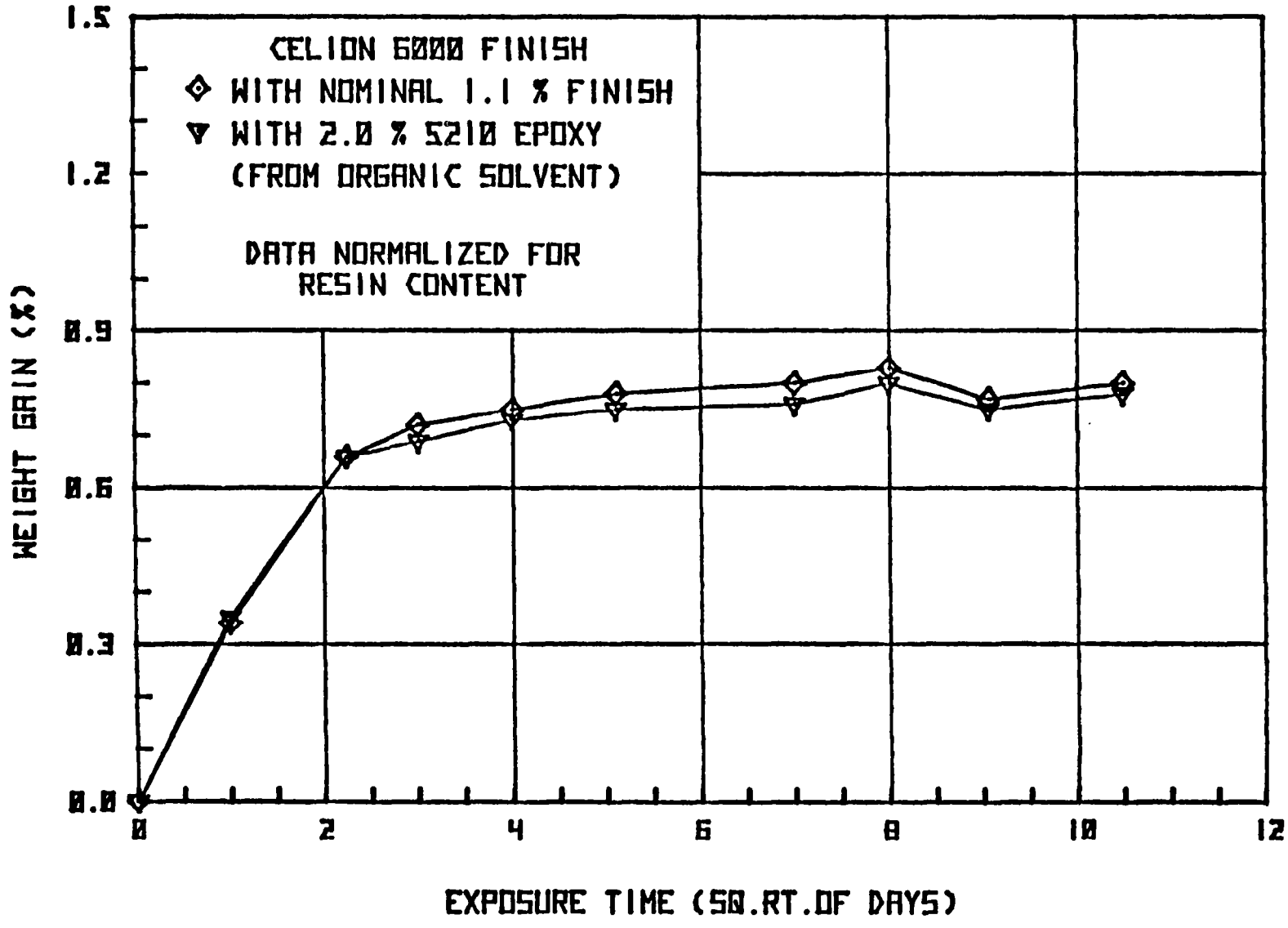

FIGURE 13. MOISTURE ABSORPTION OF CELANESE FURNISHED CELION®6000/5200 LAMINATES--SERIES 743-A AND 747-A*

*From McKague et al (Ref. 6)
Reproduced by permission.

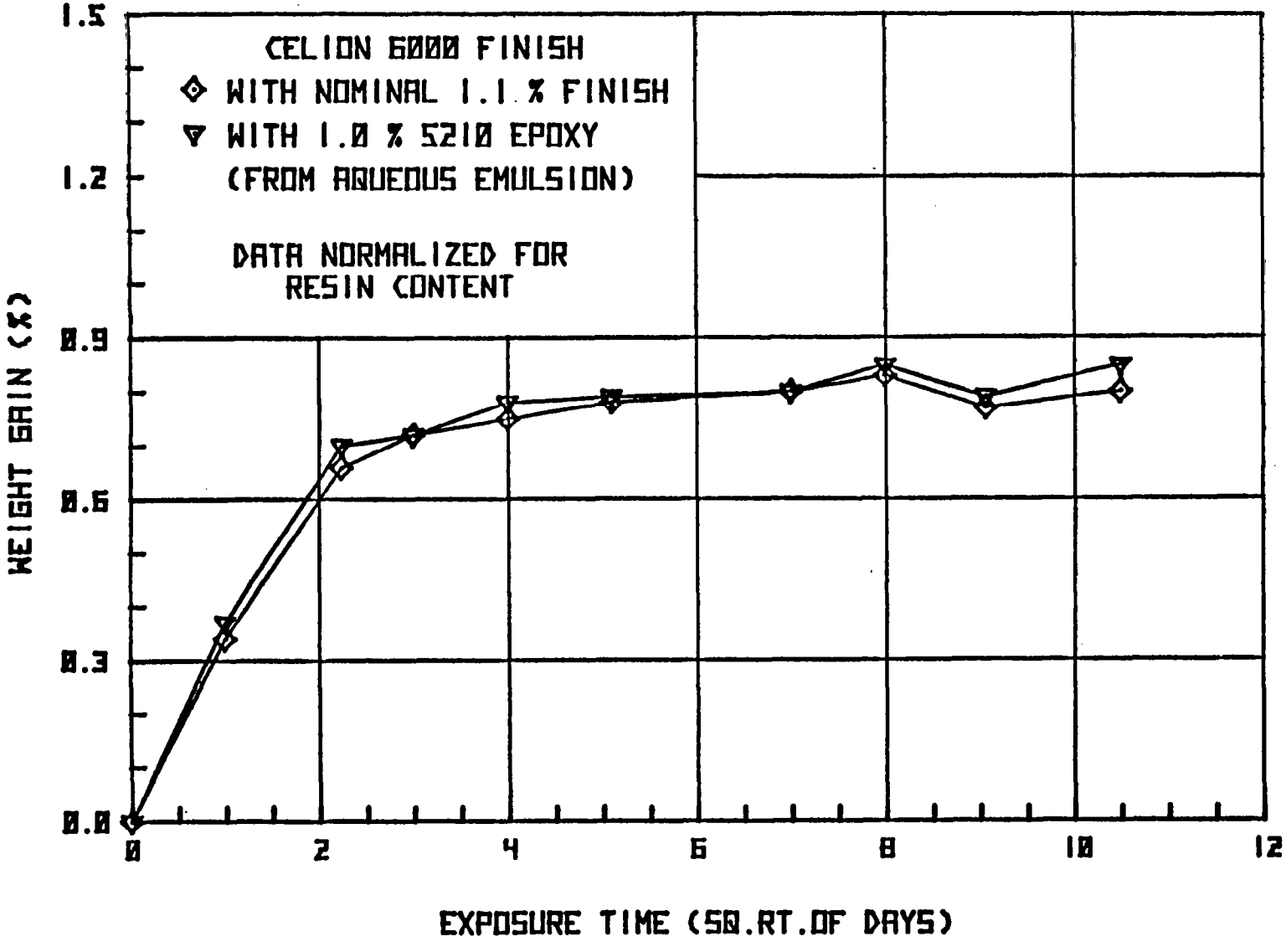

FIGURE 14. MOISTURE ABSORPTION OF CELANESE FURNISHED CELION®6000/5200 LAMINATES--SERIES 743-A AND 120-A*

*From McKague et al (Ref. 6)
Reproduced by permission.

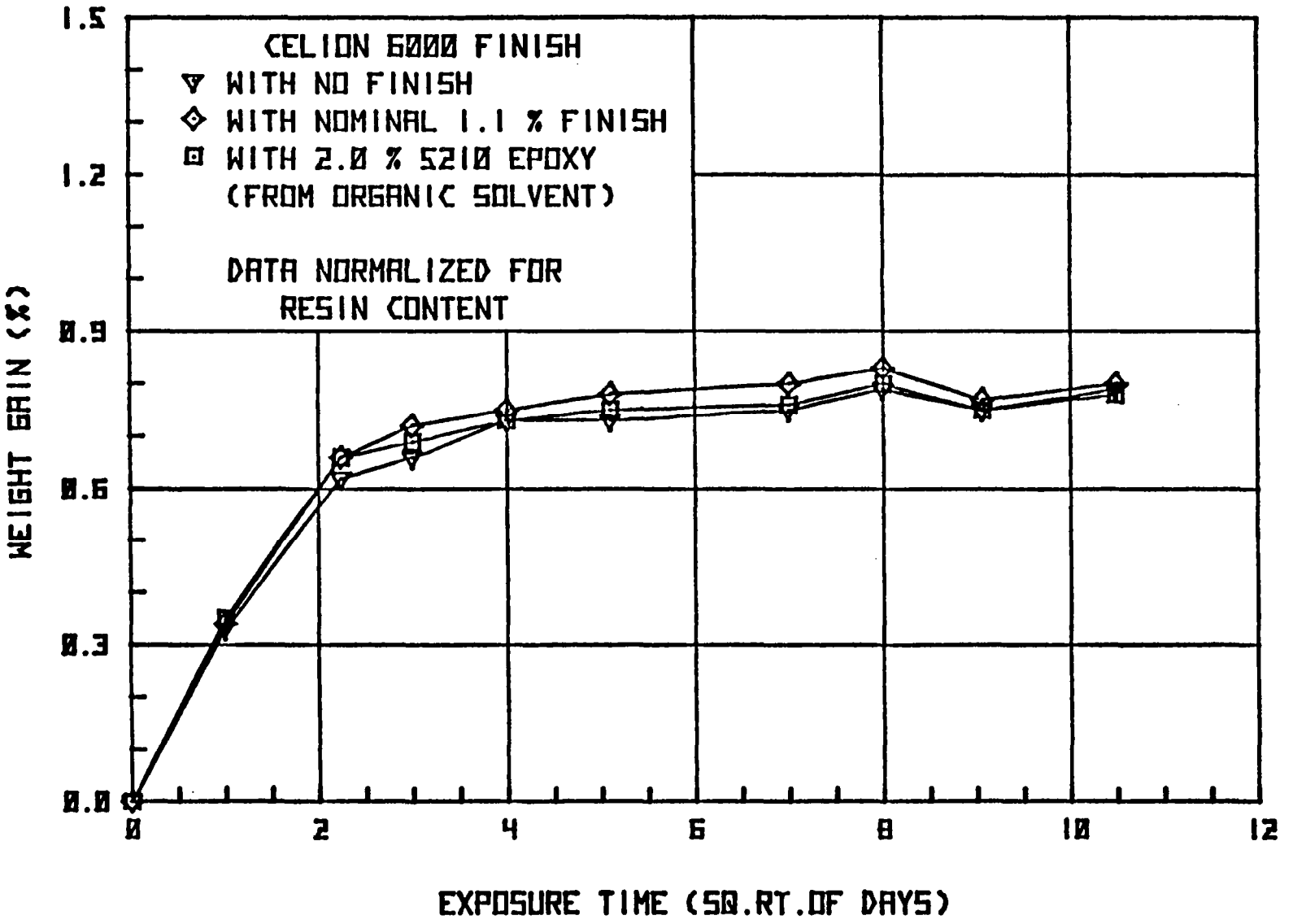

FIGURE 15. MOISTURE ABSORPTION OF CELANESE FURNISHED CELION®6000/5200 LAMINATES--SERIES 743-A, 745-A AND 747-A*

*From McKague et al (Ref. 6)
Reproduced by permission.

TABLE I. GLASS TRANSITION TEMPERATURES ON INTERPHASE VARIANTS*

Sample	Dry Tg °C (°F)	Moisture(%)	Wet Tg °C (°F)
No Finish	232 (450)	0.70	166 (330)
Normal 1.1% Finish	232 (450)	0.67	166 (330)
0.5% 5210 Epoxy	232 (450)	0.80	160 (320)
1% 5210 Epoxy	232 (450)	0.76	168 (335)
2% 5210 Epoxy	232 (450)	0.78	166 (330)
1% 5210 Epoxy (emulsion)	232 (450)	0.73	160 (320)

Note: Each value is the average of two specimens. Maximum pair difference was 43.3°C (110°F).

* From McKague et al (Ref. 6). Reproduced by permission.

TABLE II. THERMAL CYCLING DATA*

Sample	0° Flexural Properties							
	Strength				Modulus			
	Uncycled		Cycled		Uncycled		Cycled	
	MPa	ksi	MPa	ksi	GPa	Msi	GPa	Msi
No Finish	1931	280	1924	279	142.1	20.6	144.8	21.0
Normal 1.1% Finish	1869	271	1952	283	140.7	20.4	144.8	21.0
0.5% 5210 Epoxy	1876	272	1897	275	138.6	20.1	136.6	19.8
1% 5210 Epoxy	1897	275	1938	281	135.2	19.6	138.6	20.1
2% 5210 Epoxy	1841	267	1814	263	131.0	19.0	132.4	19.2
1% 5210 Epoxy (Emulsion)	1938	281	1986	288	142.1	20.6	139.3	20.2

*From McKague et al. (Ref. 6).
Reproduced by permission.

References to Effect of Moisture on the Carbon Fiber/Epoxy Interface

(1) W. D. Bascom, "Water at the Interface," Proc. 25th Ann. Tech. Conf. of SPI, 13-C (1970).

(2) J. V. Gauchel and H. C. Nash, "The Effect of Long-Term Water Immersion on the Fracture Toughness, Strength and Modulus of Graphite-Epoxy Composites," Organic Chemistry Branch, Chemistry Division, Naval Research Laboratory, Wash. DC 20375.

(3) G. S. Springer and A. C. Loos, "Moisture Absorption of Epoxy Matrix Composites Immersed in Liquids and in Humid Air," AFML-TR-79-4175, Final Report, (1979).

(4) J. M. Augl, "Prediction and Verification of Moisture Effects on Carbon Fiber-Epoxy Composites," NSWC-TR-79-43, (1979).

(5) J. M. Augl and A. E. Berger, "The Effect of Moisture on Carbon Fiber Reinforced Composites," NSWC/NOL-TR-77-61 (1977).

(6) L. McKague, J. Fruit and J. Reynolds, "Tests of Graphite Fiber Sizing Effects Upon Laminate Properties," SAMPE J, Nov-Dec, (1979) 6-11.

ADHESION THEORY

Adhesion, in physical chemistry, is the force of attraction between a solid surface and a second phase. The second phase can be a solid or a liquid. Adhesion leads to sorption, which may be adsorption on a surface or adsorption into a surface layer. Adhesion can be due to electrostatic forces, to van der Waals forces or to "chemical" valence forces. In the latter case, one speaks of "chemisorption." The magnitude of the adhesive forces is derived from equilibrium measurements of adsorption energies by thermodynamic methods.

In adhesion technology, only the interaction between a solid surface and a second liquid or solid phase is termed adhesion. The technical process of producing adhesion between two solids is called adhesive bonding. The bonded system is not necessary in a thermodynamic equilibrium; frequently the bonding process is irreversible. Therefore, surface interactions cannot be separated experimentally from bulk properties of the system.

In addition, the state of fundamental knowledge concerning the nature of the forces of attraction between bodies, determination of the magnitude of such intrinsic forces, and their relation to measured adhesive joint strengths undoubtedly lags behind state-of-the-art applied technology. One of the main reasons why developing theory has followed behind technology is that the science of adhesion is a truly multi-disciplined subject. The adhesion scientist often needs to consider aspects of surface chemistry and physics, chemistry, polymer chemistry, polymer physics, rheology, stress analysis and fracture phenomena to interpret his data fully.

The mechanisms of adhesion are still not fully understood and many theories are to be found in the current literature. Much of present confusion results from the fact that test methods commonly employed to measure the strengths of adhesive joints are not well suited to theoretical analysis. They introduce geometrical factors and loading factors which are difficult to analyze, and the measured joint strength includes indeterminate contributions from rheological energy losses in the adhesives and substrate. Thus, although the intrinsic adhesion forces acting across the adhesive/substrate interface may affect joint strength they are usually completely obscured by other contributions, and information concerning the magnitude of such forces may only be indirectly obtained. This inability to measure the interfacial interactions has been the main obstacle to the development of a comprehensive theory of adhesion.

The four principal mechanisms of adhesion which have been proposed and widely discussed are:

1. Mechanical Interlocking
2. Diffusion Theory
3. Electronic Theory
4. Adsorption Theory

These are discussed in the following paragraphs.

Mechanical Interlocking

This theory proposes that mechanical keying or interlocking of the adhesive into the irregularities of the substrate surface is the major source of intrinsic adhesion. Much work[1-7] in this area has shown the importance of surface topography/rugosity in intrinsic adhesion forces. However, the observed increase in measured joint strength with increasing surface rugosity may be attributable to other mechanisms.

Diffusion Theory

The diffusion theory of adhesion is based upon the intrinsic adhesion of high polymers to themselves (autohesion), and to each other, due to the mutual diffusion of polymer molecules across the interface. This requires that the macromolecules or chain segments of the polymers (adhesive and substrate) possess sufficient mobility and are mutually soluble, that is, they possess similar values of the solubility parameter. The solubility parameter, δ, is defined by

$$\delta = \frac{\Delta H_V - RT^{\frac{1}{2}}}{V} \qquad (1)$$

where

ΔH_V = molar heat of vaporization
R = gas constant
T = temperature (°K)
V = molar volume

Voyutskii[8] and others[9-13] have presented the evidence of molecular diffusion and their significant contributions to the intrinsic adhesion. However, with polymer systems which are highly crosslinked and have a high degree of crystallinity, diffusion theory is not likely to be the principal mechanism of adhesion.

Electronic Theory

The electronic theory of adhesion arises from the different electronic bond structures of the adhesive and the substrate which cause some electron transfer on contact to balance Fermi levels. This will result in the formation of a double layer of electrical charge at the interface which contributes to the intrinsic adhesion. This theory was proposed by Deryaguin[14-16] and supported by other workers.[17-24] However, the arguments were not strong enough to show its significant contribution to the intrinsic adhesion. Nonetheless, surface electronic states should not be overlooked.

Adsorption Theory

The adsorption theory of adhesion is by far the most generally accepted theory and has been discussed in depth by many authors.[25-28] This theory proposes, provided that sufficiently intimate intermolecular contact is achieved at the interface, that materials will adhere because of the surface forces acting between the atoms in the two surfaces. The most common of such forces are the van der Waals forces (secondary bonds). In addition, chemisorption may well occur and thus ionic, covalent and metallic bonds may operate across the interface (primary bonds).

The thermodynamic work of adhesion required to separate a unit area of two phases forming an interface, W_A, may be related to the surface free energies by the Young-Dupre equation.[29] In the absence of chemisorption and inter-diffusion, the reversible work of adhesion, W_A, in an inert medium may be expressed by

$$W_A = \gamma_1 + \gamma_2 - \gamma_{12} \qquad (2)$$

where

γ_1 = surface free energy of phase 1
γ_2 = surface free energy of phase 2
γ_{12} = interfacial free energy between the phases

This equation only applies to a solid/liquid or liquid/liquid interface. However, by assuming that the surface energy of a liquid does not change significantly where it solidifies isothermally and ignoring the shrinking stresses, it may be applied to solid adhesives/substrate interfaces.

Dukes[30] and others[31-34] have been trying to correlate measured strengths of adhesive joints with the thermodynamic work of adhesion, W_A. However, only some of the authors have confirmed correlations while others have found no correlations at all. The major cause of this conflict arises from the use of test methods for

measuring the strengths of adhesive joints which are not well suited to theoretical analysis. Moreover, correlation can only be expected when the locus of joint failure is purely interfacial. Therefore, even though the thermodynamic work of adhesion affects joint strength, it is often obscured by other contributions.

Although it has been shown that secondary bonding forces alone can give rise to acceptable joint strengths at the interface, many adhesion scientists believe that the additional presence of primary bonding can increase the joint strength and is certainly a must for establishing environmentally stable interfaces. Evidence of the presence of primary interfacialy bonding has been shown via the use of sophisticated, surface-specific, analytical techniques such as Laser-Raman spectroscopy,[35] x-ray photoelectron spectroscopy,[36] secondary-ion mass spectroscopy,[37,38] and attenuated total reflectance infra-red spectroscopy.[39]

It was recognized by adhesion scientists that the establishment of an intimate molecular contact at the interface is a necessary, though sometimes insufficient, requirement for developing strong adhesive joints. In other words, the adhesive needs to be able to be spread over the solid substrate surface and needs to displace air and any other contaminants that may be present on the surface. Ideally, an adhesive should conform to the following conditions:[40]

1. Adhesives in the liquid state must exhibit a zero or near-zero contact angle with the solid substrate.

2. The adhesive should have a relatively low viscosity (a few centipoises) at some time during the bonding operation.

3. The adhesive should be brought together with the substrate at a rate and in a manner that will promote the displacement of any trapped air at the interface.

In order to assess the ability of a given adhesive/substrate combination to meet these criteria, it is necessary to consider wetting equilibria, to ascertain values of the surface free energies of the adhesive and substrate and the free energy of the adhesive/substrate interface. In addition, the kinetics of the wetting process should also be examined.

References to Adhesion Theory

(1) E. M. Borroff and W. C. Wake, "Adhesion of Rubber to Textiles," Trans. Institute of the Rubber Industry, 25 (1949) 190.

(2) W. C. Wake, "Adhesion and the Formulation of Adhesives," Applied Science Publishers, London, (1976).

(3) D. E. Packham, K. Bright and B. W. Malpass, "Mechanical Factors in the Adhesion of Polyethylene to Aluminium," J. Appl. Poly. Sci., 18, (1974) 3237.

(4) J. R. Evans and D. E. Packham, "Adhesion-1," K. W. Allen, editor, Applied Science Publishers, London, (1977).

(5) C. W. Jennings, "Surface Preparation for Adhesive Bonding," Appl. Polymer Sympos., 19 (1972), 49.

(6) W. D. Bascom, C. O. Timmons and R. L. Jones, "Apparent Interfacial Failure in Mired-Mode Adhesive Fracture," J. Mat'l. Sci., 10, (1975) 1037.

(7) D. R. Mulville and R. Vaishnav, "Interfacial Crack Propagation," J. Adhesion, 7 (1975), 215.

(8) S. S. Voyutskii, "Autohesion and Adhesion of High Polymers," John Wiley and Sons, New York, (1963).

(9) J. N. Anand and H. J. Karam, "Interfacial Contact and Bonding in Autohesion," J. Adhesion, 1 (1969), 16.

(10) R. M. Vasenin, "Adhesion, Fundamentals and Practice," McLaren and Son, London, (1969).

(11) R. P. Campion, "The Influence of Structure on Autohesion (Self-Tack) and Other Forms of Diffusion into Polymers," J. Adhesion, 7 (1975), 1.

(12) F. Bueche, W. M. Cashin and P. Debye, "The Measurement of Self Diffusion in Solid Polymers," J. Chem. Phys., 20 (1952), 1956.

(13) W. V. Titow, "Adhesion 2," K. W. Allen, editor, Applied Science Publishers, London, (1978).

(14) B. V. Deryaguin, "Theory of Heterocoagulation, Interaction and Mutual Adhesion of Different Particles in Electrolytic Solutions," Research, 8 (1955), 70.

(15) B. V. Deryaguin, N. A. Krotova, V. V. Karassev, Y. M. Kivillova and I. N. Aleinikova, "Proceedings of the 2nd International Congress on Surface Activity III," Butterworths, London, (1957) 417.

(16) B. V. Deryaguin and V. P. Smilga, "Adhesion, Fundamentals and Practice," McLaren and Son, London, (1969) 152.

(17) C. L. Weidner, "Pressure-Sensitive Adhesive Compounds from Rubber, Tackifying Resins, Polyamines and Peroxides," Adhesive Age, 6 (7) (1963), 30.

(18) S. M. Skinner, R. L. Savage and J. E. Rutzler, "Electrical Phenomena in Adhesion, I, Electron Atmospheres in Dielectrics," J. Appl. Phys., 24 (1953), 439.

(19) H. Graf von Harrach and B. N. Chapman, "Charge Effects in Thin Film Adhesion," Thin Solid Films, 13 (1972), 157.

(20) C. Weaver, "Aspects of Adhesion 5," D. J. Alner, editor, University of London Press, London (1969).

(21) C. Weaver, "Adhesion of Metals to Polymers," Faraday Special Discussions, 2 (1972), 18.

(22) B. N. Chapman, "Aspects of Adhesion 6," D. J. Alner, editor, University of London Press, London (1970).

(23) J. Oroshnik and W. K. Croll, "Adhesion Measurements of Thin Films, Thick Films and Bulk Coating," K. L. Mittal, editor, Amer. Soc. Testing Materials, Special Tech. Publication 640 (1977), 158.

(24) C. T. H. Stoddart, D. R. Clarke and C. J. Robbie, "Thin Film Adhesion: Effect of Glow Discharge on Substrate," J. Adhesion, 2 (1970), 270.

(25) C. Kemball, "Adhesion," D. D. Eley, editor, Oxford University Press, London (1961), 19.

(26) J. R. Huntsberger, "Treatise on Adhesion and Adhesives," Vol. 1, R. L. Patrick, editor, Marcel Dekker, New York (1967).

(27). A. J. Staverman, "Adhesion and Adhesives," Vol. 1, R. Houwink and G. Salmon, editors, Elsevier, Amsterdam (1965).

(28) W. C. Wake, "Reinforcement and Filler Structure in Rubbers," Royal Institute of Chemistry Lecture Series 4 (1966), 1.

(29) T. Young, "Miscellaneous Works," Trans. Roy. Soc., 95 (1805), 65.

(30) W. A. Dukes and A. J. Kinlock, "Developments in Adhesives 1," W. C. Wake, editor, Applied Science Publishers, London (1977).

(31) K. L. Mittal, "Adhesion Science and Technology," L. H. Lee, editor, Plenum Press, New York (1975).

(32) M. Levine, G. Ilkka and P. Weiss, "Adhesion and Adhesives; Effects of Surface Energetics," J. Polym. Sci., B2 (1964), 215.

(33) D. H. Kaelble, "Peel Adhesion: Influence of Surface Energies and Adhesive Rheology," J. Adhesion, 1 (1969), 102.

(34) C. A. Dahlquist, "Adhesion," ASTM, STP 360 (1974), 46.

(35) J. L. Koenig and P. T. K. Shih, "Ramon Studies of the Glass Fibers-Silane-Resin Interface," J. Colloid Interf. Sci., 36 (1971), 247.

(36) R. Bailey and J. Castle, "XPS Study of the Adsorption of Ethoxysilanes on Iron," J. Mat'l. Sci., 12 (1977), 2049.

(37) M. Gettings and A. J. Kinlock, "Surface Analysis of Polysiloxane/Metal Oxide Interfaces," Surface Interference Analysis, 1 (1980), 189.

(38) M. Gettings and A. J. Kinlock, "Surface Characterization and Adhesive Bonding of Stainless Steels. II. The Steel/Adhesive Interface," Surface Interference Analysis, 1 (1980), 189.

(39) S. Crisp, H. J. Prosser and A. D. Wilson, "An Infra-red Spectroscopic Study of Cement Formation Between Metal Oxides and Aqueous Solutions of Poly(acrylic acid)," J. Mat'l. Sci., 11 (1976), 36.

(40) W. D. Bascom and R. L. Patrick, "The Surface Chemistry of Bonding Metals with Polymer Adhesives," Adhesive Age, 17 (10).

WETTING PHENOMENA

Surface tension is a direct measurement of intermolecular forces. The tension in surface layers is due to the attraction forces exerted on the surface molecules by the bulk material. This internal attraction force leads to a reduced number of molecules at the surface which result in an increased intermolecular distance. This increase in intermolecular distance requires external work to be done which explains why surface tension/surface free energy exist.

The most common type of physical surface attractive forces are van der Waals forces which can be attributed to: (a) dispersion (London-d) forces arising from internal electron motions which are independent of dipole moments and; (b) polar (Keesom-p) forces arising from the orientation of permanent electric dipoles and the induction effect of permanent dipoles or polarizable molecules. The dispersion forces are usually weaker than the polar forces but they are universal and all materials exhibit them.

Another type of force that may operate is the hydrogen bond. Hydrogen bonding is the attraction between a hydrogen atom and a second, small and strongly electronegative atom such as fluorine, oxygen or nitrogen. A secondary bond is actually formed between the hydrogen atom and the electronegative (host) atom through an electron-pair on the host species.

Equilibrium wetting occurs when the liquid and solid phases are in contact and can no longer be perturbed by external forces. The equilibrium condition for the wetting of a solid surface by a liquid is a three-phase equilibrium of solid, liquid and vapor. As shown in Figure 16, one can describe the equilibrium point of

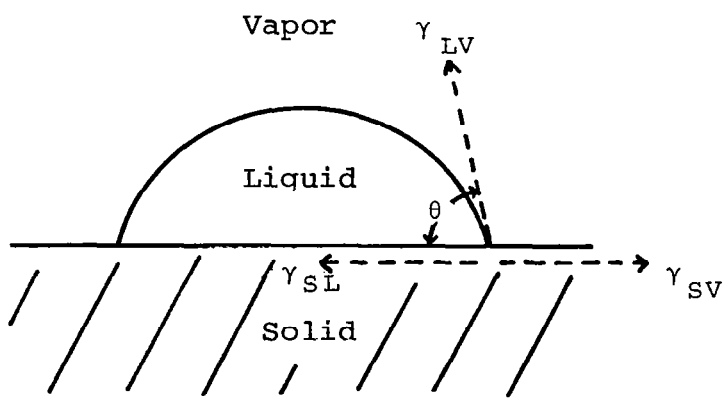

FIGURE 16. EQUILIBRIUM STATE OF A LIQUID DROP ON A SOLID SURFACE

contact as the intersection of three interfaces--solid-liquid (SL), liquid-vapor (LV), and solid-vapor (SV). The balance of these surface forces/surface tensions on this three-phase intersection is best described by the Young-Dupre equation;[1]

$$\gamma_{SV} - \gamma_{SL} = \gamma_{LV} \cos \theta \qquad (3)$$

where

γ_{SV} = surface tension at solid-vapor interface
γ_{SL} = surface tension at solid-liquid interface
γ_{LV} = surface tension at liquid-vapor interface
θ = contact angle

When $\theta \geq 90°$, the liquid is non-wetting and for $90° > \theta > 0°$, the liquid is wetting but it is nonspreading. When $\theta = 0°$, the liquid wets the solid completely and spontaneously and spreads freely over the surface at a rate depending on the liquid viscosity and solid surface roughness. Nevertheless, it is also possible for a liquid to spread and wet a solid with contact angle $\theta > 0°$ by the application of an external pressure or force to the liquid.

To apply these concepts to adhesive technology, the surface and interfacial free energies need to be evaluated. However, there are no direct methods available to measure surface free energy, γ_{SV}, which complicates the analysis. Nonetheless, the contact angle θ is a physically measurable parameter and it serves as a convenient means for describing the wettability or degree of wetting on solid surfaces.

When a liquid has a zero contact angle with a solid substrate, surface tension gradients sometimes exist at the spreading front which may either assist or hinder spreading depending upon their directions.[2,3] These surface tension gradients arise from thermal gradients, or, in the case of liquids, from the presence of a more volatile component of different surface free energy (e.g., a trace of impurity). The effect of the surface tension gradients on the spreading rates are relatively small. However, it might have an effect on the redistribution of the wetting liquid after it wets the solid surface.

The topography of the substrate surface also has an effect on the kinetics of wetting. A liquid can spread along fine pores, scratches and other inhomogeneities via capillary action. This spontaneous spreading occurs even if the liquid is non-wetting on a smooth, planar surface. A fifty per cent increase in spreading rate was reported by Bascom et al[2] and Cottington et al.[4] Again, topography plays a minor role in affecting the rate of spreading, especially if the liquid is forcibly spread over the substrate surface. Nonetheless, topography does affect the redistribution of the wetting liquid after its initial "wet-out."

Much work(5-12) has been done to obtain quantitative expressions for wetting upon various types of substrate surface topography. Fundamental understanding of the importance of wetting kinetics upon wetting processes (e.g., a process to eliminate trapped air at the interface during wetting) and interfacial bond strength have yet to be studied.

Dynamic wetting occurs when the liquid or the solid or both are kept in motion relative to the other phase throughout the wetting process. This process is best described by a sessile drop placed on an inclined plane where two contact angles are present. As shown in Figure 17, the advancing angle is the larger, frontier angle as the liquid is progressing to "wet" the solid surface. The advancing angle reflects the tendency of the liquid to wet a virgin surface. The receding angle is the smaller, tail end angle where the liquid is retreating from the "wetted" surface. The receding angle is a measure of the ability of the solid surface to remain wetted.

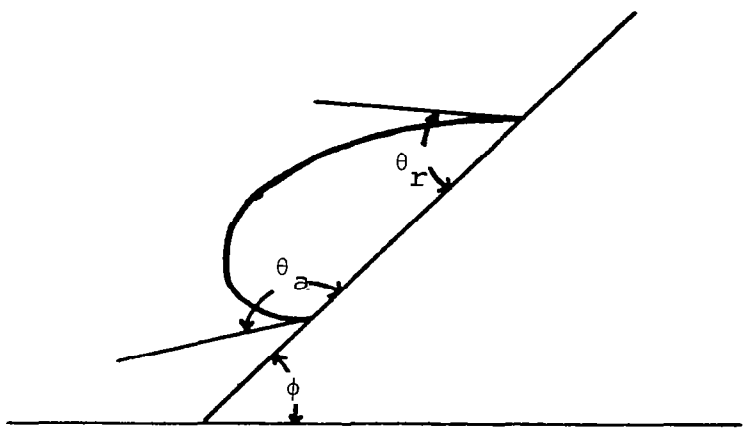

FIGURE 17. A SESSILE DROP ON AN INCLINED PLANE (GRADIENT = tanϕ) SHOWING THE ADVANCING θ_a AND RECEDING θ_r ANGLES

The dynamic wetting angles best characterize the condition where the wetting liquid is forcibly spread onto the substrate surface. Moreover, the advancing angle is very sensitive to surface contamination and surface heterogeneity. This property enables the characterization of the substrate surface and provides insight on the wetting process. The receding angle can be related to the uniformity of the coating after the liquid has wetted the substrate surface.

In addition, wetting hysteresis can be obtained by the difference between the advancing angles and the receding angles. The hysteresis of wetting is due to the presence of a large number of metastable states which differ slightly in energy at the surface and are separated from each other by small energy barriers. These metastable states are generally attributed to either surface roughness or surface chemical heterogeneity, or both. Surface heterogeneity can also arise from impurities concentrated at the surface, from crystal imperfections or from differences in the properties of different crystal faces. In general, surfaces are both rough and heterogeneous. It is possible to compare surface roughness and heterogeneity by measuring the hysteresis of wetting.

Experimental Techniques

The surface energetics of fibers can critically affect the wetting behavior and the end-use performance of fibrous materials, e.g., in composite structures. The measurement of spontaneous surface wetting is one of the few experimental techniques available for the study of the solid-surface energetics.

Assessing contact angle measurements on filamentous material is a very difficult experimental task due to the fiber geometry. A preferred technique in direct contact-angle measurement for fibers is a derivative of the tilted plate concept.[13] This involves a small reservoir of liquid which is pierced by the fiber and an arrangement whereby the fiber can be tilted relative to the liquid surface until the meniscus disappears. The contact angle is then measured from the fiber to the liquid surfaces. However, considerable precaution must be taken to obtain the true contact angle. This experimental technique is extremely difficult to apply on fibers with small-cross sectional areas.

An alternate experimental approach which does not require the direct measurement of contact angles is the wetting force measurement based on the Wilhelmy balance principle.[14] This technique is deemed to be promising with filamentous materials, especially with small denier (fine) fibers because of the development of high sensitivity microbalances and the ability to assess both equilibrium and dynamic wetting data. For fibrous composites, dynamic wetting data is very significant because of its ability to prescribe the conditions for prepregging processes.

The wetting force measurement, according to Wilhelmy,[14] is the force exerted on a vertical rod (fiber) inserted into a liquid. This force is expressed by:

$$F_W = \pi D \gamma_{LV} \cos \theta \qquad (4)$$

where

F_W = wetting force

D = diameter of the fiber

γ_{LV} = surface tension

θ = contact angle

A mathematical derivation of this expression was performed by A. J. G. Allan.[15] The balance of forces acting on the fiber before and after contact with liquid is illustrated in Figure 18. An important feature of this technique is its applicability to both equilibrium and dynamic conditions. The advancing wetting force can be obtained during the fiber penetrating into the wetting liquid. The equilibrium wetting force is obtained during the stable condition when the fiber is not in motion with respect to the liquid. The receding wetting force can be measured during the pulling out of the fiber from the wetting liquid. The corresponding wetting force expressions are:

$$F_W = \pi D \gamma_{LV} \cos \theta \qquad (5)$$

$$F_a = \pi D \gamma_{LV} \cos \theta_a \qquad (6)$$

$$F_r = \pi D \gamma_{LV} \cos \theta_r \qquad (7)$$

where

F_W and θ are the equilibrium wetting force and contact angle respectively

F_a and θ_a are the advancing wetting force and contact angle respectively

F_r and θ_r are the receding wetting force and contact angle respectively

By measuring the wetting force, F_W, and the surface tension of the wetting liquid, γ_{LV}, work of adhesion, W_A can be determined.

$$W_A = \gamma_{LV} + \gamma_{LV} \cos \theta \qquad (8)$$

or

$$W_A = \gamma_{LV} + \frac{F_W}{\pi D} \qquad (9)$$

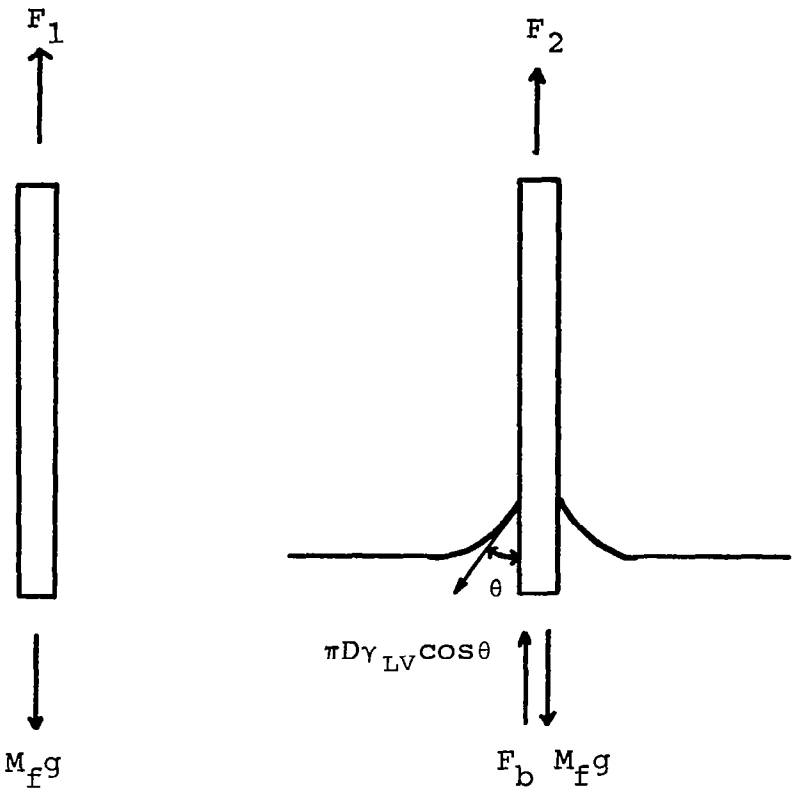

(a) Filament suspended freely

(b) Filament partially immersed

where:

F_b = buoyancy force

$M_f g$ = gravitational force

F_W = wetting force

D = diameter of fiber

γ_{LV} = surface tension of wetting liquid

θ = contact angle

assuming F_b is negligible

then

$$F_W = F_2 - F_1 = \pi D \gamma_{LV} \cos \theta$$

FIGURE 18. FORCES ACTING ON A SUSPENDED FILAMENT BEFORE AND AFTER CONTACT WITH WETTING LIQUID

Furthermore, by attaching a microprocessor to the microbalance and controlling the fiber immersion/emersion operation, a continuous monitoring of the advancing wetting force and receding wetting force along the fiber can be achieved. This would enable the determination of fiber surface heterogeneity and provide insight into the uniformity of the liquid film adhered to the fiber surface. Moreover, this information also shows the frequency of occurence of critical surface contamination which prevents wetting/bonding.

Critical surface contamination is present in those areas of the surface that has a surface energy lower than the wetting liquid. This lower surface energetics create a thermodynamically unstable condition for the higher surface energy liquid to "wet" the solid surface. Therefore, a localized rejection of the wetting liquid occurs and this leads to the formation of voids during composite fabrication.

In addition, the hysteresis of wetting can also be studied by this technique. A plot of the immersion force/emersion force along the fiber immersion length can be used to map the wetting hysteresis. Figure 19 shows a typical plot and identifies the hysteresis of wetting.

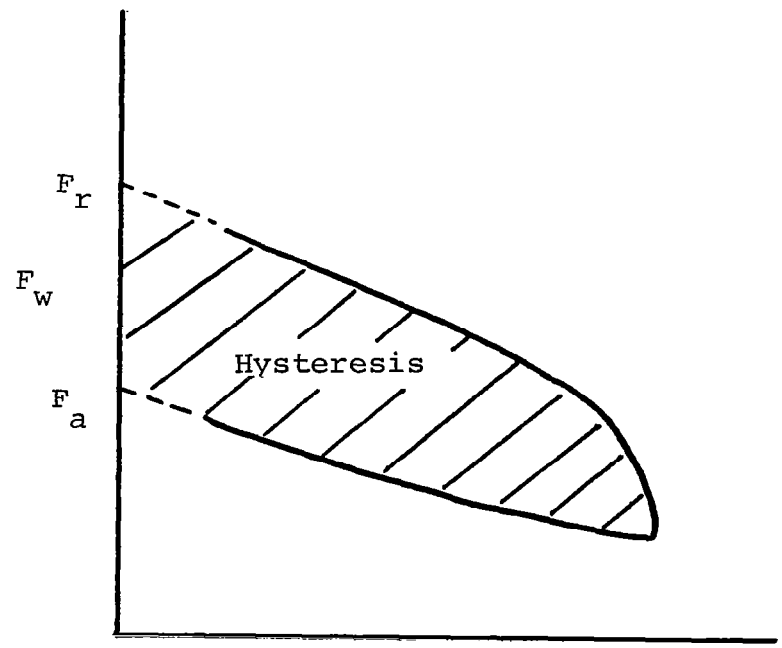

FIGURE 19. HYSTERESIS OF WETTING MEASURED BY PLOTTING ADVANCING AND RECEDING WETTING FORCE VERSUS IMMERSION FIBER LENGTH

Although the Wilhelmy wetting force measurement can provide much information, one experimental parameter can affect the accuracy of all these data.[16] The rate of the fiber penetrating into and receding out of the wetting liquid critically affects the measurables. As shown in Figure 20, a 90° contact angle (total disappearance of the meniscus) is created by this dynamic phenomena at the "critical penetration velocity." This phenomenon cannot be totally eliminated. However, the degree of meniscus depression/elevation can be minimized and controlled by operating at a much slower fiber immersion/emersion rate than the critical velocity and maintaining this rate throughout all studies. This technique has been used by many authors[17-23] and information on small denier fibers, such as, carbon fibers and polyester fibers, have been reported.

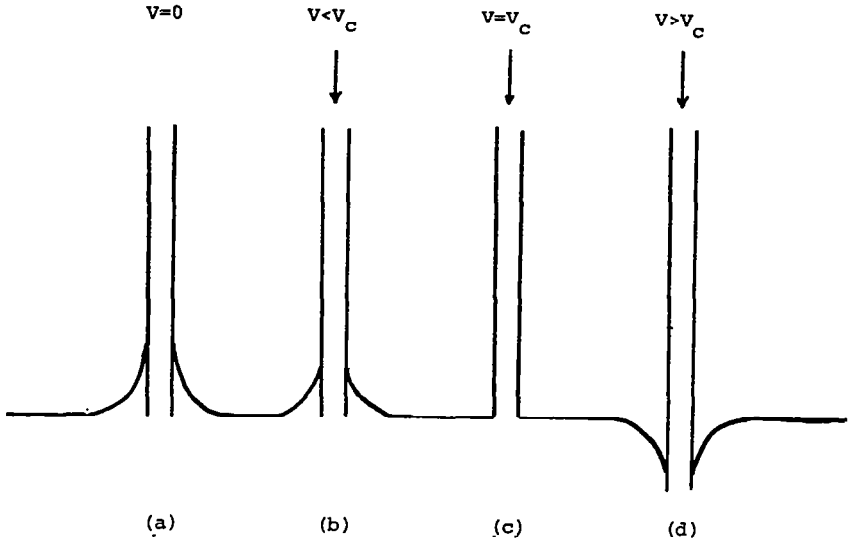

where

V = fiber penetration velocity

V_c = critical velocity at which meniscus disappears as in (c)

FIGURE 20. EFFECT OF FIBER PENETRATION VELOCITY ON CONTACT ANGLES

Carbon Fiber Surface Energetics

Hammer and Drzal[19] studied the surface energetics of Hercules Type A carbon fibers via the micro-Wilhelmy wetting force technique. Correlations were found between the oxygen concentration measured by x-ray photoelectron spectroscopy (XPS) and the change in polar/dispersive ratios of the carbon fibers. This indicated that surface treatments of carbon fibers which promote better fiber matrix adhesion resulted from an increase in the surface free energy. This increase in surface free energy was due to the addition of surface oxygen concentration during the surface treatment process. Some of the contact angle data are shown in Table III while Table IV lists the measured surface free energies of carbon fibers with their polar and dispersive components.

TABLE III. CONTACT ANGLES FOR CARBON FIBERS*

Liquid	γ_{LV} (mJ/m^2)	AU		AS	
		As Received	300°C V.T.	As Received	300°C V.T.
Water	72.8	41° ± 4°	44° ± 4°	29° ± 4°	33° ± 4°
Glycerol	64.0	33° ± 2°	40° ± 1°	25° ± 1°	42° ± 9°
Formamide	58.3	37°	24° ± 7°	22° ± 5°	27° ± 3°
Methylene Iodide	50.8	23° ± 5°	41° ± 11°	23° ± 5°	30° ± 12°
Ethylene Glycol	48.3	35° ± 6°	30° ± 6°	31° ± 7°	29° ± 2°
Bromonaphthalene	44.6	29° ± 3°	20° ± 4°	26° ± 3°	21° ± 3°
Polypropylene Glycol PG 1200	31.3	3° ± 3°	25° ± 1°	3° ± 3°	25° ± 1°
n-Hexadecane	27.6	18° ± 8°	27° ± 7°	22° ± 7°	23° ± 7°

γ_{LV} = surface tension of liquid

AU = Hercules Type A high strength carbon fiber non-surface treated

AS = Hercules Type A high strength carbon fiber surface treated

V.T. = vacuum treated

*From Hammer and Drzal (ref. 19).
Reproduced by permission.

TABLE IV. SURFACE FREE ENERGIES OF CARBON FIBER*

Fibers	Surface Free Energies		
As Received	γ^{P}_{SV} (mJ/m^2)	γ^{D}_{SV} (mJ/m^2)	γ_{SV} (mJ/m^2)
AU	23.6 ± 2.6	27.4 ± 0.3	51.0 ± 2.6
AS	30.0 ± 1.7	26.4 ± 0.1	56.4 ± 1.7
300°C V.T.			
AU	24.1 ± 1.4	26.3 ± 1.1	50.4 ± 1.4
AS	26.8 ± 1.4	26.0 ± 1.2	52.8 ± 1.4

γ^{P}_{SV} - Keesom-polar surface free energy of solid.

γ^{D}_{SV} - London-dispersion surface free energy of solid.

γ_{SV} - Surface free energy of solid, $\gamma_{SV} = \gamma^{P}_{SV} + \gamma^{D}_{SV}$

AU - Hercules Type A carbon fiber--non-surface treated.

AS - Hercules Type A carbon fiber--surface treated.

V.T. - Vacuum treated.

*From Hammer and Drzal (ref. 19).
Reproduced by permission.

Sell[18] studied the wetting properties of carbon fibers and measured the effect of surface treatments on wetting properties. Figure 21 summarizes his reported results.

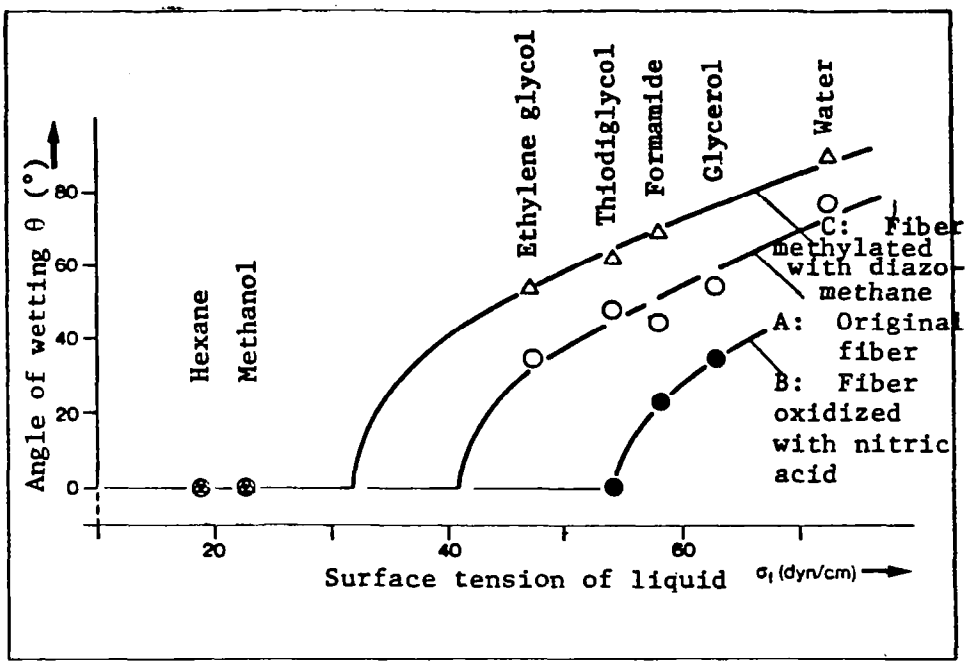

FIGURE 21. ANGLE OF WETTING θ OF VARIOUS LIQUIDS WITH RESPECT TO CARBON FIBERS*

*From Sell (ref. 18).
Reproduced by permission.

Kaelble et al[21,24-25] have intensively studied carbon fiber surface energetics via the micro-Wilhelmy balance technique. Some of his data on the contact angles of carbon fibers are shown in Table V. Kaelble also extended the information on the Keesom-polar and London-dispersive surface free energy with the modified Griffith fracture energy. This enabled the prediction of the interfacial conditions to promote good bond strength and environmental stability. This expression was done through the extension of the adsorption theory of interfacial interactions.[26] The critical value of the Griffith fracture stress, σ_c under normal plane stress loading can be expressed by the following relationships:

$$\sigma_c = \left(\frac{2E\gamma_G}{\pi C}\right)^{\frac{1}{2}} = \left(\frac{2E}{\pi C}\right)^{\frac{1}{2}} (R^2 - R_o^2)^{\frac{1}{2}} \geq 0 \qquad (10)$$

$$\gamma_G = R^2 - R_o^2 \qquad (11)$$

$$R_o^2 = 0.25[(\alpha_1 - \alpha_3)^2 + (\beta_1 - \beta_3)^2] \qquad (12)$$

$$R^2 = (\alpha_2 - H)^2 + (\beta_2 - K)^2 \qquad (13)$$

$$H = 0.5(\alpha_1 + \alpha_3) \qquad (14)$$

$$K = 0.5(\beta_1 + \beta_3) \qquad (15)$$

$$\alpha_1 = (\gamma_{LV}^d)^{\frac{1}{2}} \qquad (16)$$

$$\beta_1 = (\gamma_{LV}^p)^{\frac{1}{2}} \qquad (17)$$

$$\alpha_3 = (\gamma_{SV}^d)^{\frac{1}{2}} \qquad (18)$$

$$\beta_3 = (\gamma_{SV}^p)^{\frac{1}{2}} \qquad (19)$$

α_2 and β_2 = surface properties of the immersion phase at the crack tip

For air: $\alpha_2 = \beta_2 = 0$

For water: $\alpha_2 = 4.67\ (mJ/m^2)^{\frac{1}{2}}$

$\beta_2 = 7.14\ (mJ/m^2)^{\frac{1}{2}}$

TABLE V. WILHELMY BALANCE MEASUREMENTS OF HERCULES TYPE AU AND TYPE AS CARBON FIBER AT 23°C*

		AU				AS			
Liquid	γ_{LV} (mJ/m^2)	F_a (μg)	$\cos\theta_a$	θ_a	W_a (mJ/m^2)	Fa (μg)	$\cos\theta_a$	θ_a	W_a (mJ/m^2)
Water	72.8	181	0.8299	33.9°	133.22	172	0.8966	26.3°	138.07
Glycerol	64.0	182	0.9492	18.3°	124.75	161	0.9547	17.3°	125.10
Formamide	58.3	131	0.7500	41.4°	102.03	120	0.7811	38.6°	103.84
Diiodomethane	50.8	115	0.7556	40.9°	89.18	102	0.7620	40.4°	89.51
Ethylene Glycol	48.3	137	0.9467	18.8°	94.03	120	0.9429	19.5°	93.84
1-Bromonapthalene	44.6	126	0.9430	19.4°	86.66	111	0.9445	19.2°	86.72
Glycol PG-E-1200	43.5	130(1)	1.000	0°	---	114	1.000	0°	---
Glycol PG-15-200	36.6	106	0.9667	14.8°	71.98	94	0.9747	12.9°	72.27
Glycol PG-P-1200	31.3	94(1)	1.000	0°	---	83(1)	1.000	0°	---
n-Dodecane	25.4	71	0.933	21.1°	49.10	63	0.9413	19.7°	49.31
Ethanol (abs)	22.4	---	---	---	---	56.3	0.9413	19.7°	43.49

γ_{LV} - surface tension of liquid

F_a - advancing wetting force

θ_a - advancing contact angle

W_a - work of adhesion

AU - Hercules type A non-surface treated carbon fiber

AS - Hercules type A surface treated carbon fiber

(1) Wetting conditions with cosine θ = 1.0.

*From Kaelble et al (ref 21)
Reproduced by permission.

Through this thermodynamic analysis, Kaelble predicted that in order to have a moisture insensitive interface, a non-polar surface for the fiber and the matrix [β_1, $\beta_3 \leq 1.0 (mJ/m^2)^{1/2}$] was necessary. To assure spontaneous wetting to enhance interfacial bonding, an increase in London-dispersive contribution to the fiber surface free energy [$\alpha_3 \geq 6.0 (mJ/m^2)^{1/2}$] is required.

Penn et al[22] studied the advancing and receding contact angles of carbon fibers and the effect of wetting hysteresis. The advancing angle is used to demonstrate how readily the liquid wets the fiber surface; the receding angle is to illustrate how well the fiber surface remains wetted. The data is presented in Table VI. According to Penn, hysteresis of wetting would disappear below a critical surface tension of the wetting liquid. In addition, Penn also tried to correlate the wetting properties of carbon fibers to composite shear strength.[23] Penn sized the carbon fiber with a silicone fluid to create a hydrophobic surface and also had a hydrophilic size to compare the effect of sizings to composite properties both unconditioned and conditioned.

Some of these data are shown in Table VII. However, the reported composite data do not correlate with the wetting angles measured. The hydrophilic sized fiber showed the smallest contact angles (best wetting) but it had the lowest short beam shear strength both conditioned and unconditioned. Furthermore, silicone fluid has a poor compatability with epoxy and during prepregging, the silicone fluid could diffuse away from the fiber surface to the prepreg surface. This effect would be more pronounced with filament winding procedures. This is because the filament winding resin systems are more fluid and molecule mobility is enhanced. The similarity of the composite short beam shear strength of the silicone fluid sized fiber and the unsized fiber could be the reflection of the disappearance of the silicone size from the fiber surface. Moreover, Penn stated that silicone fluid was found on the surface of the laminates.*

Overall, much work has been done in measuring contact angles of carbon fibers and theoretical analyses have been made. However, reported values are generally scattered and the conditions at which these measurements were made are not generally clear. Above all, fiber origins, types and properties have not been generally characterized and specified. Therefore, attempting to correlate the reported data is difficult and unclear. This report is intended to clarify some of the gray areas and to try to correlate wetting properties of carbon fibers to fiber matrix adhesion and composite properties.

*Private communication with Dr. Lynn Penn.

TABLE VI. ADVANCING AND RECEDING CONTACT ANGLES OF CARBON FIBERS*

Liquid	γ_{LV} (mJ/m^2)	Carbon Fiber(1) $\cos\theta_a$	θ_a	$\cos\theta_r$	θ_r
Water	72.4	-0.067	93.8°	0.713	44.5°
Formamide	55.6	0.445	62.9°	0.562	55.8°
Methylene Iodide	48.6	0.824	34.5°	0.917	23.5°
Ethylene Glycol	47.5	0.538	57.5°	0.895	26.5°
Br-Naphthalene	45.3	0.957	16.9°	0.957	16.9°
Dimethyl Acetamide	36.7	0.993	6.78°	0.993	6.78°
Hexadecane	28.4	0.964	15.4°	0.964	15.4°

(1) Origin and type of carbon fiber unknown.

γ_{LV} - surface tension of liquid.
θ_a - advancing contact angle.
θ_r - receding contact angle.

*From Penn and Miller (Ref. 22).
Reproduced by permission.

TABLE VII. EFFECT OF WETTABILITY ON CARBON FIBER/EPOXY COMPOSITE SHEAR STRENGTH*

Fiber Variants	θ_a	θ_r	Short Beam Shear (ASTM D2344)							
			RT 82.2°C (180°F)				14 Days Water Boil RT 82.2°C (180°F)			
			MPa	ksi	MPa	ksi	MPa	ksi	MPa	ksi
AS-4 (unsized)	52.3°	22.0°	98.6±4.8	14.3±0.7	78.6±2.1	11.4±0.3	80±2.1	11.6±0.3	58.6±0.7	8.5±0.1
AS-4 (hydrophobic size) (silicone fluid)	78.6°	24.6°	90.3±2.8	13.1±0.4	76.6±1.4	11.1±0.2	81.4±2.8	11.8±0.4	58.6±2.1	8.5±0.3
AS-4	26.7°	0.00°	69.7±0.3	10.1±0.05	57.2±4.1	8.3±0.6	42.8±4.1	6.2±0.6	33.8±2.1	4.9±0.3

*From Desalvo et al (ref 23)
Reporduced by permission.

References to Wetting Phenomena

(1) T. Young, "Miscellaneous Works," Proc. Roy. Soc., Dec. (1804), and Phil. Trans., (1805), 65.

(2) W. D. Bascom and R. L. Patrick, "The Surface Chemistry of Bonding Metals with Polymer Adhesives," Adhesive Age, 17 (10), (1974) 25.

(3) W. D. Bascom, R. L. Cottington and C. R. Singleterry, "Advances in Chemistry Series, 43," R. F. Gould, editor, A.C.S., Washington (1964), 355.

(4) R. L. Cottington, C. M. Murphy and C. R. Singleterry, "Advances in Chemistry Series, 43," R. F. Gould, editor, A.C.S., Washington (1964), 341.

(5) R. N. Wenzel, "Contact Angles on Rough Surfaces," Ind. Eng. Chem., 28 (1963), 988.

(6) F. E. Bartell and J. W. Shepard, "Surface Roughness as Related to Hysteresis of Contact Angles. I--The System Paraffin-Water-Air," J. Phys. Chem., 57 (1953) 211.

(7) A. W. Neumann and R. J. Good, "Thermodynamics of Contact Angles," J. Colloid, Interf. Sci., 38 (1972), 341.

(8) J. C. Oliver and C. Huh and S. G. Mason, "The Apparent Contact Angle of Liquids on Finely-Grooved Solid Surfaces-- A SEM Study," J. Adhesion, 8 (1977), 223.

(9) H. Schonhorn, C. Frisch and T. K. Kwei, "Kinetics of Wetting of Surfaces by Polymer Melts," J. Appl. Phys., 37 (1966), 4967.

(10) B. W. Cherry and C. M. Holmes, "Kinetics of Wetting of Surfaces by Polymers," J. Colloid Interf. Sci., 29 (1969), 174.

(11) S. Newman, "Kinetics of Wetting of Surfaces by Polymers; Capillary Flow," J. Colloid Interf. Sci., 26 (1968), 209.

(12) B. W. Cherry and S. El Muddaris, "Wetting Kinetics and the Strength of Adhesive Joints," J. Adhesion, 2 (1970), 193.

(13) P. C. Hiemenz, "Principles of Colloid and Surface Chemistry," Ch. 6, Marcel Dekker, Inc. (1977).

(14) J. Wilhelmy, Ann Physik, 119, 117 (1863).

(15) A. J. G. Allan, "Wilhelmy's Plate and Young's Equation," J. of Colloid Sci., 13, 273-274 (1958).

(16) A. M. Schwartz and Silvestre B. Tejada, "Studies of Dynamic Contact Angles on Solids," J. of Colloid Interf. Sci., 38, No. 2 (1972), 359.

(17) R. L. Bendure, "Dynamic Adhesion Tension Measurement," J. of Colloid Interf. Sci., 42, No. 1 (1973), 137.

(18) P. J. Sell, "Wetting Properties of Carbon Fibers," Umschau, 72 (13), (1972) 433.

(19) G. E. Hammer and L. T. Drzal, "Graphite Fiber Surface Analysis by X-Ray Photoelectron Spectroscopy and Polar/Dispersive Free Energy Analysis," Appl. of Surf. Sci., 4 (1980), 340-355.

(20) G. Mozzo and R. Chabord, "Contribution to the Study of Glass-Resin Adhesion," Proc. of the 23rd Ann. Tech. Conf. of SPI, 1968, Sec. 9-C.

(21) D. H. Kaelble, P. J. Dynes and E. H. Cirlin, "Interfacial Bonding and Environmental Stability of Polymer Matrix Composites," J. Adhesion, 6 (1974), 23.

(22) L. S. Penn and B. Miller, "A Study of the Primary Cause of Contact Angle Hysteresis on Some Polymeric Solids," J. of Colloid Interf. Sci., 78, No. 1 (1980), 238.

(23) G. D. M. DiSalvo, L. S. Penn, F. A. Bystry, "Silicone Fluids as Hydrophobic Sizing in Graphite/Epoxy Composites: Physiochemical Analysis," Symp. on Adv. in Polymer Composites I. The Interface Poly. Preprints for ACS Nat'l. Meeting, 22, No. 2, August 1981.

(24) D. H. Kaelble, "Interface Degradation Processes and Durability," Polym. Eng. and Sci., 17, No. 7, July 1977, 474.

(25) D. H. Kaelble and P. J. Dynes and L. Maus, "Surface Energy Analysis of Treated Graphite Fibers," J. Adhesion, 6, (1974) 239.

(26) D. H. Kaelble, "A Relationship Between the Fracture Mechanics and Surface Energetics Failure Criteria," J. of Appl. Polym. Sci., 18 (1974), 1869.

STRESS TRANSFER FROM MATRIX TO FIBER

When a tensile load is applied to an elastic matrix, the matrix will elongate to a value proportional to the load. However, if fiber with a higher elastic modulus is embedded in the matrix, the fiber will restrict the matrix from freely elongating in the region of the fiber. Shear stresses are produced on planes parallel to the axis of the fibers in the direction of this axis. The tensile stresses in the fiber are introduced by these interfacial shear stresses. These stress patterns can be identified and evaluated by birefringence techniques.[1,2]

A number of models have been proposed for calculating the longitudinal tensile stress distribution in an embedded fiber. The models of Cox,[3] Dow[4] and Rosen[5] considered the case of an elastic fiber in an elastic matrix. If the matrix deforms elastically, the interfacial shear stresses peak at a maximum value near the fiber ends and then decay rapidly toward the center length of the fiber. Conversely, the tensile stresses in the fiber will build to a maximum value provided that the fiber is sufficiently long. The tensile strain of the fiber and the tensile strain of the matrix are nearly equal in the mid-length.

When the load is applied to the fiber by shear stress at the interface, physically, at equilibrium, one must always have:

$$\frac{dP}{dx} = \pi \, d_f \, \tau_{x,r=\frac{1}{2}d_f} \qquad (20)$$

where

x = distance from end of fiber

P = tensile load in the fiber

d_f = diameter of the fiber

$\tau_{x,r=\frac{1}{2}d_f}$ = the shear stress evaluated at the fiber surface

Generally, $\tau_{x,r}$ in the matrix is a function of both x and r. The magnitude of the interfacial shear stress is largely dependent on the fiber content, on the magnitude of the applied load, and on the physical properties of the filament, matrix and interfacial bonds.

In order to obtain an expression for the shear stress, the following assumptions are made.(3-5)

1. Fiber and matrix both behave elastically.

2. Fiber is surrounded by a cylinder of matrix material.

3. The bond between fiber and matrix is perfect throughout any deformation.

4. Straight radial lines in the fiber and matrix remain straight lines after deformation.

The shear stress between fiber and matrix could then be expressed as follows: (3-5)

$$\tau_x = \frac{\lambda}{4}\left[\frac{P_{eff}}{\frac{A_m E_f}{E_m} + A_f}\right]\left[\frac{\sinh\left(\frac{\lambda}{d_f}\left[\frac{L}{2} - X\right]\right)}{\cosh\left(\frac{\lambda L}{2d_f}\right)}\right] \qquad 0 < X < \frac{L}{2} \qquad (21)$$

where:

$$\lambda = 2\sqrt{\frac{2\sqrt{2}\left(\frac{G_f}{E_f}\right)\left[1 + \frac{A_f}{A_m}\left(\frac{E_f}{E_m}\right)\right]}{(\sqrt{2}-1) + \left(\frac{G_f}{G_m}\right)\sqrt{\frac{A_m}{A_f} + 2 - \sqrt{2}}}} \qquad (22)$$

and

τ_x = interfacial shear stress between fiber and matrix in psi

A = cross-sectional area in in^2

E = Young's modulus in psi

G = shear modulus in psi

X = distance from end of fiber, in inches

d_f = diameter of fiber, in inches

L = effective length for load differential between fiber and matrix

$$P_{eff} = \sigma_a A_m \left(1 - \frac{E_m}{E_f} \right) \tag{23}$$

σ_a = applied field stress in psi

Subscripts:

f = fiber

m = matrix

Hence, the tensile load in the fiber at distance X is given by:(3-5)

$$P_f = P_{f,x=0} + \pi d_f \int_o^x \tau_x \, dx \tag{24}$$

Therefore, the tensile stress in the fiber at position X is obtained by integrating as follows:(3-5)

$$\sigma_f = \frac{P_{f,\ x=0}}{A_f} + \frac{\pi d_f}{A_f} \int_o^x \tau_{xy} dx' \tag{25}$$

$$= \sigma_a + \frac{\sigma_a \left(1 - \frac{E_m}{E_f} \right)}{\left(\frac{E_m}{E_f} + \frac{A_f}{A_m} \right)} \left[1 - \frac{\cosh\left(\frac{\lambda}{d_f} \left(\frac{L}{2} - x \right) \right)}{\cosh\left(\lambda \cdot \frac{L}{2d_f} \right)} \right]$$

$$= \sigma_a \cdot K \left[1 - \frac{\cosh\left(\frac{\lambda}{d_f} \left(\frac{L}{2} - x \right) \right)}{\cosh\left(\frac{\lambda L}{2d_f} \right)} \right]$$

where:

$$K = 1 + \frac{\left(1 - \frac{E_m}{E_f}\right)}{\left(\frac{E_m}{E_f} + \frac{A_f}{A_m}\right)} \qquad (26)$$

The transfer length required to build up a maximum stress equal to a fraction ϕ of the stress in an infinitely long fiber can also be calculated by the equation: (3-5)

$$\frac{\ell_c}{d_f} = \frac{1}{\lambda} \cosh^{-1}\left(\frac{1}{1-\phi}\right) \qquad (27)$$

and the load transfer pattern is demonstrated in Figure 22.

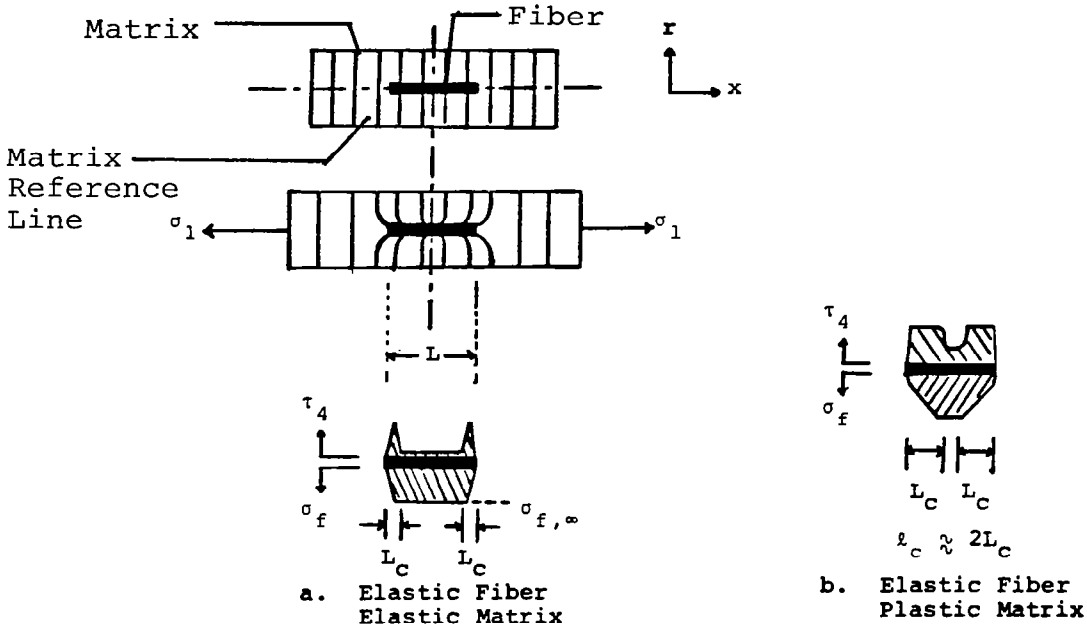

FIGURE 22. INTERFACIAL SHEAR STRESS PATTERNS FOR THE ELASTIC AND PLASTIC MATRIX CASES

From equation (21), one can see that a maximum shearing stress occurs at the ends of the fiber. When a high tensile load is applied, the shear stress is likely to exceed the yield stress of the matrix. If the matrix is unable to plastically deform, either the matrix fails or an interfacial slip occurs between the fiber and the matrix. If the matrix is able to deform, then the interfacial shear stress never rises above the yield shear strength of the matrix and equation (21) becomes irrelevant. Therefore, the plastic flow model of Kelly and Tyson[6] appears to be more appropriate.

In the case of a plastic matrix, a yield shear strength τ_y is constant throughout the deformation. Then one can obtain a tensile stress distribution in the fiber by integrating equation (20):(6)

$$P = \sigma_f \cdot A_f = \int_o^x \pi d_f \tau_y dx \qquad (28)$$

$$= \pi d_f \tau_y x$$

Equation (28) shows that the tensile load builds up linearly and a transfer length of the fiber is obtained.(6)

$$\frac{L_c}{d_f} = \frac{\sigma_f}{4\tau_y} \qquad (29)$$

or

$$\tau_y = \frac{\sigma_f d_f}{2\,\ell_c} \qquad (30)$$

where

σ_f = tensile strength of the fiber at transfer length

d_f = fiber diameter

τ_y = interfacial shear strength

L_c = critical length of the fiber required for load transfer from a fiber end

ℓ_c = critical fiber length required for load transfer, $\ell_c = 2L_c$

and the load transfer mechanism for the plastic deformable matrix is shown in Figure 22(b).

References to Stress Transfer

(1) L. B. Greszczuk, "Micromechanics Failure Criteria for Composites Subjected to Transverse Noarmal Loadking," AIAA Journal, 9, No. 7 (1971), 1274.

(2) A. Voloshin, "Stress Field Evaluation in Photoelastic Anisotropic Materials: Experimental Numerical Technique," J. Comp. Mat'l., 14 (1980), 342.

(3) H. L. Cox, "The Elasticity and Strength of Paper and Other Fibrous Materials," Brit. J. Appl. Phys., 3 (1952), 72.

(4) N. F. Dow, "Study of Stresses Near a Discontinuity in a Filament-Reinforced Composite Metal," General Electric Report TIS R635D61, AD-414673 (1963).

(5) B. W. Rosen, "Tensile Failure of Fibrous Composites," AIAA J., 2, No. 11 (1964), 1985.

(6) A. Kelly and W. R. Tyson, "Tensile Properties of Fibre-Reinforced Metals: Copper/Tungsten and Copper/Molybdenum," J. Mech. Phys. Solids, 13 (1965), 329.

METHODS FOR MEASURING INTERFACIAL BOND STRENGTH

Fiber Pullout Test

Broutman[1] developed the single filament fiber pullout test to measure the interfacial joint strength and interfacial frictional strength. A typical load-displacement curve resulting from such a test is shown in Figure 23. The geometry of the specimen for the fiber pullout test can either be a button-type sample as shown in Figure 24, or a fiber end of controlled length embedded into a bulk matrix as in Figure 25. The relationship which assumes the shear stress to be uniformly distributed along the interface is:

$$\tau = \frac{P_m}{2\pi r \ell} = \frac{\sigma_m r}{2\ell} \qquad (31)$$

where

τ = average shear strength of joint

P_m = maximum load applied to fiber

r = radius of fiber

ℓ = embedded fiber length

σ_m = maximum stress applied to fiber

The embedded fiber length is influenced by the fiber strength so that the maximum embedded length to be used is determined by:

$$\ell_{max} = \frac{\sigma_{ult} r}{2\tau} \qquad (32)$$

where

σ_{ult} = ultimated tensile strength of the fiber

The theoretical analysis of this test was performed by Lawrence[2] and Bartos[3] who concluded that this test was sensitive to interfacial adhesion properties.

However, this test is not applicable to carbon fiber/epoxy joint strength analysis because of the small diameter of the carbon fiber and the relatively high interfacial bond strength. Using the

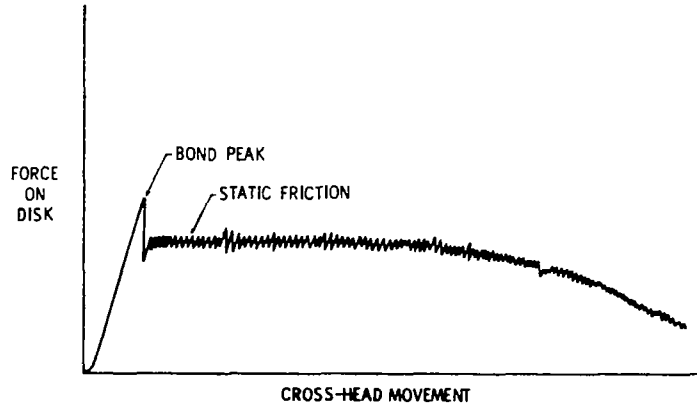

FIGURE 23. A TYPICAL LOAD-DISPLACEMENT CURVE FOR FIBER PULLOUT TEST*

*From Broutman (ref. 1)
Reproduced by permission.

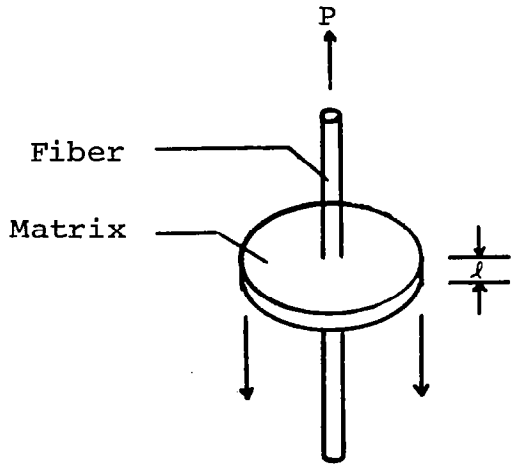

FIGURE 24. BUTTON-TYPE SPECIMEN FOR FIBER PULLOUT TEST

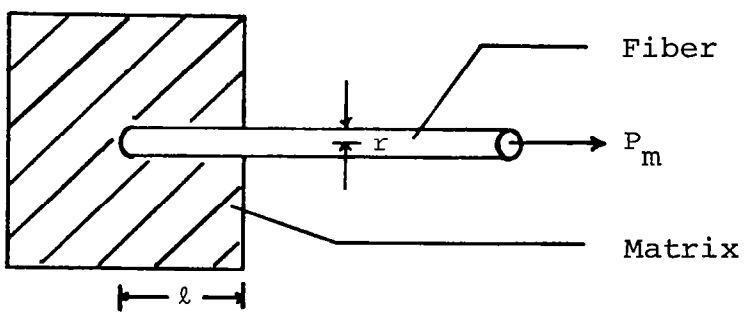

FIGURE 25. BLOCK-TYPE SPECIMEN FOR FIBER PULLOUT TEST

typical properties of carbon fiber shown in Table VIII, the maximum embedded length for carbon fiber/epoxy determined from equation (32) had to be less than 100μm (3.5 mils).

TABLE VIII. SOME TYPICAL PHYSICAL PROPERTIES OF A SINGLE FILAMENT CARBON FIBER

Tensile strength of carbon fiber at 2.54×10^{-2}m gauge length		
	σ_{ult} =	3241 MPa (470 ksi)
Diameter of carbon fiber, d	=	7×10^{-6}m (0.14 mil)
Interfacial shear strength, τ	≈	70 MPa (10 ksi)

Favre et al[4] attempted to use this technique to study the joint strength of carbon fiber in various thermoset matrix materials (epoxy, polyester and polyimide). A special fabrication technique was designed to provide a short embedded length. However, the thickness of the resin lozenge was difficult to control and large variations in the data were observed. Moreover, the critical embedment lengths of the fiber for each matrix were not determined. The critical embedment length could be determined by testing specimens with various embedded lengths and relating the fiber pullout force to the embedded length as shown in Figure 26. According to the authors, the joint strength of equation (31) should be calculated

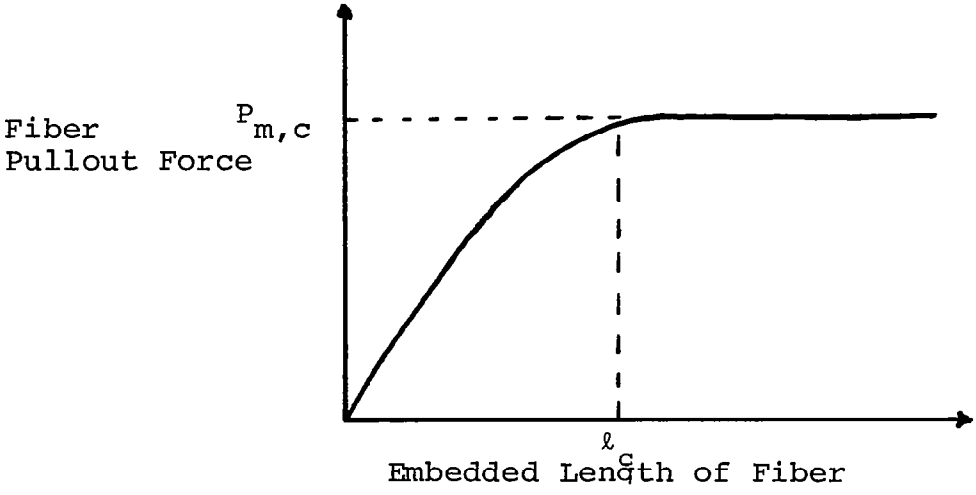

FIGURE 26. RELATIONSHIP OF RESIN LOZENGE THICKNESS TO FIBER PULLOUT FORCE

based on $P_{m,c}$ and ℓ_c as in equation (33).

$$\tau = \frac{P_{m,c}}{\pi d \ell_c} \tag{33}$$

where:

$P_{m,c}$ = fiber pullout force at maximum embedded length

ℓ_c = maximum embedded length which allows fiber pullout

This relation was not determined by Favre possibly because of the difficulties in controlling and fabricating ultrathin resin lozenges. Some of his data is shown in Tables IX and X.

TABLE IX. VALUES OF THE ADHESION STRENGTH σ_A FOR AS-RECEIVED FIBERS*

Fibre	Type	Modulus (GNm^{-2})	Matrix •	σ_A Nmm^{-2}
Courtaulds	HT (long staple)	270	Polyester A	5.4
			Polyester B	10.4
			Epoxy	9.7
			Polyimide	17.1
	HTS (continuous tow)	283	Epoxy	57.3
	HM (continuous tow)	330 (1st batch)	Epoxy	5.5
			Polyimide	12.8
		357 (2nd batch)	Epoxy	1.8
	HMS (continuous tow)	350	Epoxy	31.4
Morgan	II treated (sample)	240	Epoxy	41.9
Carbone-Lorraine	AG (short staple)	440	Epoxy	1.0
	AGT (continuous tow)	258	Epoxy	41.6
Columbia	CMR (sample)	42†	Epoxy	8.3

*Polyester A Rhodester 1108 (Rhône-Poulenc)
Polyester B Stratyl A.30 (St Gobain)
Epoxy Araldite LY 556 + HT 972 (CIBA)
Polyimide Kerimid 601 (Rhône-Poulenc)
†Manufacturer's data

*From Favre and Perrin (Ref. 4)
Reproduced by permission.

In Table IX,

$$\sigma_A = \frac{F}{\pi d \ell}$$

where

F = the force required for fiber pullout

d = diameter of the fiber

ℓ = thickness of the pastille

TABLE X. ADHESION STRENGTH OF TREATED FIBRES*
(Matrix: epoxy LY 556 + HT 972)

Fibre	Treatment	Modulus (GNm^{-2})	Tensile strength (GNm^{-2})	σ_A Nmm^{-2}
Courtaulds HT (long staple)	—	270	2.56	9.7
	benzene washing	270	2.56	7.8
	oxidation (nitric acid)	—	2.14	32.5
	oxidation (hypochlorite)	273.5	2.46	40.0
	oxidation (hot air)	—	1.96	40.5
	formation of silicon carbide	—	—	18.0
Courtaulds HM (continuous)	—	357	1.73	1.8
	oxidation (hypochlorite)	270 to 325	1.00 to 1.80	up to 26
	formation of silicon carbide	281.5	0.88	(70)
	reduction by wet hydrogen	259	1.04	3.8
	pyrolytic carbon coating -toluene	340	1.83	8.0
	-propylene	—	1.67	8.0 to 46

*From Favre and Perrin (Ref. 4)
Reproduced by permission.

Single Filament Shear Fracture Energy Test

Outwater and Murphy[5-7] developed a new test method to measure the debonding fracture energy between epoxy resin and single filament glass fibers. The authors considered an infinitely long fiber of diameter "d_f" and cross-sectional area "A_f" embedded in a semi-infinite solid as in Figure 27. Let P be the tensile load at the end of the fiber protruding a distance L from the surface of the resin and let the fiber be debonded a distance "x" into the matrix and G_{II} be the energy required to debond the fiber.

The strain energy, Ω_f in the filament is:

$$\Omega_f = \frac{P^2 L}{2AE_f} + \int_0^x \frac{(P-\tau\pi d_f x)^2}{2AE_f}\, dx \qquad (34)$$

where

τ = interfacial shear strength

E_f = Young's modulus of the fiber

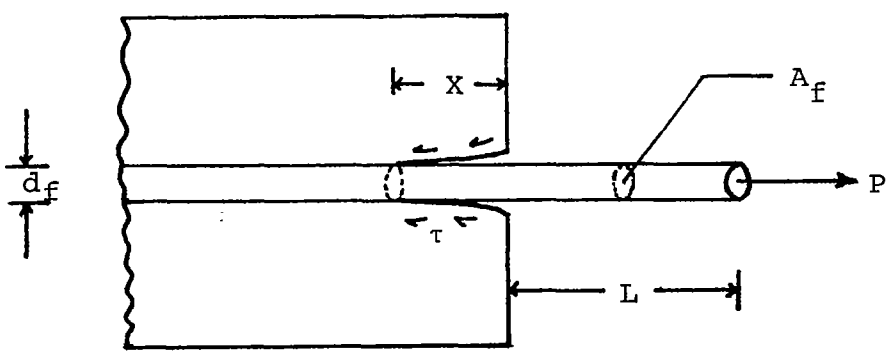

FIGURE 27. EMBEDDED SINGLE FIBER IN A SEMI-INFINITE SOLID UNDER TENSILE LOAD*

*From Outwater and Murphy (Ref. 5).
Reproduced by permission.

By equating the energy required to debond an incremental length, dx, $G_{II}\pi d_f dx$ and the strain energy released by an increment dx of debonding,

$$\frac{(P-\tau\pi d_f x)^2}{2AE_f}\,dx$$

where A = cross-sectional area, the following equation is obtained:

$$G_{II}\pi d_f = \frac{(P-\tau\pi d_f x)^2}{2AE_f} \tag{35}$$

Substituting for $P = \sigma \cdot A$, then

$$G_{II}\left(\frac{8E_f}{d_f}\right) = \left(\sigma - 4\tau\frac{x}{d_f}\right)^2 \tag{36}$$

where

σ = stress at the fiber end not embedded in resin

Directly pulling the fiber makes this measurement experimentally difficult. A modified technique is to embed the fiber in a resin block, severing the fiber at the center of the block and then loading the specimen in compression and observing the stress required to debond the fiber. A diagram of this method is shown in Figure 28. The G_{II} value was determined from:

$$G_{II} = \left[\left(\sigma_r \cdot \frac{E_f}{E_r}\right)^2 - \left(\frac{4\tau x}{d_f}\right)^2\right]\frac{d_f}{8E_f} \tag{37}$$

where

σ_r = applied stress

x = debonded length

and, for initial debonding, where x = 0, then

$$G_{II} = \frac{\varepsilon_r^2 E_f d_f}{8} \tag{38}$$

where

ε_r = compressive strain in the resin

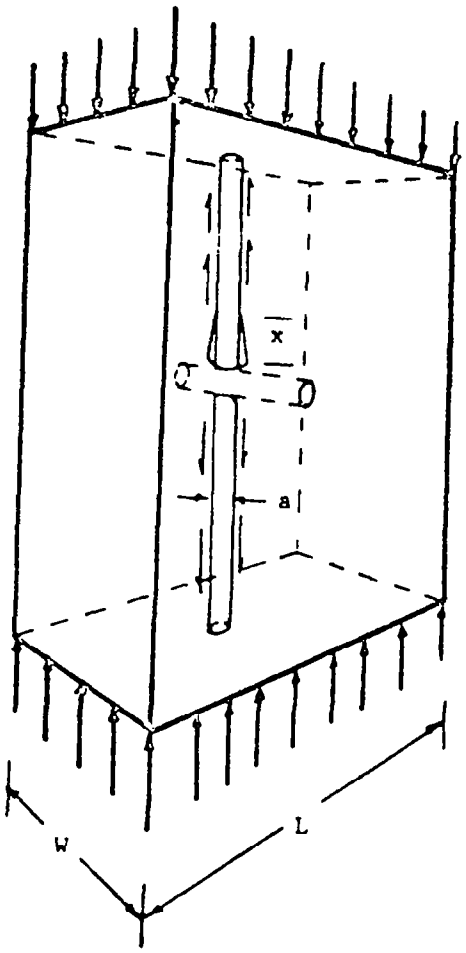

FIGURE 28. SPECIMEN FOR MEASURING THE DEBONDING ENERGY OF THE FIBER FROM THE SURROUNDING MATRIX*

*From Outwater and Murphy (Ref. 7).
Reproduced by permission.

The data obtained from this test for glass fibers in an epoxy matrix was conclusive. However, due to the small diameter and the brittle nature of the carbon fiber, this test is not applicable for a study of carbon fiber/epoxy adhesion properties. This test requires the observation of initial debonding during compression of the specimen and the small diameter of a carbon fiber makes the observation difficult if not impossible.

Single Filament Interfacial Shear and Transverse Tensile Debonding Strength Determination

Broutman[1,8,9] has also developed tests to characterize the interfacial shear debonding strength and interfacial transverse tensile strength. Interfacial shear strength is determined by embedding a single filament in the center of an epoxy casting as shown in Figure 29. Upon subjection to compression, the fiber

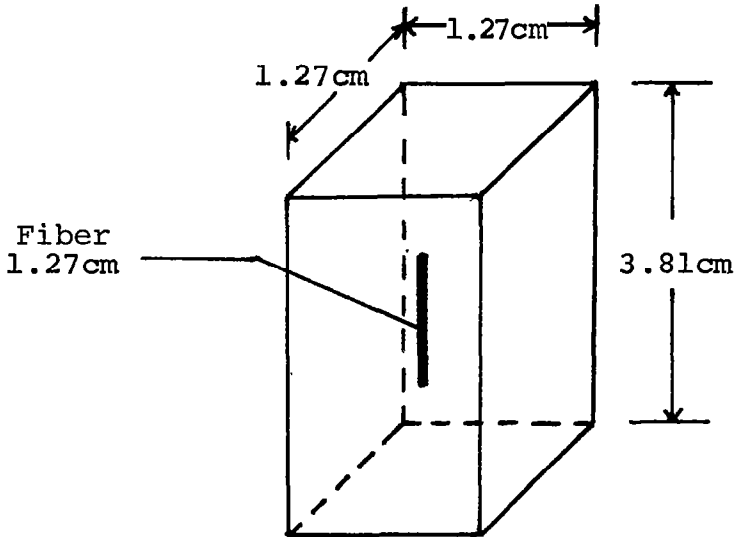

FIGURE 29. INTERFACIAL SHEAR STRENGTH SPECIMEN

will debond at the interface by shear. The shear stress can be determined from:

$$\tau = 2.5\sigma \qquad (39)$$

where

τ = interfacial shear stress

σ = axial compression stress in specimen

Interfacial transverse tensile strength was determined in a similar manner. The specimen for this test is shown in Figure 30.

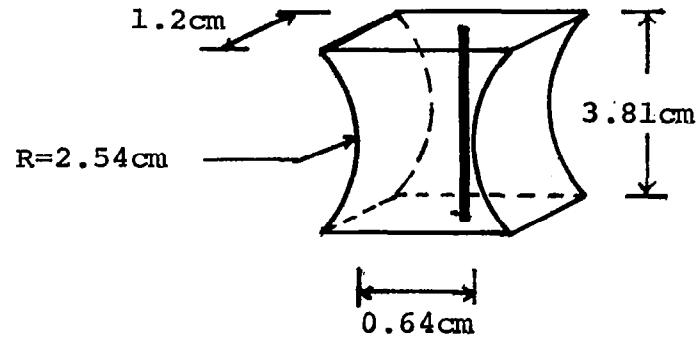

FIGURE 30. INTERFACIAL TRANSVERSE TENSILE STRENGTH SPECIMEN

Due to the curvature of the matrix and the difference in the Poisson's ratios of the fiber and the matrix, the fiber will debond at the interface through transverse tensile stress. This transverse tensile stress can be determined from:

$$S = - \frac{\sigma_m(\mu_m - \mu_f)E_f}{(1+\mu_m)E_f + (1-\mu_f-2\mu_f^2)E_m} \qquad (40)$$

where

S = transverse tensile stress

σ_m = axial compression stress on specimen

μ = Poisson's ratio

E = elastic modulus

Subscripts: f = fiber

m = matrix

These tests have been used to evaluate carbon fiber/epoxy adhesion properties by Hawthorne[10] and Mullin.[11] However, they both concluded that these tests were not applicable to carbon fibers due to the low compression strain of the carbon fibers. Compression fracture and local buckling occured prior to the debonding of the fiber.

Single Filament Critical Length Determination

The single filament critical length determination is an experimental technique derived from the load transfer analysis discussed under "Stress Transfer from Matrix to Fiber." Kelly[16] illustrated the multiple fracture phenomenon in a system consisting of tungsten wires embedded in a copper matrix. After deformation, the copper matrix was dissolved and the wire fragments extracted. On analysis of the fragment length distribution, it was found that its bounds were approximately ℓ_c and $\ell_c/2$; where ℓ_c was the critical fiber length and was determined from:

$$\ell_c = \frac{\sigma_f d_f}{2\tau_y} \tag{41}$$

where

σ_f = tensile strength of fiber at ℓ_c gauge length

d_f = diameter of fiber

τ_y = interfacial shear strength

Equation (41) is a rearrangement of equation (30). Recalling the definition of critical fiber length, this result is not unexpected. The longest fibers capable of surviving in this load situation will have a length just under ℓ_c; since longer fibers, by definition, must fracture.

Analogous experiments were run by Ongchin et al,[18] McGarry[19] and Fraser et al[12] for glass fibers in both thermoplastic and thermoset (epoxy) matrixes. Conclusive results were obtained. Wardsworth and Spilling,[17] Ishikawa et al[13] and Drzal et al[14,15] applied this technique to carbon fiber in an epoxy matrix.

Drzal[14] embedded a single filament of carbon fiber into an ASTM two-and-one-half inch length epoxy casting as in Figure 31. These specimens were then subjected to a tensile deformation. The schematic of the fiber fracture and stress distribution is presented in Figure 32 (taken from Ref. 14). Figures 33 and 34 show the transmitted polarized light micrographs of a non-surface treated (fiber A) and a surface treated (fiber B) fiber during tensile deformation and their corresponding shear strength data are presented in Table XI. The effect of carbon fiber surface treatments on adhesion is shown clearly by the histogram of the aspect ratios of the two types of fibers in Figure 35.

In addition, the failure mechanisms during debonding can also be observed and characterized.[15] The epoxy sized carbon fiber promoted a higher interfacial bond strength. The higher joint strength created matrix cracking after fiber fracture whereas no matrix cracking was observed with the non-surface treated, unsized fiber and the surface treated, unsized fiber.

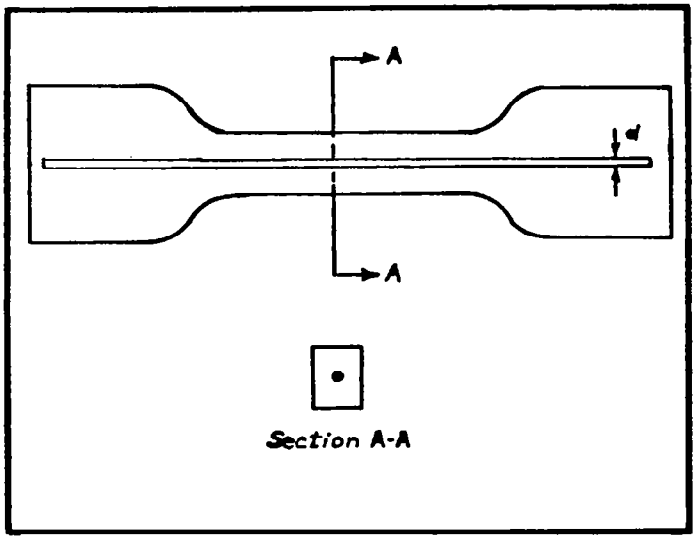

FIGURE 31. SCHEMATIC DIAGRAM OF SINGLE FIBER INTERFACIAL SHEAR STRENGTH SPECIMEN*

*From Drzal et al (Ref. 14).
Reproduced by permission.

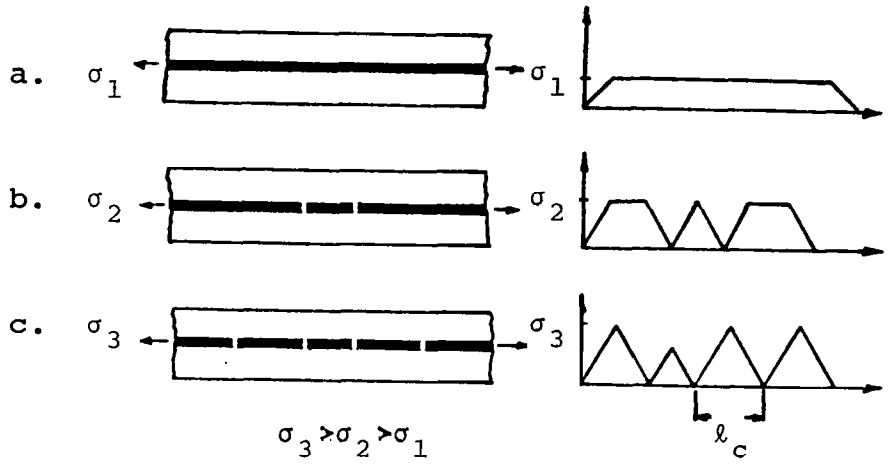

a. At low initial stress values

b. After fiber flaws and defects have broken.

c. After critical length has been reached.

FIGURE 32. FIBER FRACTURE AND STRESS DISTRIBUTION*

*From Drzal et al (Ref. 14).
Reproduced by permission

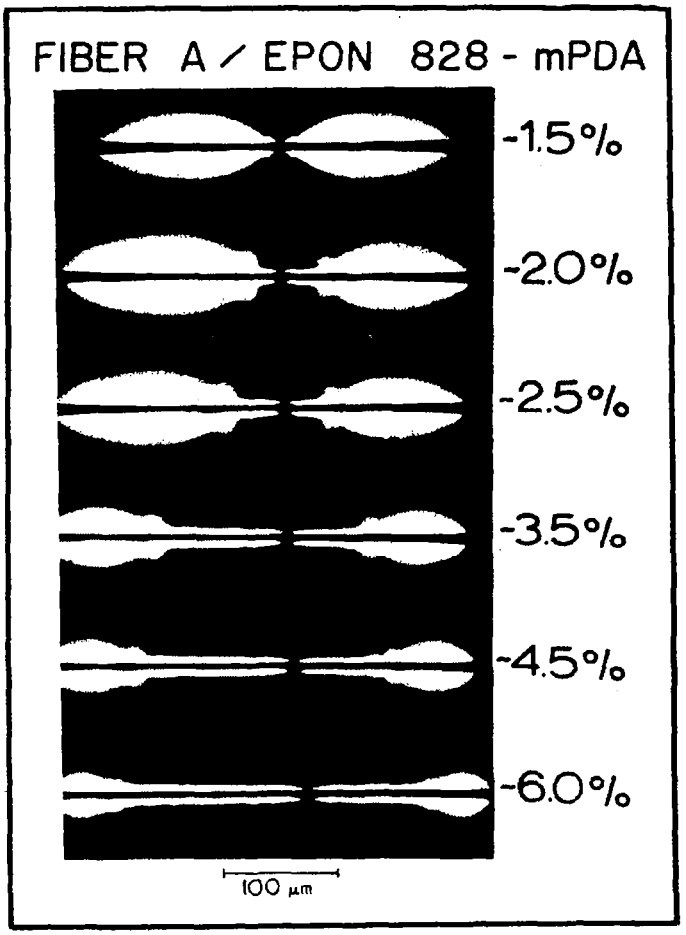

FIGURE 33. TRANSMITTED POLARIZED LIGHT MICROGRAPH OF A TYPICAL FIBER A FRACTURE AS A FUNCTION OF INCREASING STRAIN*

*From Drzal et al (Ref. 14).
Reproduced by permission.

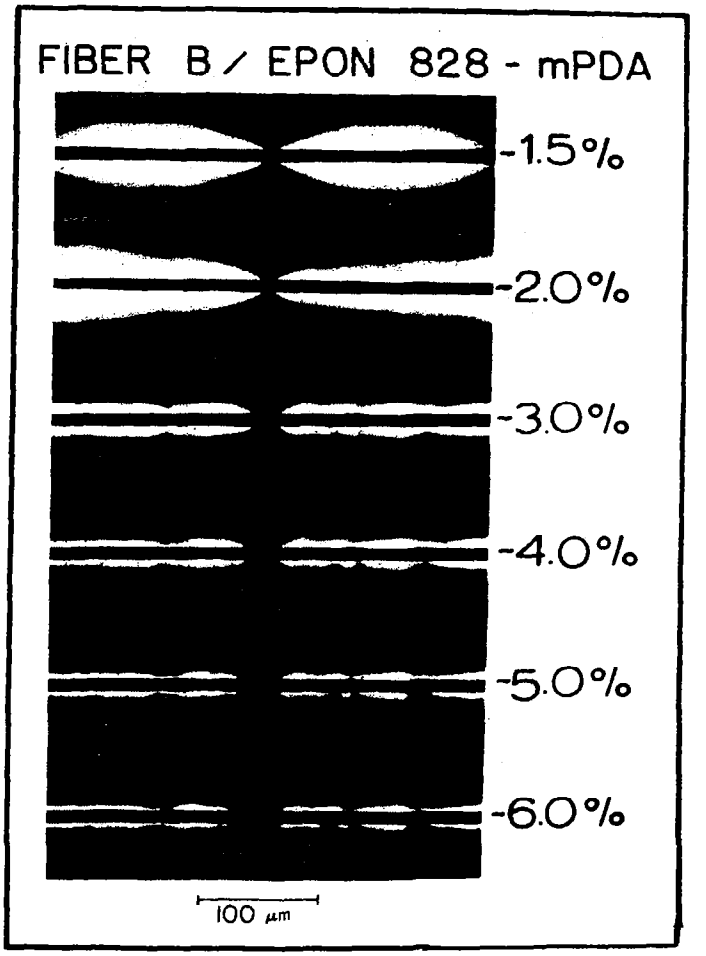

FIGURE 34. TRANSMITTED POLARIZED LIGHT MICROGRAPH OF A TYPICAL FIBER B FRACTURE AS A FUNCTION OF INCREASING STRAIN*.

*From Drzal et al (Ref. 14).
Reproduced by permission.

TABLE XI. SINGLE FILAMENT INTERFACIAL SHEAR STRENGTH OF FIBER A(1) AND FIBER B(2)*

	Fiber A(1)	Fiber B(2)
Total Specimens	15	23
Total Fragments	669	485
Weibull α (eqn. 3)	3.074	3.308
Weibull β (eqn. 4)	48.50	109.05
Fiber Tensile Strength (1" gage length)	2959 MPa (429,000 psi)	2614 MPa (379,000 psi)
E828/mPDA Yield Strength	40 MPa (5,800 psi)	40 MPa (5,800 psi)
Interfacial Shear Strength (τ) (eqn. 1)	40.86±26.21 MPa (5,925±3800 psi)	15.6±8.89 MPa (2,262±1290 psi)

(1) As-1--surface treated carbon fiber, unsized.
(2) AU-1--virgin carbon fiber with no surface treatment and unsized.

*From Drzal et al (Ref 14).
Reproduced by permission.

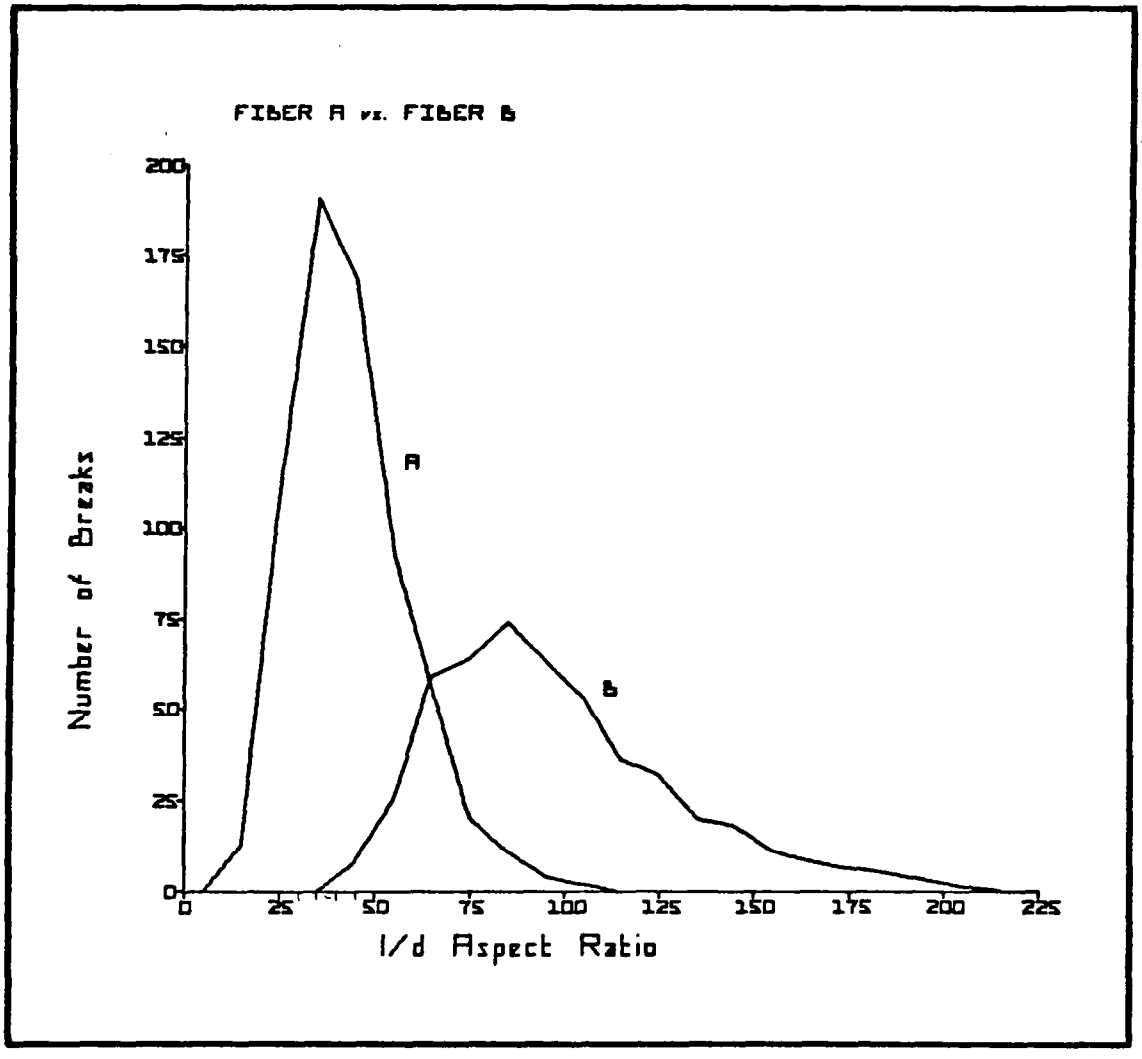

Total number of breaks as a function of length to diameter ratio.

FIGURE 35. HISTOGRAMS OF ASPECT RATIOS FOR FIBER A AND B*

*From Drzal et al (Ref. 14).
Reproduced by permission.

Overall, this test has shown some conclusive results and provided much information on the characterization of fiber/matrix adhesion. This technique has been adapted by the author to further study the effect of interphase properties on carbon fibers epoxy adhesion.

Microdebonding Test

Mandell and McGarry[20] developed a microdebonding test for in-situ measurement of fiber/matrix bond strength in fiber composites. The test involved the compressive loading of a fiber on a polished specimen surface to produce debonding as shown in Figure 36. Glass, aramid and carbon fibers in epoxy composites have been tested. Initial results of these evaluations, especially glass, on unconditioned and moisture conditioned samples were promising. For carbon fiber, experimental difficulties were encountered due to the skin-core properties of the fiber. Refinements to simplify interpretation of the debonding force in terms of interfacial shear strength and improvement on the apparatus were required in order to make the test more reproducible for carbon fibers.

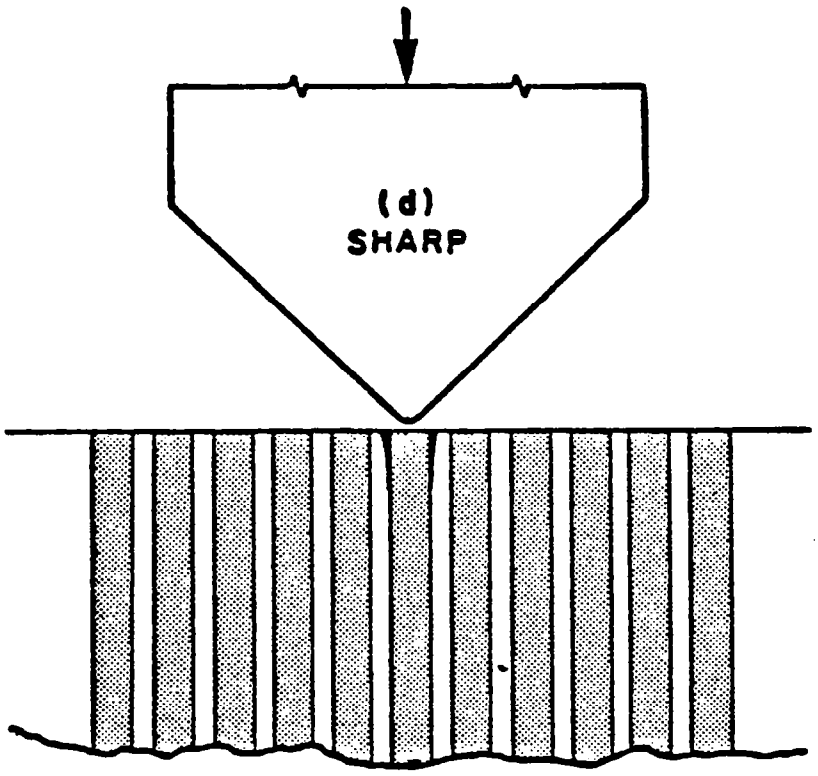

FIGURE 36. MICRODEBONDING TEST*

*From Mandell and McGarry (Ref. 20)
Reproduced by permission.

References to Methods for Measuring Interfacial Bond Strength

(1) L. J. Broutman, "Measurement of the Fiber-Polymer Matrix Interfacial Strength," Interfaces in Composite, ASTM STP 452 (1969), 27.

(2) P. Lawrence, "Some Theoretical Considerations of Fibre Pull-Out from an Elastic Matrix," J. of Mat'l. Sci., 7 (1972), 1.

(3) P. Bartoš, "Analysis of Pull-Out Tests on Fibres Embedded in Brittle Matrices," J. of Mat'l. Sci., 15 (1980), 3122.

(4) J. P. Favre, J. Perrin, "Carbon Fiber Adhesion to Organic Matrices," J. of Mat'l. Sci., 7 (1972), 1113.

(5) J. O. Outwater and M. C. Murphy, "On the Fracture Energy of Unidirectional Laminates," Proc. of the 24th Ann. Tech. Conf., SPI, Sec. 11-C, 1 (1969).

(6) J. O. Outwater and M. C. Murphy, "Fracture Energy of Unidirectional Laminates," Modern Plastics, Sept. (1970), 160.

(7) J. O. Outwater and M. C. Murphy, "The Influences of Environment and Glass Finishes on the Fracture Energy of Glass-Epoxy Joints," Proc. of the 25th Ann. Tech. Conf., SPI, Sec. 16-D, 1 (1970).

(8) L. J. Broutman, "Mechanical Requirements of the Fiber-Matrix Interface," Proc. of the 25th Ann. Tech. Conf., SPI, Sec. 13-B, 1 (1970).

(9) L. J. Broutman, "Glass-Resin Joint Strengths and Their Effect on Failure Mechanisms in Reinforced Plastics," Polym. Eng. and Sci., 6, July (1966), 263.

(10) H. M. Hawthorne and E. Teghtsoonian, "Graphite Fibre-Epoxy Matrix Interface Interactions," J. Adhesion, 6 (1974), 85.

(11) J. V. Mullin and V. F. Mazzio, "The Effects of Matrix and Interface Modification on Local Fractures of Carbon Fibers in Epoxy," J. Mech. Phys. Solids, 20 (1972), 391.

(12) W. A. Fraser, F. H. Achker and A. T. DiBenedetto, "A Computer Modeled Single Filament Technique for Measuring Coupling and Sizing Agent Effects in Fiber Reinforced Composites," Proc. of the 30th Ann. Tech. Conf. of SPI, Sec. 22-A (1975), 1.

(13) M. Ishikawa, I. Narisawa and H. Ogawa, Faculty of Engineering, Yamagata University, "A Study on the Interlaminar Shear Fracture in Carbon Fiber Composites,"

(14) L. T. Drzal, M. J. Rich, J. D. Camping, W. J. Park, "Interfacial Shear Strength and Failure Mechanisms in Graphite Fiber Composites," Proc. of the 35th Ann. Tech. Conf. of SPI, Sec. 20-C, 1 (1980).

(15) L. T. Drzal, M. J. Rich and D. L. Hall, "Structure-Property Relationships at the Composite Interphase," 15th Biennial Conference on Carbon, Amer. Carbon Society, June (1981).

(16) A. Kelly, "The Strengthening of Metals by Dispersed Particles," Proc. Roy. Soc., London, 19282, 63 (1964).

(17) N. J. Wadsworth and I. Spilling, "Load Transfer from Broken Fibers in Composite Materials," Brit. J. Appl. Phys., Ser. 2, 1 (1968), 1049.

(18) L. Ongchin, W. K. Olender and F. H. Ancker, "Fiber Matrix Adhesion and the Fracture Behavior of Glass Reinforced High Density Polyethylene," Proc. of the 27th Ann. Tech. Conf. of SPI, Sec. 11-A (1972).

(19) F. J. McGarry and M. Fujiwara, "Resin-fiber Load Transfer in Reinforced Plastics," Modern Plastics, 143, July (1968).

(20) J. F. Mandell and F. J. McGarry, "Microdebonding Test for in-situ Bond Strength Measurement," Summary of Presentation at the 3rd Annual Army Composites Research Review, Oct (1980).

EXPERIMENTAL

INTRODUCTION

After reviewing the information available in the literature, it is apparent that little effort has been spent on the correlation of theoretical analyses with experimentally determined composite properties; and there is limited evidence that the nature of the interphase can be used to optimize composite properties. In order to clarify some of these uncertain areas, the following experiments were designed to examine the relationship between wetting and interfacial shear strength. Also, various finish variants were formulated to demonstrate the effect of interphase properties on composite performance.

MATRIX RESIN

For carbon fiber composites, diglycidyl ether of bisphenol A (DGEBA) epoxies are commonly used in the matrix resin. In order to have a typical matrix that is suitable for both critical length determination and composite fabrication, system "F" was formulated for the evaluations reported herein. This resin is prepared by mixing 100 parts of Epi-Res 508* and 22.5 parts of Epi-Pure 841.* A unique feature of this system is its high tensile elongation-to-break value of 8%. A cure schedule of two hours at 93°C was used combined with a post-cure at 150°C for two hours. The tensile properties of system "F" castings, evaluated at different cure schedules, are shown in Table XII. This high elongation-to-break property of system "F" allows multiple fracture of the embedded fiber without matrix failure which enables critical length determination. Some of the other properties obtained from castings of system "F" are presented in Table XIII.

Finish Variants

To study the effect of fiber/matrix interphase on composite performance, four finish variants were developed and applied to Celion® 6000 (C-6K) unsized fiber. These four variants are:

1. C-6K/SR - RTV 615**silicone rubber
2. C-6K/FRE 25 - An organophosphazene***elastomer blended with Epon 828 at 25 parts elastomer to 100 parts epoxy

---

* Product of Celanese Plastics and Specialties Co., Louisville, Ky.
** Product of General Electric Co.
***Product of Firestone Co.

TABLE XII. TENSILE PROPERTIES OF SYSTEM "F" AT VARIOUS CURE SCHEDULES

Composition:

EPI-RES	508*	100	parts by weight
EPI-CURE	841*	22.5	parts by weight

Sample	Cure Schedule Time (Hr)	Cure Schedule Temp (°C)	Post Cure Time (Hr)	Post Cure Temp (°C)	Tensile Strength MPa	Tensile Strength ksi	Tensile Modulus GPa	Tensile Modulus Msi	Elongation-to break %
1	2	85	2	150	82.1	11.9	3.02	0.44	5.56
2	2	85	3	150	79.3	11.5	2.92	0.42	5.22
3	2	85	4	150	82.1	11.9	2.90	0.42	5.77
4	2	85	2	160	84.8	12.3	2.97	0.43	6.78
5	2	85	2	170	79.3	11.5	2.87	0.42	5.36
6	2	85	2	180	77.2	11.2	2.88	0.42	3.20
7	2	93	2	150	92.4	13.4	3.15	0.46	7.99
8	2	93	3	150	89.0	12.9	3.01	0.44	5.89
9	2	93	4	150	91.7	13.3	2.93	0.43	7.60
10	2	93	2	160	80.0	11.6	2.93	0.43	5.75
11	2	93	2	180	80.0	11.6	2.88	0.42	5.55

*Celanese Plastics and Specialties Co.

TABLE XIII. RESIN CASTING PROPERTIES OF SYSTEM "F"*

	Tensile Strength MPa	Tensile Strength ksi	Tensile Modulus GPa	Tensile Modulus Msi	Elongation-to break %	Flexural Strength MPa	Flexural Strength ksi	Flexural Modulus GPa	Flexural Modulus Msi
RT	92.4	13.4	3.15	0.456	7.99	102.8	14.9	2.90	0.420
121°C	39.3	5.7	1.93	0.280	9.71	72.4	10.5	2.01	0.292
3 Day H_2O boil, tested at RT						97.2	14.1	2.60	0.377

Transition Temperature Determined by TMA:

Initial T_g = 176°C
After 3 day H_2O Boil = 142°C
After 7 day H_2O Boil = 143°C

Heat Deflection Temperature = 155°C
[@ 1.82 MPa (264 psi)]

Notched Izod = 58.7 J/m of notch
(1.10 ft-lbs/in of notch)

*Composition: Epi-Res 508, 100 parts by weight
Epi-Cure 841, 22.5 parts by weight

Cure Schedule: 2 hours @ 93°C
2 hours @ 150°C

3. C-6K/ETP 10 - An epoxy-thermoplastic blend (in-house developed material) with 10 parts thermoplastic in 100 parts epoxy.

4. C-6K/ETP 50 - Same as item 3 except this consisted of 50 parts thermoplastic in 100 parts epoxy.

Silicone rubber (a prepolymer) was dissolved in n-hexane, then the curing agent was added to the solution before sizing. The silicone rubber was mixed at a ratio of 10 parts silicone rubber prepolymer to 1 part curing agent.

The FRE 25 sizing solution was prepared by dissolving the organophosphazene prepolymer in acetone. Then, Epon 828 was added in the ratio of 25 parts elastomer to 100 parts epoxy. Just before sizing, 1% by weight of the elastomer of Esperox 10 (t-butyl perbenzoate) was added to the solution. This organoperoxide was used as a curing agent for the organophosphazine elastomer.

ETP 50 and ETP 10 were dissolved in acetone and the concentration of all the sizing solutions were adjusted together with the sizing speed to allow approximately 1% by weight pickup by the fibers.

Silicone rubber was selected to demonstrate the effect of a very soft interphase together with a weak interfacial joint strength. FRE 25 was used to illustrate the effect of a second, soft and dispersed phase at the interphase. Organophosphazene was selected because of its high temperature performance combined with a relatively high strength for an elastomeric material; it is also tough and is compatible with epoxy resins. The purpose of the polyblend material is to maintain the strength at the interface while the elastomeric material is damping the impact and/or blunting crack tips to enhance toughness.

The same principles were applied in the selection of the thermoplastic-epoxy blend, ETP 10 and ETP 50. The only difference is that the thermoplastic epoxy blends provide higher modulus as well as strength. The difference in concentrations is to provide stepwise increases in modulus and strength at the interphase.

Although the properties of the finish variants were not characterized due to many unsuccessful attempts to make castings from these materials, it is estimated that the moduli of the interphases should be in the following order:

ETP 10 > ETP 50 > FRE 25 > SR

EXPERIMENTAL RESULTS AND DISCUSSION

Wetting Force Measurement

The Wilhelmy micro-balance wetting force technique was used to characterize the surface of carbon fibers. A micro-computer was used to control the wetting experiment as well as to carry out the data processing. The details of the apparatus construction are discussed in Appendix B and the program developed by the authors for an HP-85A micro-computer is attached in Appendix C.

To characterize the surface energetics of the carbon fiber, double distilled water was used initially. A very careful cleaning procedure for the glassware which contains the wetting liquid was required so that the surface tension of the contained water approaches 72.4×10^{-3} N/m. This vigorous cleaning process is detailed in Appendix D. By employing this cleaning process, a consistent 72.3×10^{-3} N/m $\pm$ 1×10^{-4} N/m surface tension for water was measured. Contact angles for unsized fibers were measured successfully with water as the wetting liquid. However, when the fibers contained finish, misleading wetting forces were obtained. This is primarily due to the finish slowly dissolving into and contaminating the water. As a consequence, a significant drop in surface tension of the water took place. This caused the wetting force to drop during the experiment. Some of these results are listed in Table XIV. The large scatter of data within each region with little or no hysteresis effects indicates that the surface tension of the wetting liquid was changing during the experiment. The surface tension of the water dropped as much as 5×10^{-3} N/m after experiments were conducted.

Under this condition, water, as well as other commonly used liquids with known surface tension are not applicable for this study because of the contamination/dilution process. Nevertheless, in order to understand the wetting behavior and to prescribe the optimum prepregging condition, a major component of the matrix resin should be used as the wetting liquid. Although contamination by finish from the sized fiber still continues, this is representative of the prepregging process. A DGEBA epoxy resin, Epi-Res 508, was selected to be the wetting liquid. Epi-Res 508 was chosen because of its relatively low viscosity and it is the major component of the matrix used in this study. A viscosity-temperature profile of Epi-Res 508 was determined in a Brookfield viscometer and is shown in Figure 37. An insulated clean beaker was used to contain and to maintain the resin at approximately 70°C. At this temperature, a reasonable low viscosity, 0.16 Pa (160 cps) was obtained and no significant dynamic wetting phenomenon was observed. The wetting force data obtained for a series of fibers and finishes are shown in Table XV.

Comparing the data in Table XV, the effect of finish variants on wetting behavior was demonstrated. The receding angles of all the samples are all similarly high suggesting that, once the fibers

TABLE XIV. WETTING FORCE MEASUREMENTS OF CARBON FIBERS WITH WATER AT 23°C

Sample	Advancing, μg (contact angle, θ_a)	Equilibrium, μg (contact angle, θ)	Receding, μg (contact angle, θ_r)
C-6KU[1]	82.3 ± 5.5 (60° ± 2.3°)	89.4 ± 7.2 (57° ± 3°)	97.5 ± 9.7 (53° ± 4.3°)
AS-1[2]	81.7 ± 7.5 (61° ± 3°)	91.3 ± 9.8 (57° ± 4°)	108.0 ± 8.0 (50° ± 3.3°)
C-6KE[3]	44.2 ± 14.6	41.8 ± 24.0	63.5 ± 10.0
T-6300[4]	90.9 ± 18.3	91.3 ± 23.3	100.4 ± 21.4

(1) Celion® 6000 unsized carbon fiber.
(2) Hercules AS-1 unsized carbon fiber.
(3) Celion® 6000 standard epoxy compatible sized fiber, commercial product.
(4) Thornel T-6300 standard commercial sized fiber.

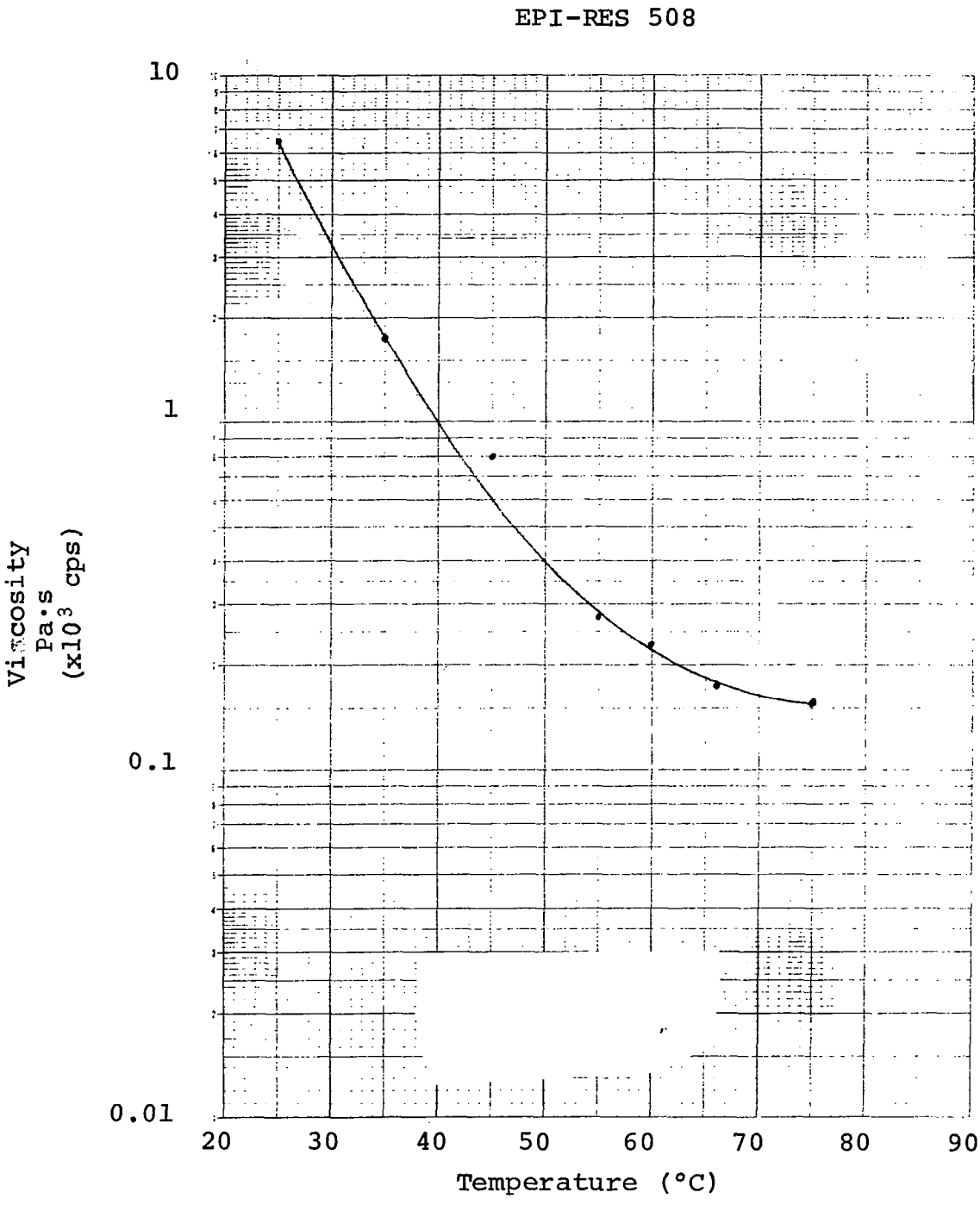

FIGURE 37. VISCOSITY-TEMPERATURE PROFILE OF EPI-RES 508 EPOXY RESIN MEASURED BY A BROOKFIELD VISCOMETER WITH SPINDLES NO. 1 AND 2.

TABLE XV. WETTING FORCE MEASUREMENTS OF CARBON FIBERS WITH EPI-RES 508 RESIN AT 70°C

Sample	Advancing, μg	Equilibrium, μg	Receding, μg
T-6300[1]	72.8 ± 27.6	95.6 ± 18.5	103.8 ± 20.2
AS-1[2]	57.2 ± 10.6	74.4 ± 5.4	87.2 ± 7.8
C-6KV[3]	67.0 ± 11.3	80.2 ± 9.9	92.2 ± 14.9
C-6KU[4]	75.6 ± 19.4	83.2 ± 19.5	88.6 ± 20.9
C-6KE[5]	55.8 ± 19.5	91.4 ± 13.3	102.4 ± 12.9
C-6K/ETP 50[6]	107.4 ± 28.4	127.2 ± 29.4	135.0 ± 29.1
C-6K/ETP 10[7]	86.0 ± 40.0	103.0 ± 39.0	109.0 ± 43.0
C-6K/FRE 25[8]	71.7 ± 10.7	82.0 ± 12.6	90.2 ± 14.9
C-6K/SR[9]	-1.6 ± 18.2	50.6 ± 4.1	99.8 ± 48.2

Note: All carbon fibers were surface treated except C-6KV.

(1) Thornel standard sized 6000 filament per tow carbon fiber.
(2) Hercules unsized carbon fiber.
(3) Celion® 6000 virgin fibers--no surface treatment and unsized.
(4) Celion® 6000 unsized carbon fiber.
(5) Celion® 6000 standard epoxy compatible size, commercial product.
(6) Celion® 6000 sized with finish variant ETP 50.
(7) Celion® 6000 sized with finish variant ETP 10.
(8) Celion® 6000 sized with finish variant FRE 25.
(9) Celion® 6000 sized with finish variant SR.

are "wetted," there is little or no rearrangement of the resin film on the surface of the fiber. However, in the advancing measurements, large variations are observed. This suggests that some finish variants have better compatibility with the matrix resin and can be wetted easier. For example, silicone rubber coated Celion® 6000 showed the lowest wetting force (negative) which indicates that, in order to wet this surface, additional external forces are needed to forcibly wet it. This will most likely also result in poor adhesion.

On the other hand, the finish variant ETP50 showed the highest advancing wetting force which suggests that the resin is highly compatible with this surface and it will probably translate to good interfacial adhesion. Furthermore, with a high advancing wetting force fiber, better quality prepreg is likely, due to the minimization of trapped air at the interface by rapid advancement of the wetting liquid/resin. In other words, improved laminate properties are anticipated.

Single Filament Adhesion Test

As previously discussed, the single filament critical length determination was identified to be one of the better methods for characterization of carbon fiber/epoxy interfacial bond strength. Recall the load transfer mechanism, wherein the critical length, ℓ_c is determined by equation (41):

$$\ell_c = \frac{\sigma_f \, d_f}{2\tau_y} \qquad (41)$$

where

σ_f is the tensile strength of the fiber at critical length

d_f is the diameter of the fiber

τ_y is the interfacial shear strength

By determining σ_f and measuring ℓ_c and d_f, the interfacial shear strength, τ_y can be obtained as already stated by rearranging equation (41) to the form shown for equation (30):

$$\tau_y = \frac{\sigma_f \, d_f}{2\ell_c} \qquad (30)$$

The critical length and the diameter of the fiber can be measured optically by embedding a single filament in an epoxy matrix and stressing the specimen to a strain value such that no additional fracture can be obtained with additional stress. However, to obtain the tensile strength of carbon fiber at the critical length is itself an involved task. Carbon fiber strength is sensitive to gauge length and the critical length of carbon fiber is too small to experimentally test in a reliable manner. Nevertheless, it was shown[1] that a linear relationship can be obtained by plotting single filament tensile strength versus the logarithm of gauge lengths. The test method is described in Appendix E.

Gauge lengths of 7.62 cm (3-inch), 2.54 cm (1-inch), 1.27 cm (½-inch), 0.635 cm (¼-inch) and 0.254 cm (1/10-inch) were tested for each fiber type and finish variant and best fit straight lines were obtained from these five data points for each variant. These straight lines were then extrapolated to the critical length and the tensile strengths were obtained. The results of these gauge length studies are presented in Appendix F.

To perform the adhesion test, a single filament of carbon fiber was aligned in the center of an ASTM 6.35 cm (2½ inch) dogbone epoxy casting. The dimensions of the dogbone specimens are 0.32 cm (1/8 inch) wide x 0.16 cm (1/16 inch) deep with a 2.54 cm (1 inch) long gauge section. Fabrication of the specimen and alignment of the fiber was accomplished with the aid of an RTV-630* silicone rubber mold. A silicone rubber mold was used because of the ease in making a flexible mold cavity by casting the rubber around standard ASTM injection-molded dogbone specimens. Moreover, the use of silicone rubber molds also prevents fiber surface contamination because they do not require the application of mold release agents.

Sprue spots were cut precisely in the center of each end for each dogbone to a depth of 0.08 cm (1/32 inch) to align and secure each fiber to be embedded. Once the fiber was aligned, a drop of rubber cement was used to hold it in place. During the fiber selection, mounting and the application of rubber cement, the section of the fibers placed in the mold cavity were not handled nor contaminated.

After the rubber cement was set, system "F" resin was introduced with an eye dropper into the cavity. Extreme care was exercised to prevent damaging and/or mis-aligning the fiber. Then the whole was degassed in a vacuum oven and cured according to the schedule previously described.

Since system "F" is an amber transparent solid, visual and microscopic evaluation of the fiber and the critical length can be performed with ease. Furthermore, system "F" also exhibits photoelastic properties which can be used to evaluate the stress patterns at the interphase.

*General Electric Co., Silicon Rubber Dept., Waterford, NY.

To apply this test to the above mentioned specimen, a special tensile fixture was designed and mounted onto a stage micrometer for a Leitz ortholux optical microscope. Long working distance objectives and polarizing condensers were used. The details of the design for the tensile fixture are presented in Appendix G.

To carry out this study, the specimen was initially examined for fiber alignment, breakage and residual stress. Due to the low cure and post cure temperatures employed with this system, together with a slow cool down rate, no apparent residual stresses were observed in the samples. The specimen was then stressed to different strain values at approximately 0.5% intervals and at each strain level, the number of the broken segments was counted. When this number remains constant with increasing strain, the critical length of the fiber is reached. This test was repeated on at least ten specimens for each fiber type/finish variant and the cumulative fiber lengths were used to determine the critical length.

Once the segment lengths of the fibers were obtained, a statistical approach to determine the critical length of the fiber was used. According to Drzal et al,[2] these data sets fit the two parameter Weibull distribution quite well.

$$F(X) = 1 - \exp\left\{-\left(\frac{X}{\beta}\right)^{\alpha}\right\} \quad \text{for } X > o \tag{42}$$

where

X is the aspect ratio, ℓ_c/d_f

α is the shape parameter

β is the scale parameter

The maximum likelihood methods were employed to estimate the parameters of the Weibull distribution. These parameters are solutions to

$$\frac{\sum_{i=1}^{n}\left(X_i\right)^{\alpha} \ell_n\left(X_i\right)}{\sum_{i=1}^{n}\left(X_i\right)^{\alpha}} - \frac{1}{\alpha} - \frac{\sum_{i=1}^{n} \ell_n\left(X_i\right)}{n} = 0 \tag{43}$$

$$\beta = \left\{\frac{1}{n} \sum_{i=1}^{n}\left(X_i\right)^{\alpha}\right\}^{1/\alpha} \tag{44}$$

A computer program was developed to evaluate these two parameters, α, β, numerically, these were then used to calculate the shear strength and the listing is attached in Appendix H. The mean and the variance of the interfacial shear strength were then obtained from

$$\bar{\tau} = \frac{\alpha_f}{2\beta} \Gamma\left(1 - \frac{1}{\alpha}\right) \tag{45}$$

and

$$VAR(\tau) = \frac{\sigma_f^2}{4\beta^2}\left\{\Gamma\left(1-\frac{2}{\alpha}\right) - \Gamma^2\left(1-\frac{1}{\alpha}\right)\right\} \tag{46}$$

where

Γ is the Gamma function

Another program was also developed to plot the cumulative function and the population density function (histogram) of the critical aspect ratio for each fiber type/finish variant. This program is also listed in Appendix I.

The results of the interfacial bond strength determinations for the different fiber types/finish variants are listed in Table XVI and the histograms of the critical aspect ratios are shown in Figures 38 through 46. The results clearly indicate that the surface treatment improved the interfacial adhesion significantly and that coating the carbon fibers with silicone rubber inhibits interfacial bonding. The remainder of the sized and unsized fibers together with the other finish variants did not show meaningful difference.

An underlying reason for the lack of additional distinctions is the large variation in the shear strengths and the 1:1 relationship between extrapolated tensile strength and shear strength. This effect is seen in the AS-1 data shown in Appendix F whereby an abnormally high extrapolated tensile strength translates directly to a proportionally high shear strength.

In conclusion, this test can be used to identify strong and weak interfacial bond strengths successfully. However, due to the nature of this test, it cannot reliably differentiate small differences.

TABLE XVI. SINGLE FILAMENT INTERFACIAL SHEAR STRENGTH

Sample	$\sigma_{f,\bar{e}_c}$ MPa	$\sigma_{f,\bar{e}_c}$ ksi	α	β	τ MPa	τ ksi
T-6300[1] (Sized)	4414	640	3.657	46.368	60 ± 29	8.682 ± 4.211
AS-1[1] (Unsized)	5931	860	3.294	41.736	92.6 ± 53.2	13.43 ± 7.707
C-6KV[2]	2772	402	3.255	71.385	25.4 ± 14.9	3.687 ± 2.159
C-6KU	4828	700	3.413	45.282	68.6 ± 37.1	9.948 ± 5.382
C-6KE[1]	5379	780	3.094	47.092	76.3 ± 48.9	11.07 ± 7.09
C-6K/ETP 50	5400	783	3.752	47.394	71.1 ± 33.2	10.31 ± 4.81
C-6K/ETP 10	5655	820	3.857	51.726	67.7 ± 30.3	9.81 ± 4.39
C-6K/FRE 25	5172	750	3.742	46.899	68.9 ± 32.3	9.99 ± 4.68
C-6K/SR	4276	620	3.001	185.952	15.57 ± 10.56	2.257 ± 1.531

(1) Commercially available carbon fibers

(2) Virgin carbon fibers with no surface treatment and unsized

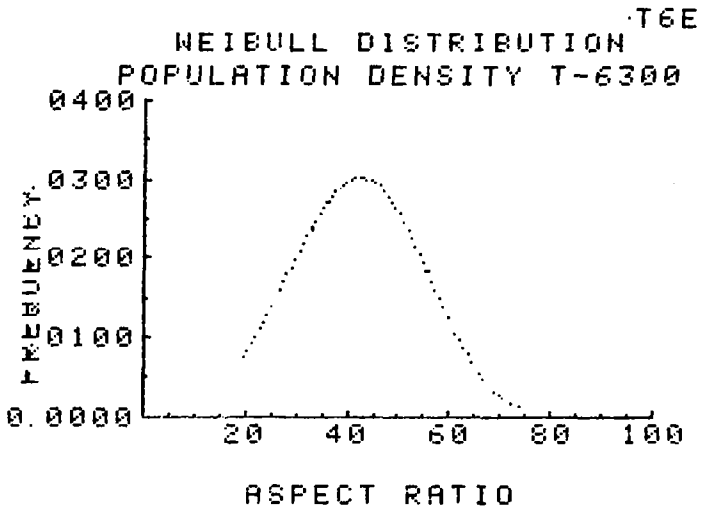

FIGURE 38. HISTOGRAPH OF CRITICAL ASPECT RATIO OF T-6300 STANDARD SIZED CARBON FIBERS

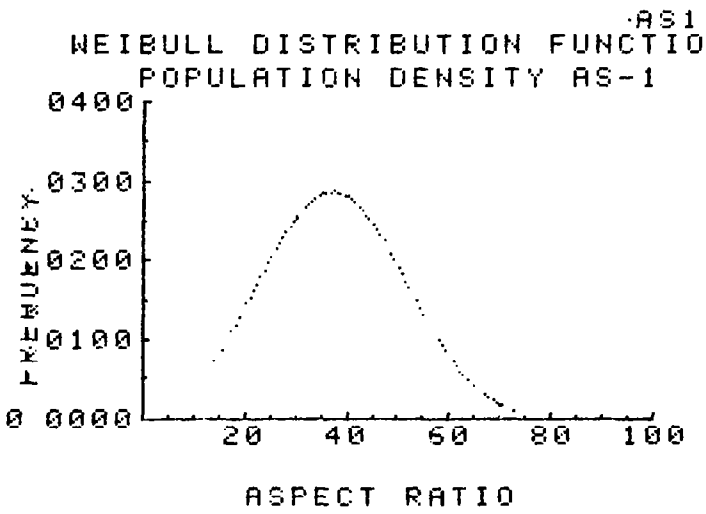

FIGURE 39. HISTOGRAPH OF THE CRITICAL ASPECT RATIO OF AS-1 UNSIZED CARBON FIBER

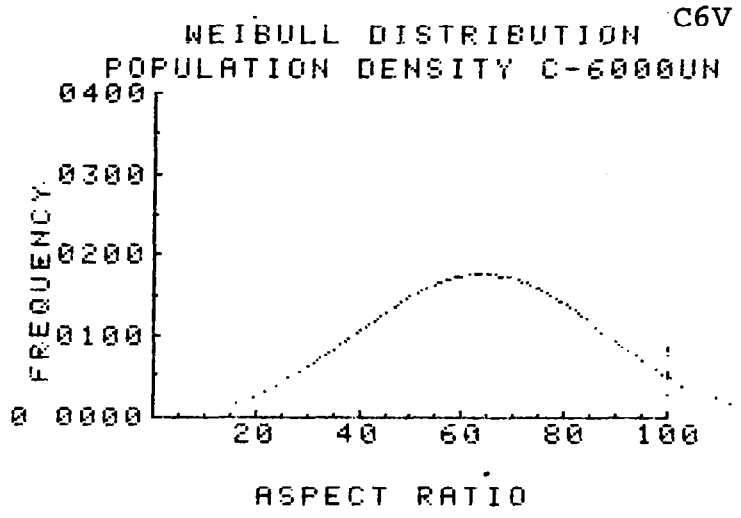

FIGURE 40. HISTOGRAM OF THE CRITICAL ASPECT RATIO OF CELION® 6000 WITH NO SURFACE TREATMENT AND UNSIZED

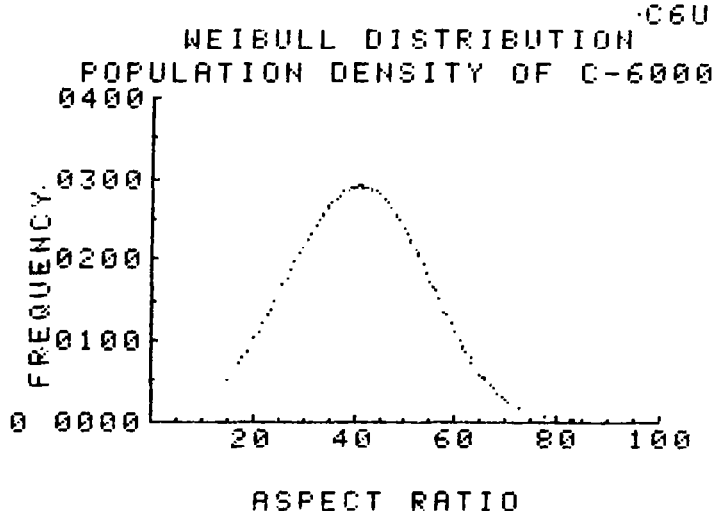

FIGURE 41. HISTOGRAM OF THE CRITICAL ASPECT RATIO OF CELION® 6000 WITH SURFACE TREATMENT BUT UNSIZED

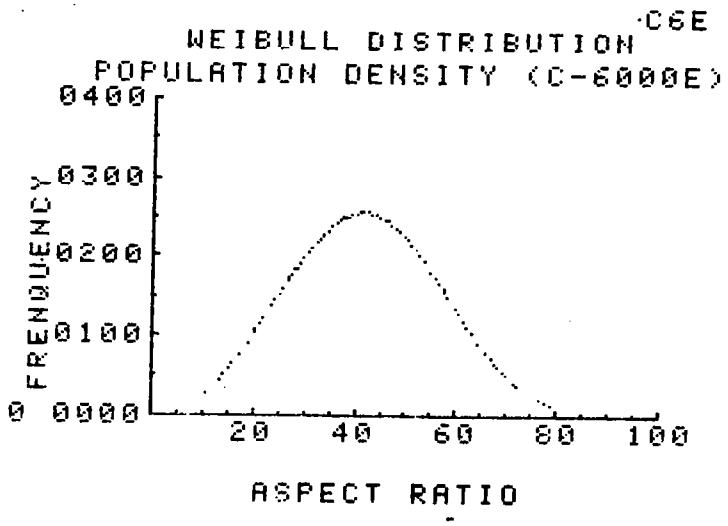

FIGURE 42. HISTOGRAM OF THE CRITICAL ASPECT RATIO OF CELION® 6000 STANDARD EPOXY COMPATIBLE SIZE (COMMERCIAL PRODUCT)

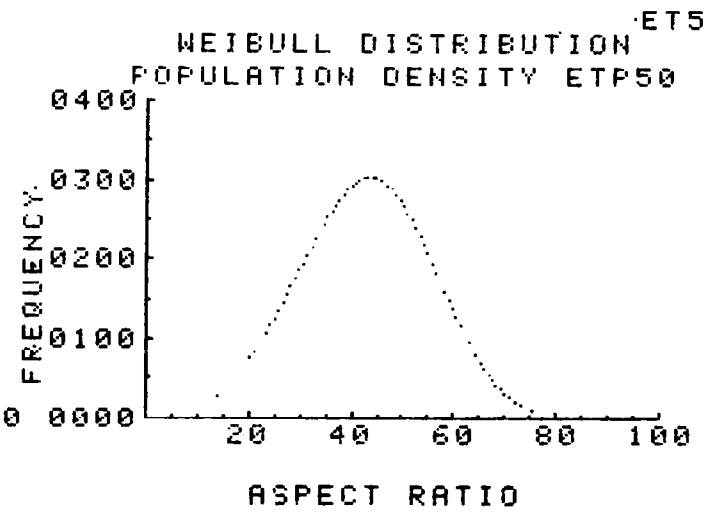

FIGURE 43. HISTOGRAM OF THE CRITICAL ASPECT RATIO OF CELION® 6000 WITH ETP-50 SIZE

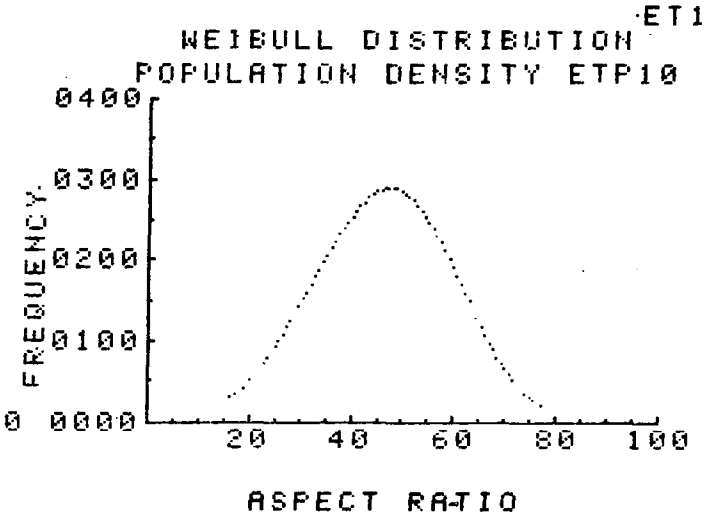

FIGURE 44. HISTOGRAM OF THE CRITICAL ASPECT RATIO OF CELION® 6000 WITH ETP-10 SIZE

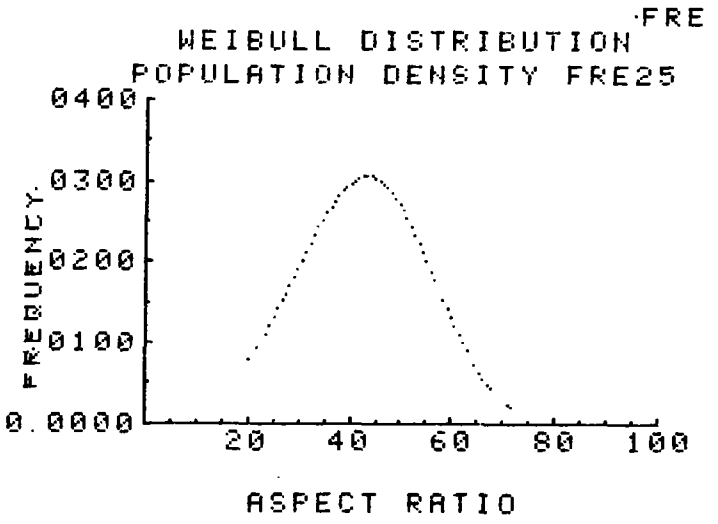

FIGURE 45. HISTOGRAM OF THE CRITICAL ASPECT OF CELION® 6000 WITH FRE-25 SIZE

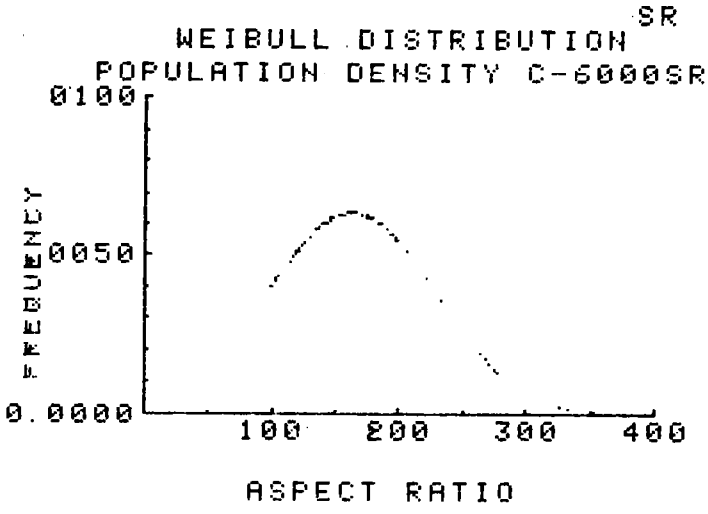

FIGURE 46. HISTOGRAM OF THE CRITICAL ASPECT RATIO OF CELION® 6000 WITH SILICONE RUBBER SIZE

Although this test cannot differentiate small differences numerically in interfacial bond strength, it does provide some information on fracture behavior of different fiber types/finish variants. Three distinctly different types of fracture behaviors were observed. The optical photomicrographs of these fracture behavior patterns are shown in Figures 47 through 49 and a schematic diagram of these three fracture modes is presented in Figure 50.

From this information, it is clear that the commercial epoxy-based sized fibers provide a higher interfacial shear strength and that brittle matrix cracks were initiated at the fiber fracture ends. However, ETP-50 sized Celion® 6000 produced a ductile, energy absorbing type of crack at the interphase. Further increase in stress on the latter fibers created a sharp, brittle crack extending into the bulk matrix material. These observations suggest that it may be possible to achieve both high shear strength and increased fracture toughness simultaneously.

CROSS POLAR TRANSMISSION PHOTOMICROGRAPH 100X

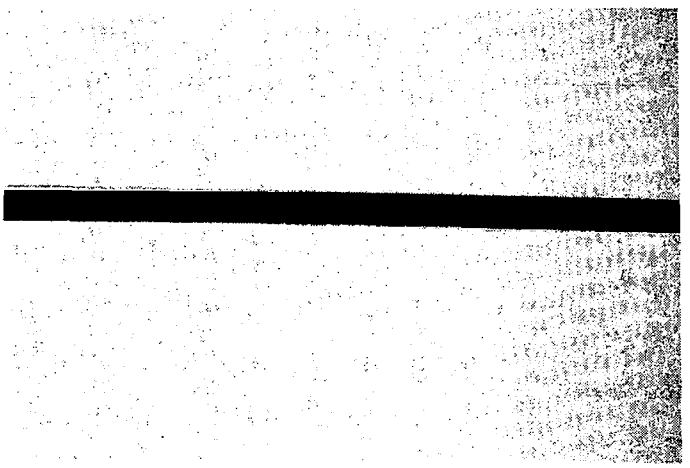

TRANSMISSION PHOTOMICROGRAPH 320X

FIGURE 47. FRACTURE MODE AT FIBER END OF LOW INTERFACIAL BOND STRENGTH (SILICONE RUBBER SIZED AND UNSIZED CARBON FIBERS)

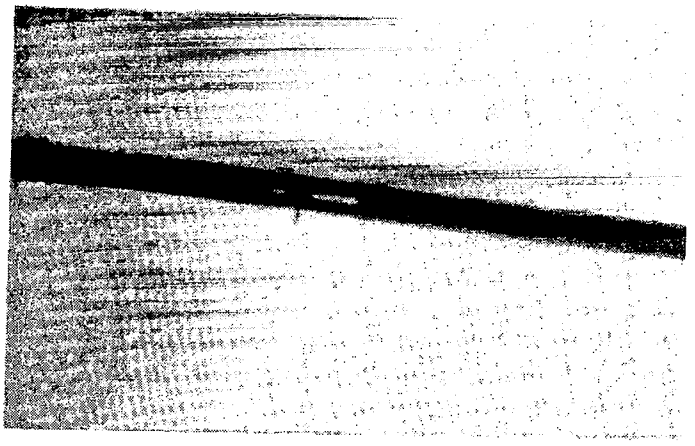

TRANSMISSION PHOTOMICROGRAPH 320X

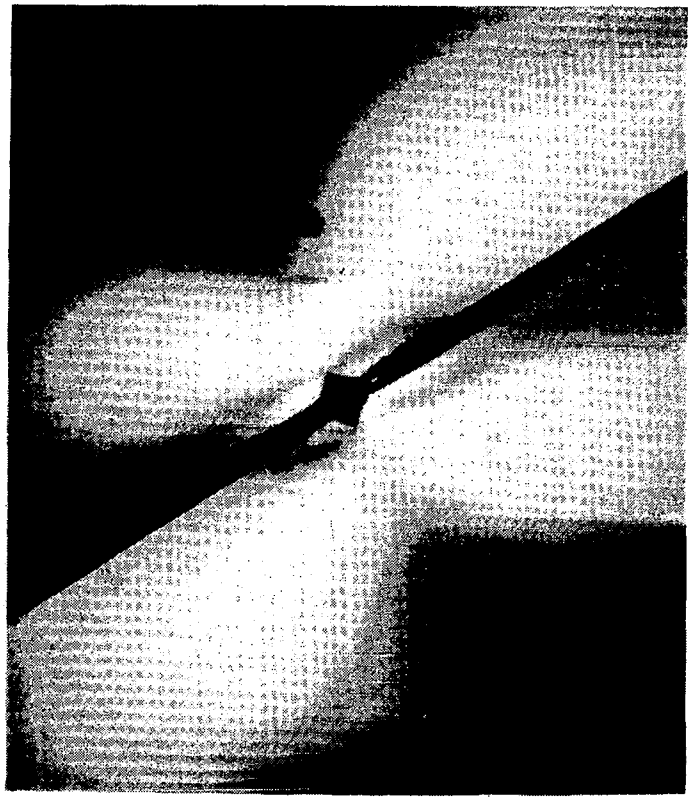

CROSS POLAR PHOTOMICROGRAPH 200X

FIGURE 48. FRACTURE MODE AT FIBER END OF HIGH INTERFACIAL BOND STRENGTH WITH STANDARD EPOXY SIZED CARBON FIBER. BRITTLE FAILURE INTO MATRIX AT FIBER ENDS.

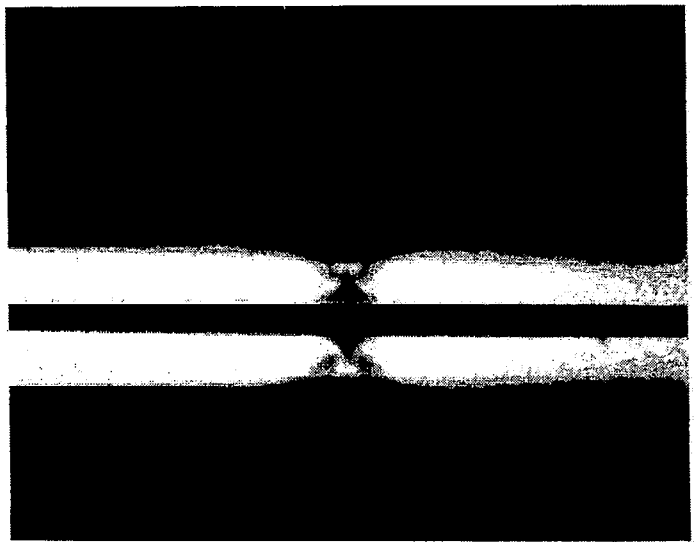

CROSS POLAR PHOTOMICROGRAPH 320X

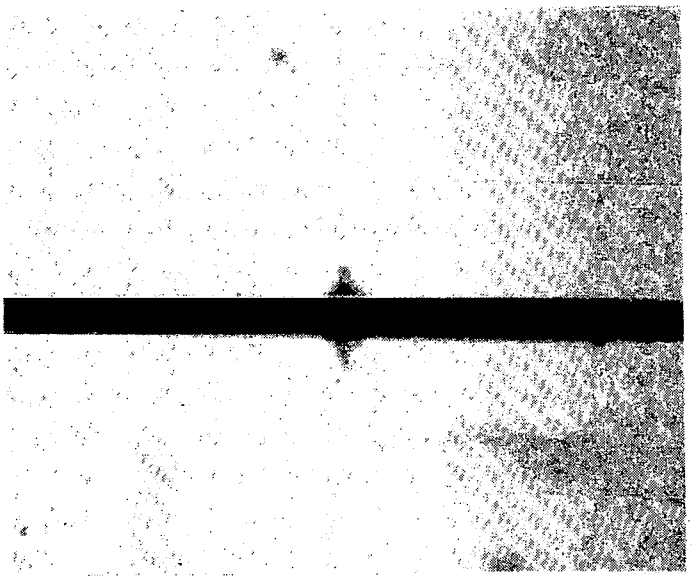

TRANSMISSION PHOTOMICROGRAPH 320X

FIGURE 49. FRACTURE MODE AT FIBER END OF LOWER MODULUS FINISH (ETP 50) CARBON FIBER. A DUCTILE FRACTURE MODE AT INTERPHASE INDICATES A TOUGH FRACTURE BEHAVIOR. THE INNERLAYER IS IDENTIFIED BY THE SHARP BRITTLE CRACK EXTENDED INTO THE BULK MATRIX MATERIAL.

a) Typical unsized fiber or weak interfacial bonding - no matrix crack.

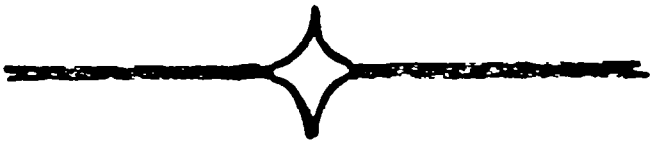

b) Celion®6000 standard epoxy sized fiber brittle cracks initiated at fiber ends.

c) Celion®6000 sized with ETP-50 different crack geometry immediately adjacent to fiber. Brittle matrix crack developed outside the interphase region.

FIGURE 50. A SCHEMATIC DIAGRAM OF THE THREE TYPES OF FAILURE MECHANISMS AT FIBER ENDS WITH DIFFERENT FINISHES

References

(1) P. E. McMahon, "Graphite Fiber Tensile Property Evaluation," SAMPLE Quarterly, Vol. 6, No. 1, Oct. (1974).

(2) L. T. Drzal, M. J. Rich, J. D. Camping and W. J. Park; "Interfacial Shear Strength and Failure Mechanisms in Graphite Fiber Composites," Proc. 35th Ann. Tech. Conf. of SPI, Sec. 20-C (1980).

Effect of Sizings on Composite Properties

The finish variants were formulated and applied to Celion® 6000 unsized carbon fiber. A three-inch wide prepreg tape with a thickness of 0.127 mm (5 mils) was prepared from each variant. Laminates were then fabricated using a match-metal-die molding technique. 0°-tensile properties together with 0°-flexural, 90°-flexural and short beam shear (SBS) at both room temperature and 93.3°C (200°F) were measured. An ETI-Dynatup drop dart instrumented impact tester (Appendix J) was used to measure the impact toughness of additional laminates. An approximately quasi-isotropic, [+45/90/-45/0/ 45/90]s lay-up was used for the impact toughness measurements. To characterize the toughess of these laminates, the maximum penetration force, P_F recorded on the tester is reported along with P_I, the force associated with initial damage. These composite properties together with the wetting force measurements and the single filament adhesion strength are presented in Table XVII.

To further evaluate this toughness enhancement obtained with resin system "F," a commercial resin system 5208 is used. Finish variant ETP-50 and a standard commercial size (serving as a control) were applied to Celion® 6000 unsized fiber and their properties are presented in Table XVIII.

Comparing the wetting force measurements with both the single filament adhesion strength and the composite shear strength, it can be seen that good wetting is required for good adhesion. However, better wetting as measured herein does not necessarily provide stronger interfacial bonding. This also suggests that once the fibers are "wetted," regardless of how the wetting is achieved, either forcibly wet or due to differences in surface energetics, then some adhesion can be achieved. This is identified in the silicone rubber sized carbon fiber composites where structural integrity is maintained in spite of chemical incompatibility. However, stronger interfacial bond strengths are clearly obtained with the other finish variants and the control. This probably arises from more favorable chemical bonding at the interface.

Although a 1:1 correlation between the single filament adhesion strength and the composite shear strength was not demonstrated, the single filament test is still very useful. This test method provides valuable insight into adhesion fundamentals, the underlying composite shear strength and the failure mechanisms involved in corresponding composites.

It is noteworthy that three of the finish variants selected in this study, ETP-50, ETP-10 and FRE-25 all show significant increases in impact toughness with no corresponding decreases in other mechanical properties either at room or elevated temperature. This impact

TABLE XVII. CELION® 6000/SYSTEM "F" LAMINATE PROPERTIES

SAMPLE	WETTING FORCE M/REPORT[5] (mg) ADVANCING	EQUILIBRIUM	RECEDING	SINGLE FILAMENT[4] CRITICAL LENGTH DETERMINED SHEAR MPa (ksi)	TENSILE[2] RT STR MPa (ksi)	RT MOD GPa (msi)	93.3°C STR MPa (ksi)	93.3°C MOD GPa (msi)	0° FLEXURAL[2] RT STR MPa (ksi)	RT MOD GPa (msi)	93.3°C STR MPa (ksi)	90° FLEXURAL[1] RT STR MPa (ksi)	RT MOD GPa (msi)	93.3°C STR MPa (ksi)	ILSS[1] RT MPa (ksi)	93.3°C MPa (ksi)	IMPACT[3] P_i N (lb)	P_f N (lb)	E_t (J) (ft-lb)
T-6300 (sized)	72.8±27.6	95.6±18.5	103.8±20.2	59.9±29.0 (8.68±4.21)	1669 (242)	142.8 (20.7)	NA	NA	1800 (261)	121.4 (17.6)	NA	99.31 (14.4)	8.83 (1.28)	NA	93.10 (13.5)	NA	NA	NA	
AS-1 (unsized)	57.2±10.6	74.4±5.4	87.2±7.8	92.6±53.2 (13.43±8.71)	1669 (242)	131.0 (19.0)	NA	NA	1676 (243)	115.9 (16.8)	NA NA	77.93 (11.3)	7.17 (1.04)	NA	83.45 (12.1)	NA	NA	NA	
C-6KV	67.0±11.3	80.2±9.9	92.2±14.9	25.5±13.9 (3.69±2.02)	1841 (267)	144.2 (20.9)	NA	NA	1331* (193)*	127.5 (18.5)	NA	NA	NA	NA	49.66 (7.2)	NA	NA	NA	
C-6KU	75.6±19.4	83.2±19.5	88.6±20.9	68.6±37.1 (9.95±5.38)	2069 (300)	153.8 122.3	1952 (283)	151.7 (22.0)	1910 (277)	123.4 (17.9)	NA NA	NA NA	NA NA	NA NA	86.21 (12.5)	NA	NA	NA	
C-6KE	55.8±19.5	91.4±13.3	102.4±12.9	76.3±48.9 (11.07±7.09)	1793 (260)	141.4 (20.5)	1855 (269)	144.8 (21.0)	1848 (268)	123.4 (179)	1069 (155)	81.38 (11.8)	7.45 (1.08)	71.03 (10.3)	95.86 (13.9)	57.24 (8.3)	1188 (267)	1481 (333)	8.45 (6.23)
C-6K/ETP50	107.4±28.4	127.2±29.4	135.0±29.1	71.1±33.2	1766 (256)	130.3 (18.9)	1828 (265)	146.2 (21.2)	2090 (303)	127.6 (18.5)	931 (135)	84.83 (12.3)	7.52 (1.09)	74.48 (10.8)	86.90 (12.6)	57.24 (8.3)	1468 (330)	1926 (433)	10.47 (7.72)
C-6K/ETP10	86.0±40.0	103.0±39.0	109.0±43.0	67.7±30.3	2034 (295)	141.4 (20.5)	1883 (273)	133.1 (19.3)	1586 (230)	122.1 (17.7	979 (142))	66.21 (9.6)	8.83 (1.28)	71.03 (10.3)	85.52 (12.4)	56.55 (8.2)	1472 (331)	1939 (436)	10.67 (7.87)
C-6K/PRE-25	71.7±10.7	82.0±12.6	90.2±14.9	68.9±32.3	1731 (251)	145.5 (21.1)	1786 (259)	133.1 (19.3)	1931 (280)	127.6 (18.5)	1090 (158)	74.48 (10.8)	8.21 (1.19)	63.45 (9.2)	91.03 (13.2)	57.24 (8.3)	1397 (314)	1837 (413)	9.34 (6.89)
C-6K/ER	-1.6±18.2	50.6±4.1	99.8±48.2	15.57±10.56 (2.257±1.531)	1621 (235)	127.6 (18.5)	1434** (208)	135.9 (19.7)	806.9 (117)	130.3 (18.9)	745 (108)	26.21 (3.8)	7.59 (1.10)	20.00 (2.9)	34.48 (5.0)	28.28 (4.1)	1886 (424)	2220 (499)	11.82 (8.72)

* Failed intralaminar shear.
** Failed at tab due to low shear strength.

1 Data obtained as tested.
2 Data normalized to 62% vol.fraction.
3 Normalized to 0.15cm (0.060 in.) thickness.
4 Average of 10 specimens.
5 Average of 30 specimens.

Note: Impact data is an average of 6 samples. Each composite properties is an average of 5 samples.

TABLE XVIII. CELION® 6000/5208 LAMINATE PROPERTIES

PROPERTY		CONDITION	TEST TEMPERATURE	SAMPLE C-6KE	SAMPLE C-6K/EPT50
Impact[1]			RT		
P_F (N)				1348	1744
E_T (J)				7.46	9.53
Tensile[2]	STR (MPa)		RT	1669	1834
	MOD (GPa)			140.7	142.1
	STR (MPa)		132°C	1738	1814
	MOD (GPa)			154.5	153.1
	STR (MPa)	WET[3]	132°C	1745	1786
	MOD (GPa)			156.6	153.1
0° Flex[2]	STR (MPa)		RT	1972	2041
	MOD (GPa)			118.6	121.4
	STR (MPa)		132°C	1731	1986
	MOD (GPa)			119.3	119.3
	STR (MPa)	WET[3]	132°C	1076	869
90°C Flex	STR (MPa)		RT	87.6	82.8
	MOD (GPa)			9.31	9.03
	STR (MPa)		132°C	63.5	56.6
	STR (MPa)	WET[3]	132°C	31.0	26.9
SBS	STR (MPa)		RT	117.2	111.7
	STR (MPa)		132°C	79.3	80.7
	STR (MPa)	WET[3]	132°C	53.8	49.0
±45° Tension	STR (MPa)		RT	161.4	159.3
	MOD (GPa)			4.76	4.35
	STR (MPa)		132°C	144.8	131.7
	MOD (GPa)			3.72	3.24
	STR (MPa)	WET[3]	132°C	129.7	112.4
	MOD (GPa)			2.69	2.28

(1) Normalized to 1.5×10^{-3} meter thickness.
(2) Normalized to 62% vol. fraction.
(3) Immersed in water at 71.1°C for 14 days.
Note: All data except impact are average of 5 specimens.
An average of 6 specimens is used for impact data.

toughness improvement is also shown in the 5208 resin system. The mechanisms involved are not fully understood. It is postulated that the softer innerlayer at the interphase diminishes some of the internal residual stresses and thereby eliminates stress concentrations. The significant improvements in impact toughness may arise from damping effects of shock waves at each fiber interphase where an energy dissipating material is not present. In any case, this study has demonstrated that tailoring of the interphase properties can enable significant improvement of composite performance.

MODEL DEVELOPMENT

The analytical model discussed under the section, "Stress Transfer from Matrix to Fiber," is valid only if there is no interphase region. However, it was shown by Drzal et al[1] and by the authors that an interphase does exist and its effect on composite properties is significant. Therefore, a modification of the existing analytical model is essential.

From the observations and the results of this study, several recommendations can be made by the authors to support the development of a new analytical model which includes a third phase - the interphase region.

Experimentally, the authors have shown that incorporation of a lower modulus interphase region results in the observation of a different fracture mechanism. This energy absorbent inner layer also improves the impact toughness of the composite. Further, there is some indication that the transverse matrix crack which occurs at a fiber fracture is blunted and that the tensile strength of a laminate is slightly enhanced. However, it has to be made clear that not only the physical properties of the interphase are important, but the chemical nature of the interphase also has to be considered. This is because some chemical bonding is required to provide strong interfacial shear strength to maximize the load transfer across the interface. The thickness of this interphase may itself be crucial. An annulor layer which is too thin may not be effective in improving impact resistance, while too thick a layer may lower other laminate properties such as transverse tension and compression, etc.

A schematic diagram of the modified model with the incorporated inner layers is shown in Figure 51. A micromechanistic approach can be taken to analyze the stresses in each region. Two approaches with different assumptions can be taken.

First, consider the fiber to be very rigid, when under stress and the true deformation of the fiber to be negligible compared to the matrix and the inner layer. In this case, a ductile inner layer of low shear modulus combines with the matrix to undergo large deformations in transferring tensile load to the fiber. Or second, consider the fiber to be an inclusion in the inner layer material, then treat the fiber/inner layer composite with its inherent characteristics as an inclusion in the bulk matrix.

After the stress states are determined, then classical micromechanistic approach can be used to study the composite properties. The resulting analytical model should include a third phase introduced by either (or both) of the approaches illustrated in Figure 51.

To incorporate the experimental results reported here, some refining experiments are necessary:

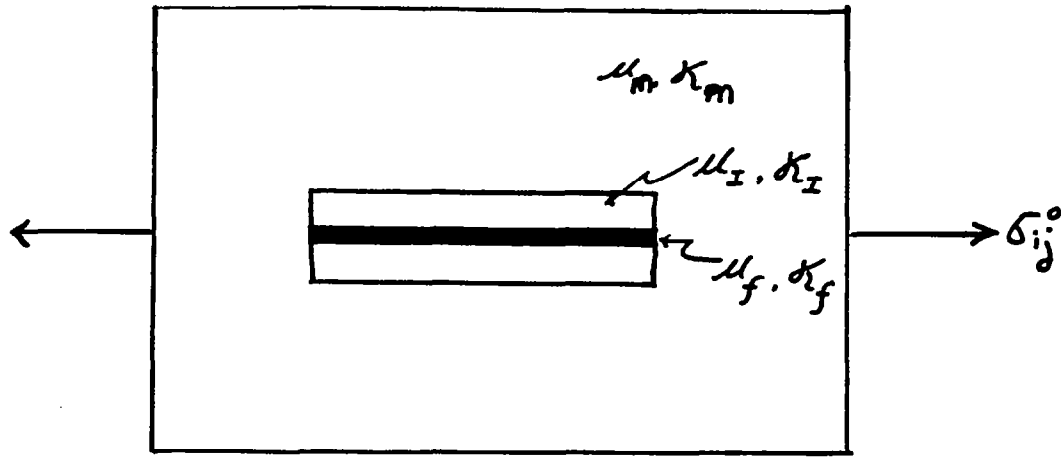

μ is the shear modulus

κ is the bulk modulus

and subscript

m = matrix

I = interphase

f = fiber

FIGURE 51. A SCHEMATIC DIAGRAM OF AN INNERLAYERED INCLUSION

- What is the modulus of the interphase?

- What is the composition gradient (and property gradient) across the interphase?

- What is the effect of interphase thickness?

- What is the degree of bonding required at the fiber surface? (Is the perfect bonding assumption a valid one?)

- What is the effect of finish on the load transfer to an adjacent fiber? (What is the loaded length of the adjacent fiber in the vicinity of a fracture?)

The answers to these questions and additional experimental observations would be amenable to analytical modelling to predict and account for the observed phenomenon. A valid model must be consistent with the observations.

CONCLUSIONS AND RECOMMENDATIONS

An extensive literature review on the role of interface and interphase in composite properties has been completed and experiments were designed to clarify some of the uncertainties encountered in this survey.

Wetting angle measurement on fiber surfaces is the most commonly used technique to predict adhesion strength due to wetting. However, no direct correlation has been shown between wetting angle measurements and fiber-to-matrix bond strength. In this study, wetting behavior has been characterized by the Wilhelmy wetting force measurement and interfacial shear strengths have been studied via the single filament critical length determination. The results indicate that intimate contact is necessary for adhesion, but chemical bonding may be responsible for higher interfacial bond strength.

Further, the results also indicate that by tailoring the interphase, different failure mechanisms can be achieved without significant loss in interfacial bond strength. This approach was investigated more thoroughly by an in depth evaluation of laminate properties. A significant improvement in impact toughness was obtained without loss of static mechanical properties. The conclusions of this study can be summarized as the following:

1. Good wetting properties are essential to provide good bondability, but better wetting properties do not necessarily provide stronger adhesive joint strengths.

2. Single filament critical length determination is a good analytical tool to characterize carbon fiber/epoxy adhesion properties and inherent failure mechanisms.

3. Single filament adhesion strength and composite shear strength are only loosely correlated.

4. Different failure mechanisms are identified in testing of single filaments of carbon fiber with different finish variants embedded in an epoxy matrix.

5. A significant 30% increase in impact toughness was measured without loss at room, elevated temperatures and hot-wet mechanical properties by incorporation of a "tailored-interphase" into the composite.

6. A modified analytical model is necessary to better understand the effect of the interface and interphase on composite performance.

7. A better understanding of the load transfer mechanisms involved in this more complex 3-component composite environment is necessary to prescribe the optimum interphase properties.

APPENDIX A. CALCULATIONS FOR THE THICKNESS OF A 1.5% BY WEIGHT EPOXY SIZE ON CARBON FIBER

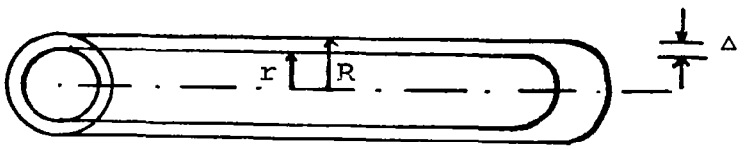

Density of carbon fiber, $\rho_f = 1.76$ g/cc

Diameter of carbon fiber, $r = 7 \times 10^{-4}$ cm

Density of epoxy size, $\rho_s = 1.182$ g/cc

Assume unit length, $\ell = 1$ cm

Volume of the fiber, $V_f = \pi r^2 \ell = 1.539 \times 10^{-6}$ cc

Weight of the fiber, $W_f = V_f \rho_f = 2.709 \times 10^{-6}$ g

$\therefore$ Weight of the epoxy size, $W_s = 1.5\%\ W_f$

$= 4.064 \times 10^{-8}$ g

Volume of the epoxy size, $V_s = W_s/\rho_s$

$= 3.438 \times 10^{-8}$ cc

But, $V_s = \pi(R^2-r^2)\ell = 3.438 \times 10^{-8}$ cc

$\therefore R = 7.08 \times 10^{-4}$ cm

Thickness of epoxy size, $\Delta = R-r = 800$ Å

APPENDIX B. APPARATUS FOR WETTING FORCE MEASUREMENT

A Cahn 26 automatic electrobalance was used to measure the wetting force of a single filament carbon fiber. This electrobalance was interfaced through a BCD interface module to an HP-85A microcomputer. This arrangement allowed the data to be stored, plotted and manipulated during the experiment.

In order to assess the advancing, receding and equilibrium wetting force, a constant speed moving stage for the wetting liquid was required. This stage was made from a modified micromanipulator and a high torque, variable speed electric motor. The electric motor was controlled automatically by the microcomputer to allow automation of this experiment. The program developed for this process is listed in Appendix C and a schematic diagram of this set-up is presented in Figure B-1.

A single filament of carbon fiber was selected and attached to the end of a thin gauge hang-down wire with rubber cement. This fiber was then connected to the balance and the weight of the fiber was tared. The wetting liquid contained in a perfectly cleaned beaker was raised by the micromanipulator until the fiber end was just immersed in the liquid. Then the program would automatically accumulate the data from the microbalance and control the stage to obtain the wetting force during the advancing, stationary and receding positions.

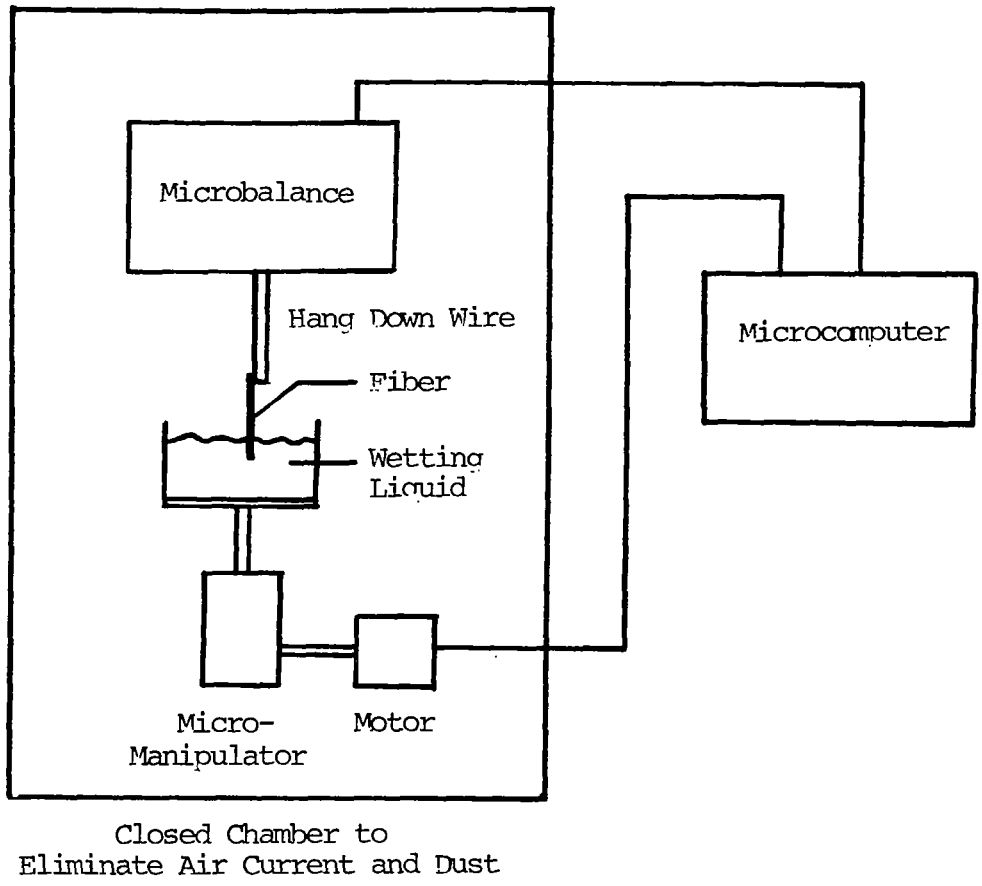

FIGURE B-1. APPARATUS ASSEMBLY FOR WETTING FORCE MEASUREMENT

APPENDIX C. WETTING FORCE MEASUREMENT PROGRAM

```
10 REM --->AUTOST
15 OPTION BASE 1
40 ON ERROR GOTO 80
50 LOADBIN "REDZER"
60 OFF ERROR
70 CHAIN "WETBAL"
80 IF ERRN=25 THEN 100
90 PRINT "Error number ";ERRN;" was encountered at line ";ERRL;"." @ GOT
O 120
100 PRINT "A binary program is already in  memory causing an error. Plea
se"
105 PRINT "eliminate this binary (i.e. by  turning machine off or execut
ing"
110 PRINT "'SCRATCH'). Then you may begin  the program again."
120 END
```

Introduction

REDZER is a binary program designed to enhance array manipulation capabilities of the HP-85. An array can be reorganized (redimensioned) or initialized to zero with use of one of the two statements offered. This binary program can be loaded into the HP-85 by the following command:

```
LOADBIN "REDZER"
```

For a further discussion of binary programs, see page 193 of the HP-85 Owner's Manual and Programming Guide.

ARRAY (RE)ORGANIZATION

You can reorganize an array into a more useful configuration by redimsioning that array. This changes the working size of the array; subsequent statements affect only the elements included in the new working size. However, elements not included in the new working size are still associated with the array. The values of these elements are not changed, and they can be accessed if the array is again redimensioned.

```
REDIM array (redim subscripts) [,array (redim subscripts)...]
```

The redimensioning subscripts are numeric expressions, variables, or constants that specify a new upper bound for each dimension. The number of subscripts must be the same as the number specified in the original DIM, REAL, SHORT, or INTEGER statements. Furthermore, the total number of elements in the new working size cannot exceed the number originally dimensioned.

Examples:

`DIM A(4),B(2,4),C(1,9)`	OPTION BASE Ø assumed.
`REDIM A(3)`	Redimensions working size from five to four elements.
`REDIM B(3,2)`	Redimensions B from 3 x 5 matrix (15 elements) into 4 x 3 matrix (12 elements).
`REDIM A(4),B(2,4)`	Redimensions A and B back to original sizes.
`X=2 @ REDIM C(2*X-1,1Ø/X-1)`	Redimensions C from 2 x 10 matrix into 4 x 5 matrix.

When a matrix is redimensioned, the values of its elements are reassigned to different positions within the matrix. Values of matrix elements are stored in order from left to right along each row, from the first row to the last. The redimensioning takes the elements out of the matrix in that order, and reassigns them in accordance with the new working size of the matrix.

The following example shows how values of matrix elements are reassigned when a matrix originally declared to be 3 x 3 is redimensioned into a 2 x 2 matrix. The values of the original matrix elements are integers that indicate the order in which the elements are stored before the redimensioning.

Example:

```
10 OPTION BASE 1
20 DIM A(3,3)                          Array A is originally dimensioned as
                                       3 x 3.
30 DATA 1,2,3,4,5,6,7,8,9
40 FOR I-1 TO 3                        Assigns values 1 through 9 to the
50 READ A(I,1),A(I,2),A(I,3)           elements of matrix A.
60 NEXT I
70 K=3 @ GOSUB 130                     Displays original 3 x 3 matrix.
80 REDIM A(2,2)                        Redimensions A down to a 2 x 2
                                       matrix.
```

```
 90 K=2 @ GOSUB 130
100 REDIM A(3,3)
110 K=3 @ GOSUB 130
 120 END
 130 FOR I=1 TO K
 140 FOR J=1 TO K
 150 DISP A(I,J);
 160 NEXT J
 170 DISP
 180 NEXT I
 190 DISP
 200 RETURN
```

Displays redimensioned 2 x 2 matrix.

Redimensions A back up to a 3 x 3 matrix.

Displays redimensioned 3 x 3 matrix.

Subroutine that displays matrix A.

RUN

```
 1 2 3
 4 5 6
 7 8 9

 1 2
 3 4

 1 2 3
 4 5 6
 7 8 9
```

Nine elements of original 3 x 3 matrix.

Four elements of redimensioned 2 x 2 matrix. Values of elements have been reassigned sequentially within new working size.

Nine elements of 3 x 3 matrix with original values still assigned.

Note that redimensioning a matrix does not isolate a submatrix. In other words, if you redimension a 3 x 3 matrix into a 2 x 2 matrix, the resulting matrix is not the 2 x 2 submatrix from the upper left corner of the original matrix.

```
5 ! WILHELMY BALANCE DATA ACQUISITION...PROGRAM WETBAL...G.V. NELSON 5/7
/81...VERSION 5.12.81
8 OPTION BASE 1
9 DIM D(1,1400),S2(10),S1$[60],V1$[84]
10 DIM Y(700),M(3),S(3),A$[20]
15 I=0 @ D2=1400
16 DISP USING "7/" ; @ DISP "         WILHELMY BALANCE" @ DISP "         D
ATA ACQUISITION"
17 DISP "Data from tape file(Y/N)" @ INPUT Y$
18 IF UPC$(Y$[1,1])="Y" THEN 2000
21 DISP USING "3/" ; @ DISP "Enter data collection interval (1-3 seconds
/point)"
22 INPUT S2
23 DISP "Enter no. of points to be collected for Advancing Region (300 m
ax)"
24 INPUT N1
26 DISP "Enter no. of points to be collected for Still Region (200 max)"

27 INPUT N2
28 CLEAR @ ON KEY# 1,"START" GOTO 50
29 ON KEY# 6,"UP" GOSUB 6200
30 ON KEY# 7,"DOWN" GOSUB 6250
31 ON KEY# 8,"STOP" GOSUB 6300
32 OFF KEY# 3 @ OFF KEY# 4 @ OFF KEY# 2
37 !
38 GCLEAR @ CLEAR @ KEY LABEL
39 GOSUB 6000 ! INITIALIZE INTERFACE
40 GOTO 40
50 DISP "Enter Sample Description (20 Chars max, no commas)"
51 INPUT A$
52 PRINT USING "7/" ; @ PRINT "         WILHELMY BALANCE" @ PRINT "
  DATA ACQUISITION" @ PRINT
53 PRINT A$
54 PRINT @ PRINT "DATA INTERVAL=";S2;" SECONDS/POINT"
55 PRINT "ADVANCING REGION=";N1;" POINTS"
56 PRINT "STILL REGION=";N2;" POINTS"
57 PRINT "RECEEDING REGION=";N1;" POINTS"
58 PRINT @ PRINT
80 Y1=0 @ Y2=0 @ M=0
85 GOSUB 7000 @ D1=D/100 @ D2=D1 ! START TIMER
86 LOCATE 0,130,0,100
87 FRAME
90 SCALE 0,2*N1+N2,0,D1
100 MOVE N1,0 @ DRAW N1,D1
102 MOVE N1+N2,0 @ DRAW N1+N2,D1
103 LORG 6 @ MOVE N1/2,D1 @ LABEL "ADVANCING"
104 MOVE N1+N2/2,D1 @ LABEL "STILL"
105 MOVE N1+N2+N1/2,D1 @ LABEL "RECEDING"
120 MOVE 0,0
135 GOSUB 6230 ! MOTOR ON-FWD
140 I=0 @ J=I
150 IF I=J THEN 150
155 GOSUB 5030
160 Y(I),Y=D
170 J=I
180 GOSUB 770
182 PEN 1
185 MOVE I,Y(I)
```

```
190 PLOT I,Y(I)
200 IF I=N1 THEN GOTO 220
210 GOTO 150
220 !
225 GOSUB 6330 ! MOTOR OFF
230 PRINT
250 OFF TIMER# 1 @ PRINT "ADVANCING:"
254 PRINT USING "10A,6D.3D,/,10A,6D.3D" ; "  MEAN  = ";M;"  STDEV = ";SQ
R(S1)
260 PRINT
270 M(1)=M @ M=0 @ Y1=0 @ Y2=0
280 ! TURN ON TIMER FOR STILL REGION
290 GOSUB 7000 ! START TIMER
310 I=0 @ J=I
320 IF I=J THEN 320
325 GOSUB 5030
330 Y(N1+I),Y=D @ J=I
340 GOSUB 770
342 MOVE N1+I,Y(N1+I)
344 DRAW N1+I,Y(N1+I)
346 IF I=N2 THEN 390
350 GOTO 320
390 OFF TIMER# 1 @ PRINT "STILL:"
400 PRINT USING "10A,6D.3D,/,10A,6D.3D" ; "  MEAN  = ";M;"  STDEV = ";SQ
R(S1)
410 PRINT
420 M(2)=M @ M=0 @ Y1=0 @ Y2=0
430 ! TURNON TIMER FOR RECEDING REGION
450 GOSUB 7000 ! START TIMER
455 GOSUB 6280 ! MOTOR REV
460 I=0 @ J=I
470 IF I=J THEN 470
475 GOSUB 5030
480 Y(N1+N2+I),Y=D @ J=I
490 GOSUB 770
492 MOVE N1+N2+I,Y(N1+N2+I)
494 DRAW N1+N2+I,Y(N1+N2+I)
496 IF I=N1 THEN 510
500 GOTO 470
510 ! STOP ROUTINE
520 GOSUB 6300 ! STOP MOTOR
530 OFF TIMER# 1 @ PRINT "RECEDING REGION:"
540 PRINT USING "10A,6D.3D,/,10A,6D.3D" ; "  MEAN  = ";M;"  STDEV = ";SQ
R(S1)
550 PRINT @ COPY
554 ON KEY# 5,"STORE" GOTO 1000
555 ON KEY# 3,"LIST" GOTO 900
556 ON KEY# 4,"PLOT" GOTO 560
557 GOTO 37
558 ON KEY# 2,"READ" GOTO 1900
559 GOTO 37
560 ! REPLOT GRAPH TO SCALE
561 GCLEAR
562 DISP "WHICH REGION DO YOU WANT TO PLOT (A=ADVANCING; S=STILL; R=RECE
DING)"
563 INPUT A1$@ N3=0
564 IF UPC$(A1$[1,1])="A" THEN N3=1 @ N4=N1 @ M$="ADVANCING"
565 IF UPC$(A1$[1,1])="S" THEN N3=N1+1 @ N4=N1+N2 @ M$="STILL"
```

```
566 IF UPC$(A1$[1,1])="R" THEN N3=N1+N2+1 @ N4=2*N1+N2 @ M$="RECEDING"
567 IF N3=0 THEN 562
570 PRINT USING "4/" ;
580 Y8=-1.E99 @ Y9=1.E99
590 FOR I=N3 TO N4
600 Y8=MAX(Y(I),Y8) @ Y9=MIN(Y(I),Y9)
610 NEXT I
611 CLEAR @ DISP "MIN Y VALUE=";Y9 @ DISP "MAX Y VALUE=";Y8 @ DISP "DO Y
OU WANT TO SET SCALE(Y/N)";
612 INPUT A1$@ IF UPC$(A1$[1,1])="Y" THEN 613 ELSE 614
613 DISP "ENTER Ymin,Ymax" @ INPUT Y9,Y8@ GOTO 615
614 Y9=0 @ Y8=D1
615 LOCATE 30,120,20,80
616 SCALE N3-1,N4,Y9,Y8
617 FXD 0,3 @ LAXES -(N4-N3+1)/10,(Y8-Y9)/10,N3-1,Y9,2,2
618 SETGU @ MOVE 70,3 @ LORG 4 @ LABEL "TIME(sec)"
619 MOVE 8,45 @ LDIR 90 @ LABEL "FORCE(mg)" @ LDIR 0 @ SETUU
635 MOVE (N3+N4)/2,Y8+(Y8-Y9)*3/20 @ LORG 4 @ LABEL M$
640 MOVE N3-1,0
650 FOR I=N3 TO N4
655 MOVE I,Y(I)
660 LORG 5
665 IF N4-N3>40 THEN PLOT I,Y(I) ELSE LABEL "+"
670 NEXT I
680 COPY
690 PRINT USING "7/" ;
715 GOTO 37
720 END
770 ! RUNNING AVERAGE,  STD DEV
780 M=((I-1)*M+Y)/I
790 Y1=Y1+Y
800 Y2=Y2+Y*Y
810 S1=(Y2-Y1*Y1/I)/I
820 RETURN
900 ! LIST
902 CLEAR
904 DISP "WHICH REGION DO YOU WANT TO LIST (A=ADVANCING; S=STILL; R=RECE
DING)"
906 INPUT A1$@ N3=0
908 IF UPC$(A1$[1,1])="A" THEN N3=1 @ N4=N1 @ M$="ADVANCING"
910 IF UPC$(A1$[1,1])="S" THEN N3=N1+1 @ N4=N1+N2 @ M$="STILL"
912 IF UPC$(A1$[1,1])="R" THEN N3=N1+N2+1 @ N4=2*N1+N2 @ M$="RECEDING"
914 IF N3=0 THEN 904
915 PRINT USING "3/" ; @ PRINT M$ @ PRINT "TIME(sec)  FORCE(mg)"
920 DISP "ENTER NUMBER OF DATA POINTS PER PRINTED VALUE" @ INPUT N5
950 FOR I=N3 TO N4 STEP N5
952 F9=3
954 IF D2>20 THEN F9=2
956 IF D2<=2 THEN F9=4
958 ON F9 GOTO 959,959,960,965
959 PRINT USING "DDDZ.DD,4X,DDDZ.DD" ; I*S2,Y(I) @ GOTO 970
960 PRINT USING "DDDZ.DD,4X,DDDZ.DDD" ; I*S2,Y(I) @ GOTO 970
965 PRINT USING "DDDZ.DD,4X,DDDZ.DDDD" ; I*S2,Y(I)
970 NEXT I
980 PRINT USING "7/" ;
990 GOTO 37
1000 ! STORE ACCORDING TO BSDM FORMAT
1010 O1=2*N1+N2 @ N7=2 @ S7=3
```

```
1020 V1$="TIME  FORCE "
1030 S1$="ADV.  STILL RECED."
1040 S2(1)=1 @ S2(2)=N1+1 @ S2(3)=N1+N2+1
1045 REDIM D(N7,01)
1050 FOR I=1 TO 01
1060 D(1,I)=S2*I
1070 D(2,I)=Y(I)
1080 NEXT I
1140 CLEAR
1150 DISP "   * * * * STORE DATA * * * *  " @ PRINT
1160 DISP "File names must be <= 6 charac- ters long. (Type 'E' to exit)
"
1170 DISP "Name of data file = ";@ INPUT F$
1180 IF LEN(F$)>0 AND LEN(F$)<7 THEN 1210
1185 IF F$="E" OR NOT LEN(F$) THEN 1530
1190 GOSUB 1590
1200 GOTO 1140
1205 IF F$[1,1]="E" AND LEN(F$)=1 THEN 1530
1210 DISP "Is data medium placed in tape   drive(Type 'E' to exit)";@ IN
PUT N$
1220 ON FNA(N$) GOTO 1210,1230,1210,1530
1230 CLEAR
1240 ON ERROR GOSUB 1710
1250 X=0
1260 ASSIGN# 1 TO F$
1270 OFF ERROR
1280 IF X=1 THEN 1360
1290 DISP "A file of this name has been    found.  Do you wish to store"

1300 DISP "present data set under this     name and destroy old data set
";@ INPUT N$
1310 ON FNA(N$) GOTO 1290,1370,1140,1530
1330 GOSUB 1590
1340 CLEAR @ GOTO 1290
1360 CREATE F$,(8+02*8) DIV 700+2,700
1370 ASSIGN# 1 TO F$
1375 CLEAR
1390 PRINT# 1,1 ; A$,01,N7,V1$,S7,S1$,S2(,)
1400 READ# 1,2
1410 PRINT# 1 ; D(,)
1420 ASSIGN# 1 TO *
1430 CLEAR
1440 PRINTER IS 2
1450 PRINT "**********************************";"*";TAB(32);"*"
1460 PRINT "*";TAB(14);"STORE";TAB(32);"*"
1470 PRINT "*";TAB(32);"*";"**********************************"
1480 PRINT
1490 PRINT "Data and related information is stored in ";F$;"."
1500 PRINT
1510 DISP "Is program medium replaced in device ";@ INPUT N$
1520 ON FNA(N$) GOTO 1510,1530,1510,1530
1530 CLEAR
1560 GOTO 37
1590 BEEP
1600 DISP "Improper response--please try   again."
1610 WAIT 1500
1620 RETURN
1710 IF ERRN=67 THEN X=1
```

```
1720 RETURN
1730 DEF FNA(A$)
1740 IF LEN(A$)=0 THEN FNA=1 ELSE FNA=POS("YNE",UPC$(A$[1,1]))+1
1750 FN END
1900 ! TRAP FOR UNINTENDED LOSS OF DATA
1905 CLEAR
1910 DISP "Reading data from tape will overwrite current memory"
1920 DISP "Continue (E to exit)";@ INPUT N$
1930 ON FNA(N$) GOTO 1920,2000,554,554
2000 ! READ DATA FROM TAPE BSDM FORMAT
2005 CLEAR
2010 DISP "Name of data file=";@ INPUT F$
2020 DISP "Is data medium placed in tape   drive(Type 'E' to exit)";@ IN
PUT N$
2030 ON FNA(N$) GOTO 2020,2040,2020,2190
2040 CLEAR
2050 ON ERROR GOTO 2080
2060 ASSIGN# 1 TO F$
2070 OFF ERROR @ GOTO 2090
2080 DISP "File ";F$;" not found" @ GOTO 2010
2090 READ# 1,1 ; A$,O1,N7,V1$,S7,S1$,S2(,)
2100 REDIM D(N7,O1)
2110 READ# 1,2
2120 READ# 1 ; D(,)
2130 ASSIGN# 1 TO *
2140 PRINT "DATA ENTERED FROM TAPE FILE ";F$ @ PRINT
2150 N1=S2(2)-1 @ N2=S2(3)-S2(2)
2160 FOR I=1 TO O1
2170 Y(I)=D(2,I)
2180 NEXT I
2185 S2=D(1,2)-D(1,1)
2186 D1=D(2,O1/2)
2190 GOTO 554
4900 !
4910 ! INTERRUPT PROCESSING
4920 !
5000 ENTER 3 ; Q3,Q4 ! READ VALUE
5001 IF ABS(Q3)<60000 THEN 5000
5010 I=I+1
5020 RETURN
5021 !
5022 ! INPUT DECODING
5023 !
5030 Q1=Q3
5031 Q2=Q4
5032 IF Q1#Q3 THEN 5030
5040 IF INT(Q2/10)=1 THEN 5045
5042 DISP "Overrange"
5045 Q2=RMD(Q2,10)
5050 IF Q2>0 AND Q2<9 THEN 5100
5060 !
5070 Q2=1
5075 DISP "Exponent Error"
5080 GOTO 5190
5090 ON Q2 GOTO 5140,5160,5060,5180,5060,5060,5060,5185
5100 ON Q2 GOTO 5140,5160,5060,5180,5060,5060,5060,5185
5140 Q2=.1
5150 GOTO 5190
```

```
5160 Q2=.01
5170 GOTO 5190
5180 Q2=.001
5184 GOTO 5190
5185 Q2=.0001
5190 D=Q1*Q2
5210 RETURN
6000 !
6010 ! DATA INITIALIZATION
6020 !
6030 RESET 3
6040 CONTROL 3,1 ; 0 ! NO INTERRUPTS
6050 CONTROL 3,2 ; 0 ! CLEAR OUTPUT BITS
6060 CONTROL 3,3 ; 5 ! 5 DIGITS
6070 CONTROL 3,4 ; 0 ! NO EXPONENT
6080 CONTROL 3,5 ; 2 ! 2 FUNCTIONS
6090 CONTROL 3,6 ; 0 ! NO DECIMAL
6100 CONTROL 3,7 ; 0 ! NO HANDSHAKE
6110 CONTROL 3,8 ; 0
6120 CONTROL 3,9 ; 15
6130 CONTROL 3,10 ; 0
6140 RETURN
6200 !
6210 ! MOTOR ON-FWD
6220 !
6230 CONTROL 3,2 ; 1
6240 RETURN
6250 !
6260 ! MOTOR ON-REV
6270 !
6280 CONTROL 3,2 ; 3
6290 RETURN
6300 !
6310 ! MOTOR OFF
6320 !
6330 CONTROL 3,2 ; 0
6340 RETURN
7000 GOSUB 5000 ! READ START VALUE
7005 GOSUB 5030 ! DECODE VALUE
7010 D=49999*Q2 ! SET MAX VALUE
7020 ON TIMER# 1,1000*S2 GOSUB 5000
7030 RETURN
```

APPENDIX D. PROCEDURES FOR CLEAN GLASSWARE TO PREVENT CONTAMINATION OF WETTING LIQUIDS

1. Glassware is placed in boiling 1:1 diluted nitric acid for five minutes.
2. Then it is rinsed with double distilled water.
3. It is next steamed with double distilled water for thirty minutes.
4. It is then vacuum dried at 150°C for ten hours.
5. Finally, it is individually wrapped in aluminum foil and stored in a dessicator.

APPENDIX E. SINGLE FILAMENT GRAPHITE FIBER TENSILE TEST

A representative number (generally 20) of single filaments are randomly selected from a tow sample. The filaments are center-line mounted on special slotted paper tabs as shown in Figure E-1. The paper tabs are gripped such that the test specimen is uniaxially aligned in the jaws of an Instron. An Instron constant cross-head speed of 0.02 inch/min and a chart speed of ten inches/min are employed. The procedure of mounting the graphite fiber on the tabs is as follows:

1. The strand bundle is placed loosely on a suitable work surface.

2. A dental pick is used to gently separate the filaments and a suitable test specimen is selected.

3. A tab of pre-punched slot is used as the mounting medium. The single filament is centered along the slot of a mounting tab and a small strip of tape is used to anchor one end to this tab.

4. The filament is lightly stretched and the opposite end is anchored in the same manner.

5. A small amount of sealing wax is carefully placed on top of the filament at each edge of the slot to secure the filament to the tab.

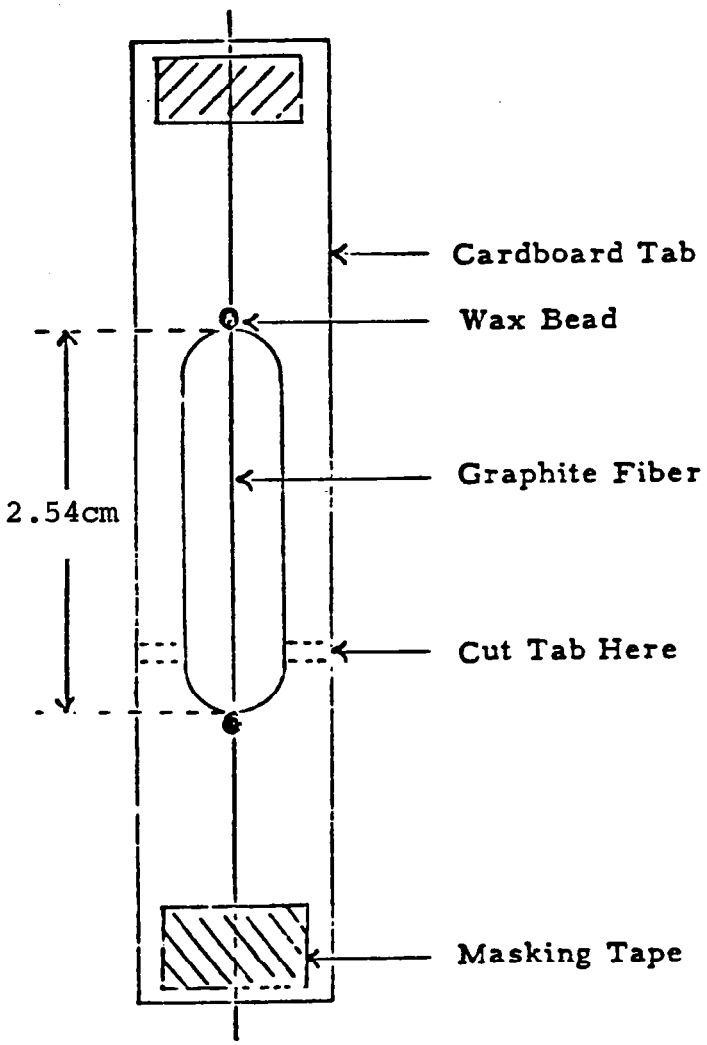

FIGURE E-1. GRAPHITE FIBER MOUNTED ON A TAB

APPENDIX F. SINGLE FILAMENT TENSILE STRENGTH AT VARIOUS GAUGE LENGTHS

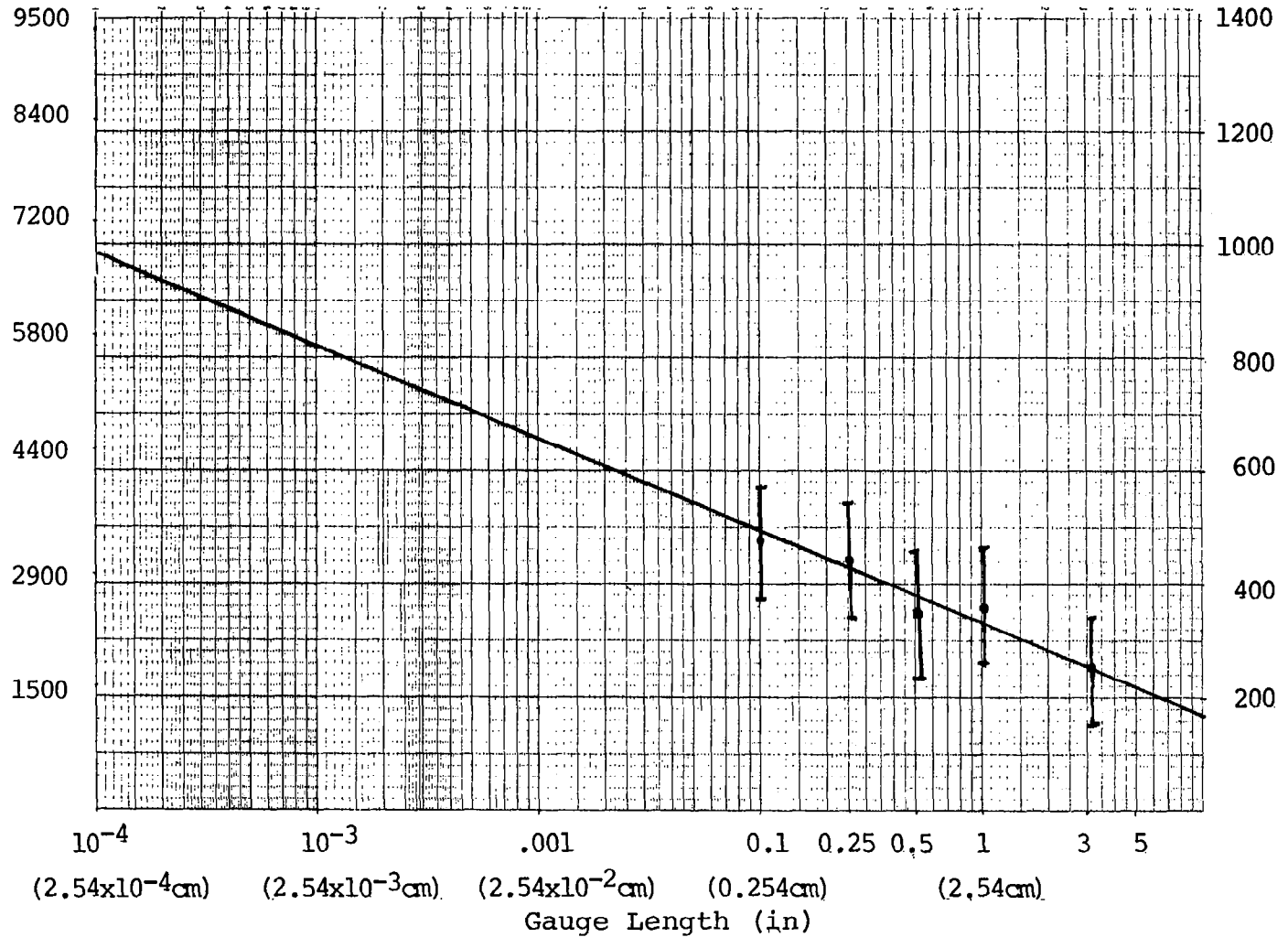

FIGURE F-1. T-6300 (STANDARD SIZED PRODUCT) LOT #1141-4

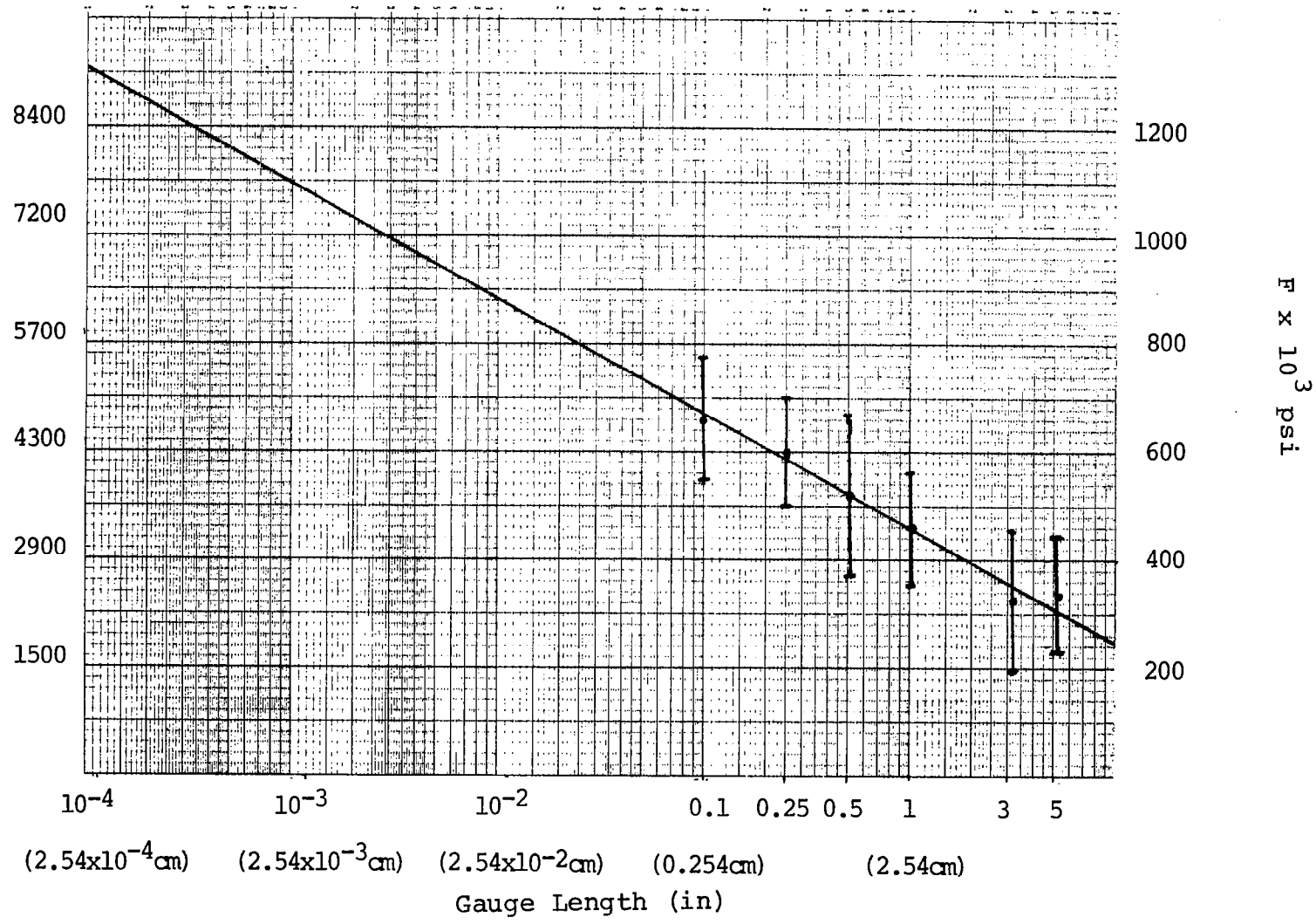

FIGURE F-2. AS-1 (STANDARD UNSIZED PRODUCT) LOT #156-3

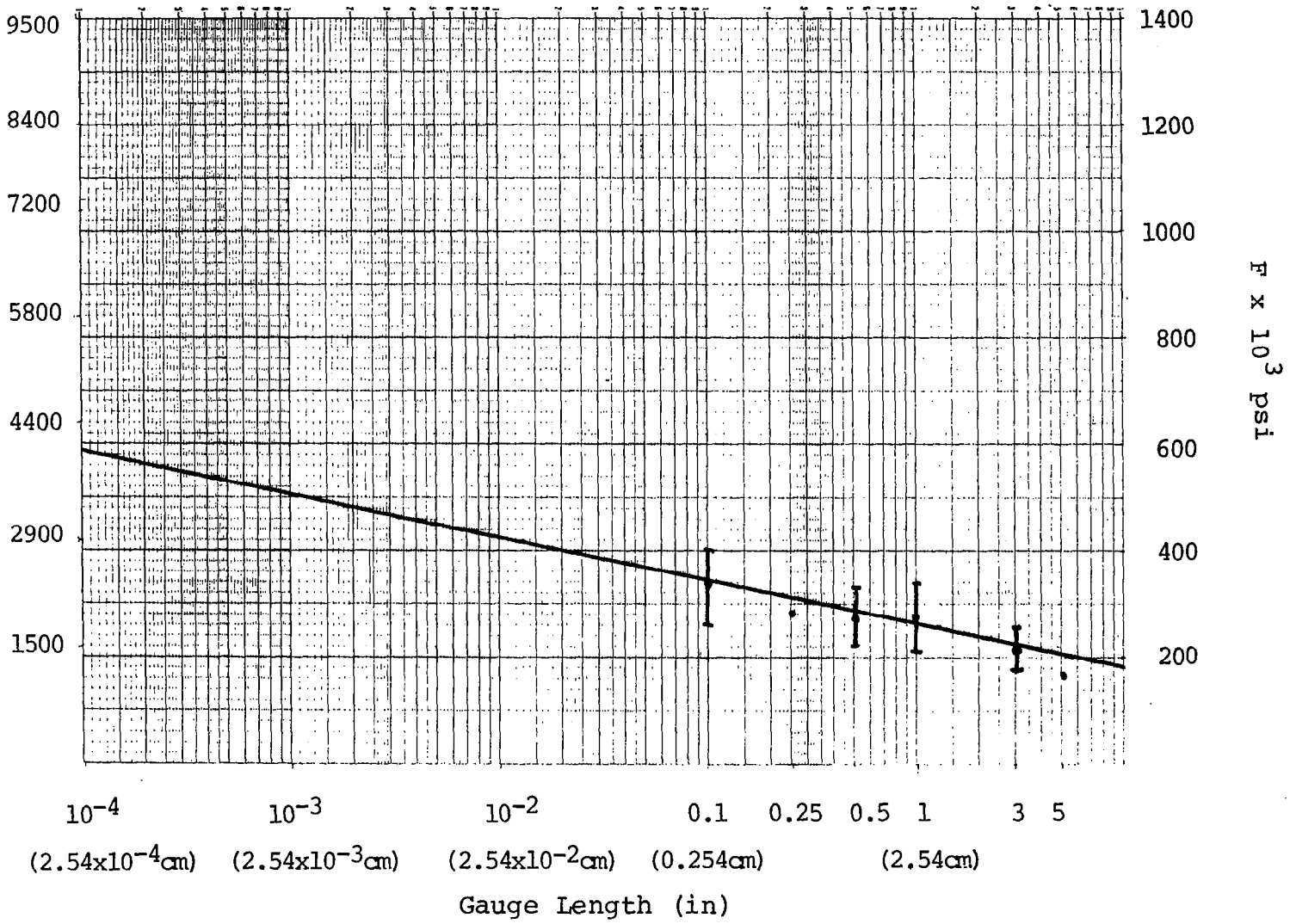

FIGURE F-3. C-6KV (UNSIZED, NONTREATED) LOT #7411

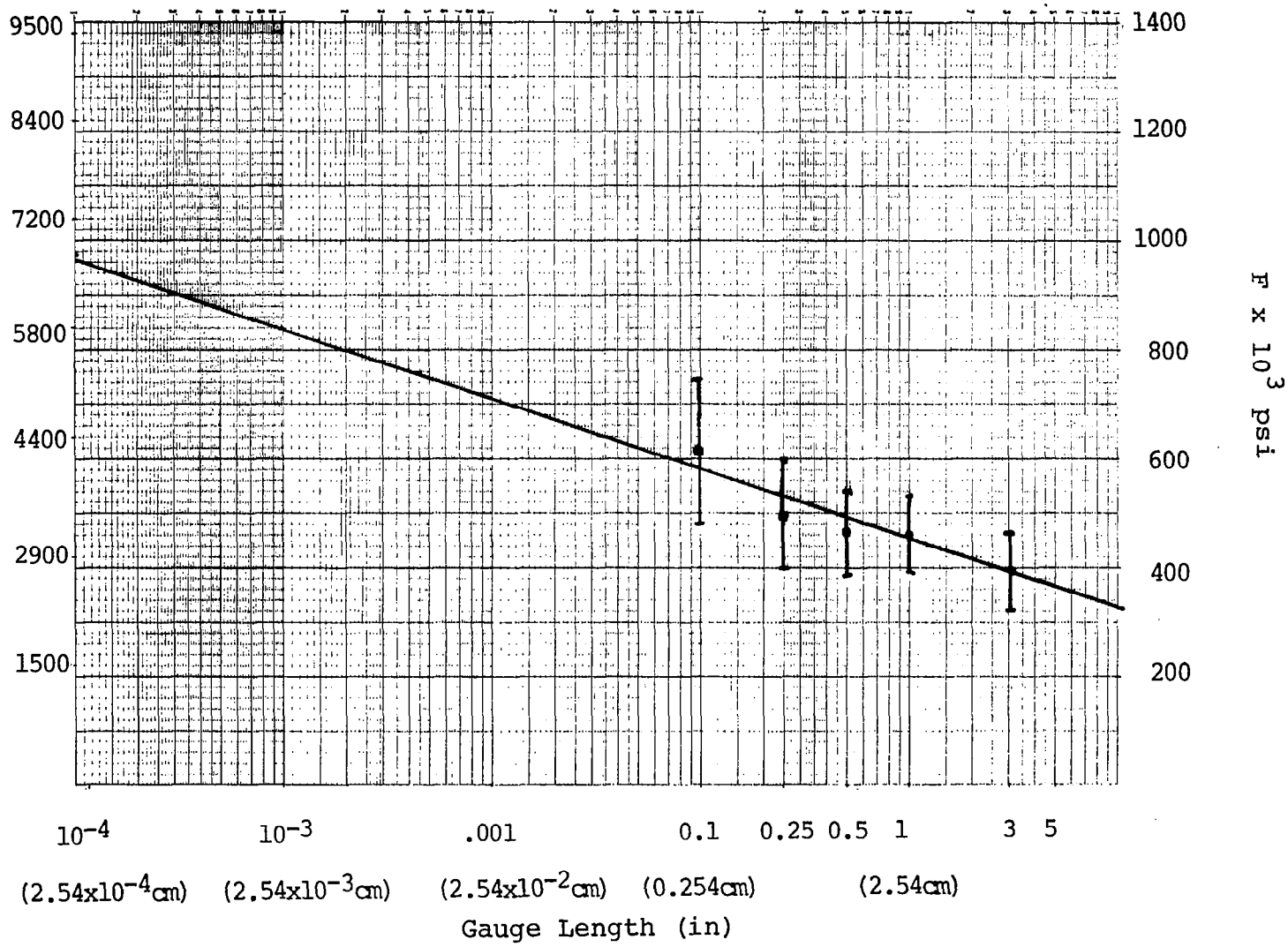

FIGURE F-4. C-6K (UNSIZED) LOT #9621

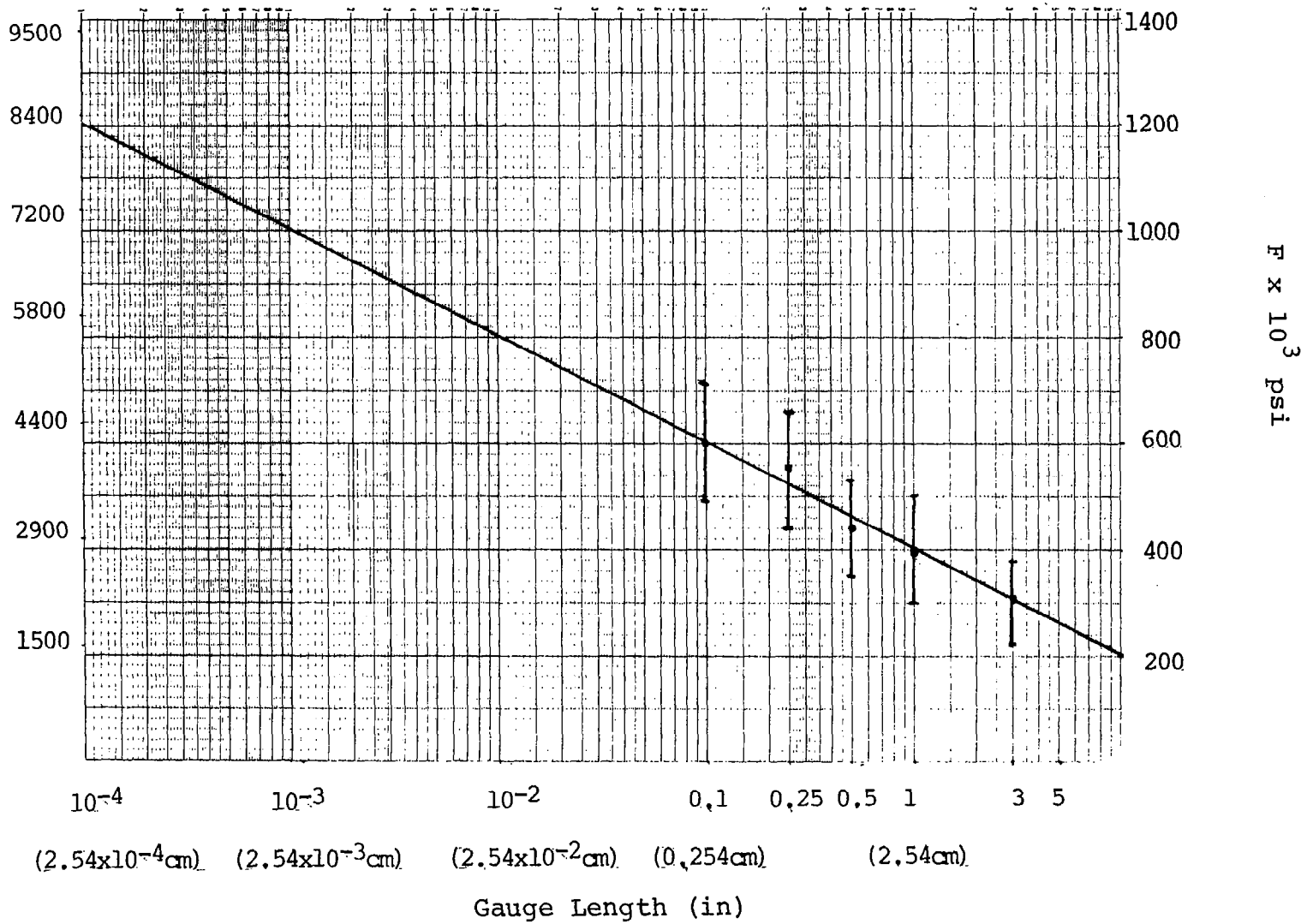

FIGURE F-5. C-6KE (STANDARD SIZE) LOT #0431

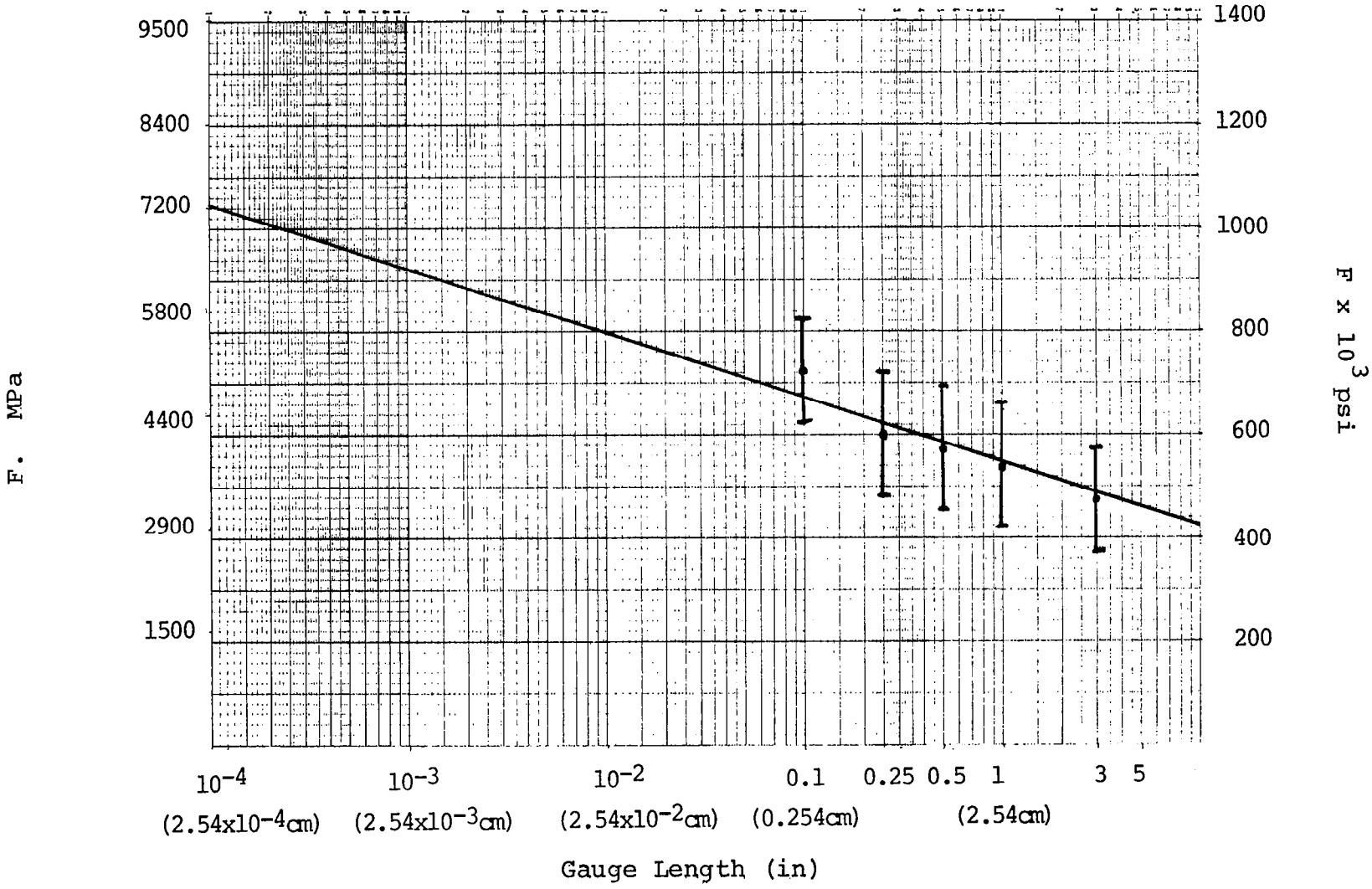

FIGURE F-6. C-6K/ETP-50 LOT #9431

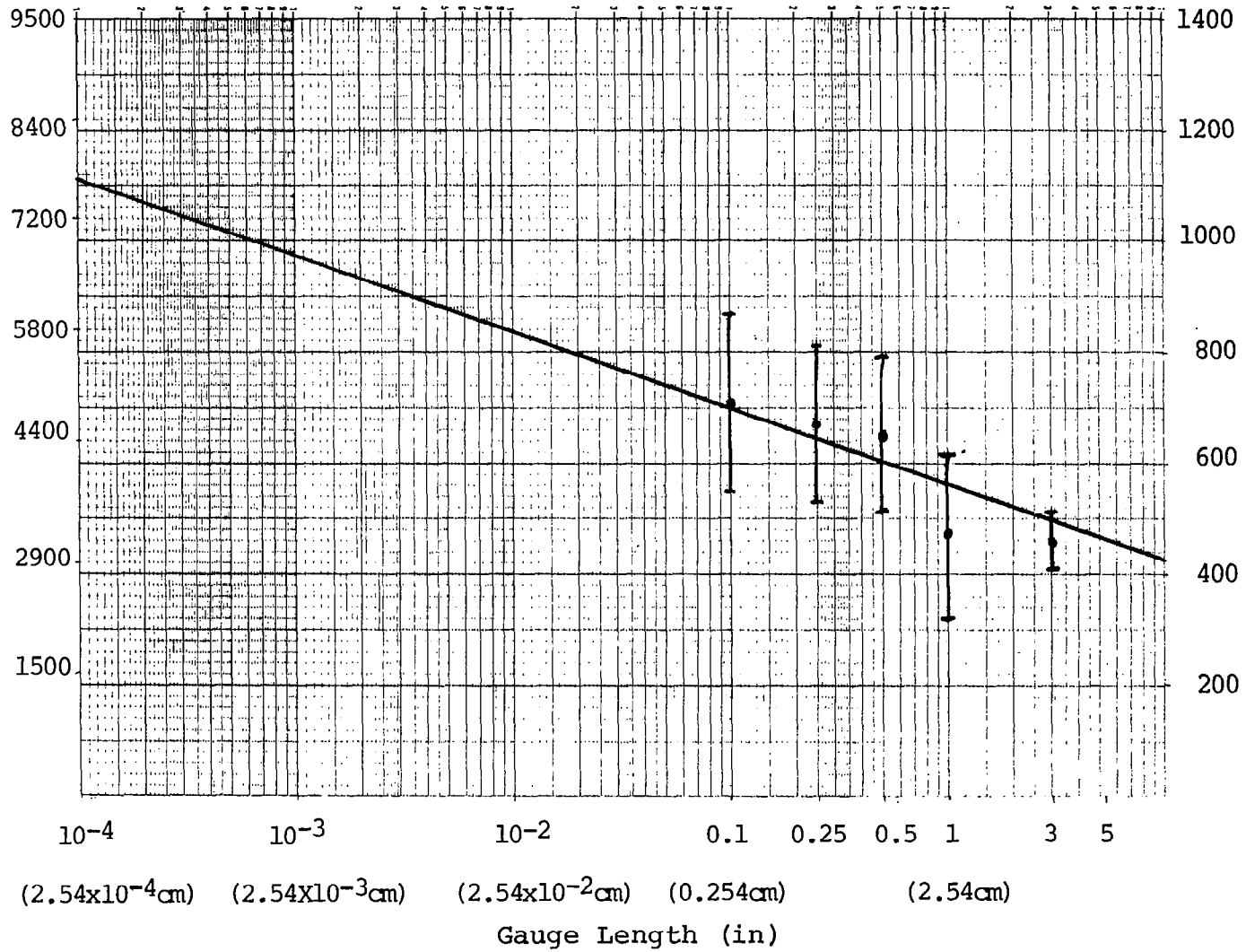

FIGURE F-7. C-6K/ETP-10 LOT #9Y31

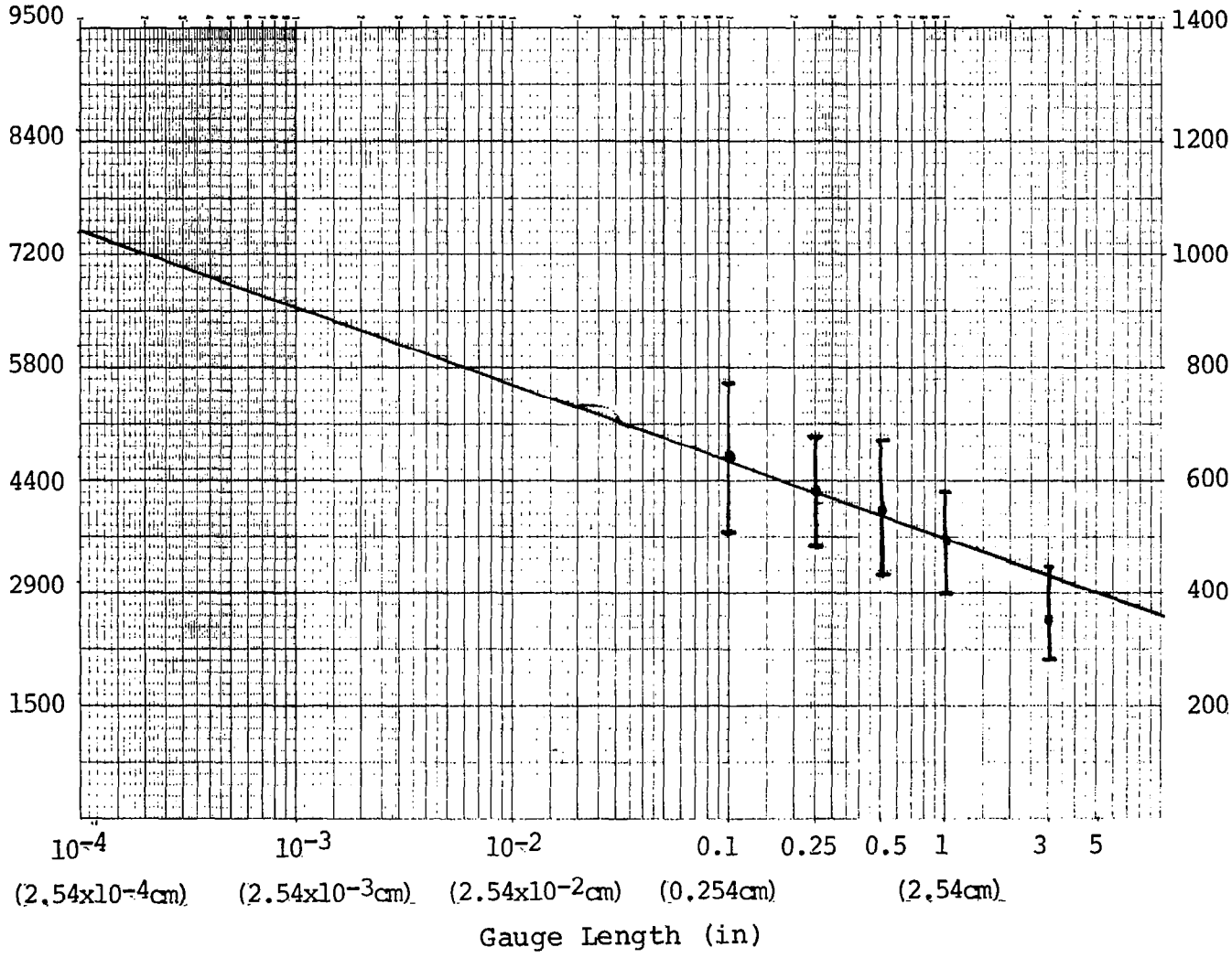

FIGURE F-8. C-6K/FRE-25 LOT #9732

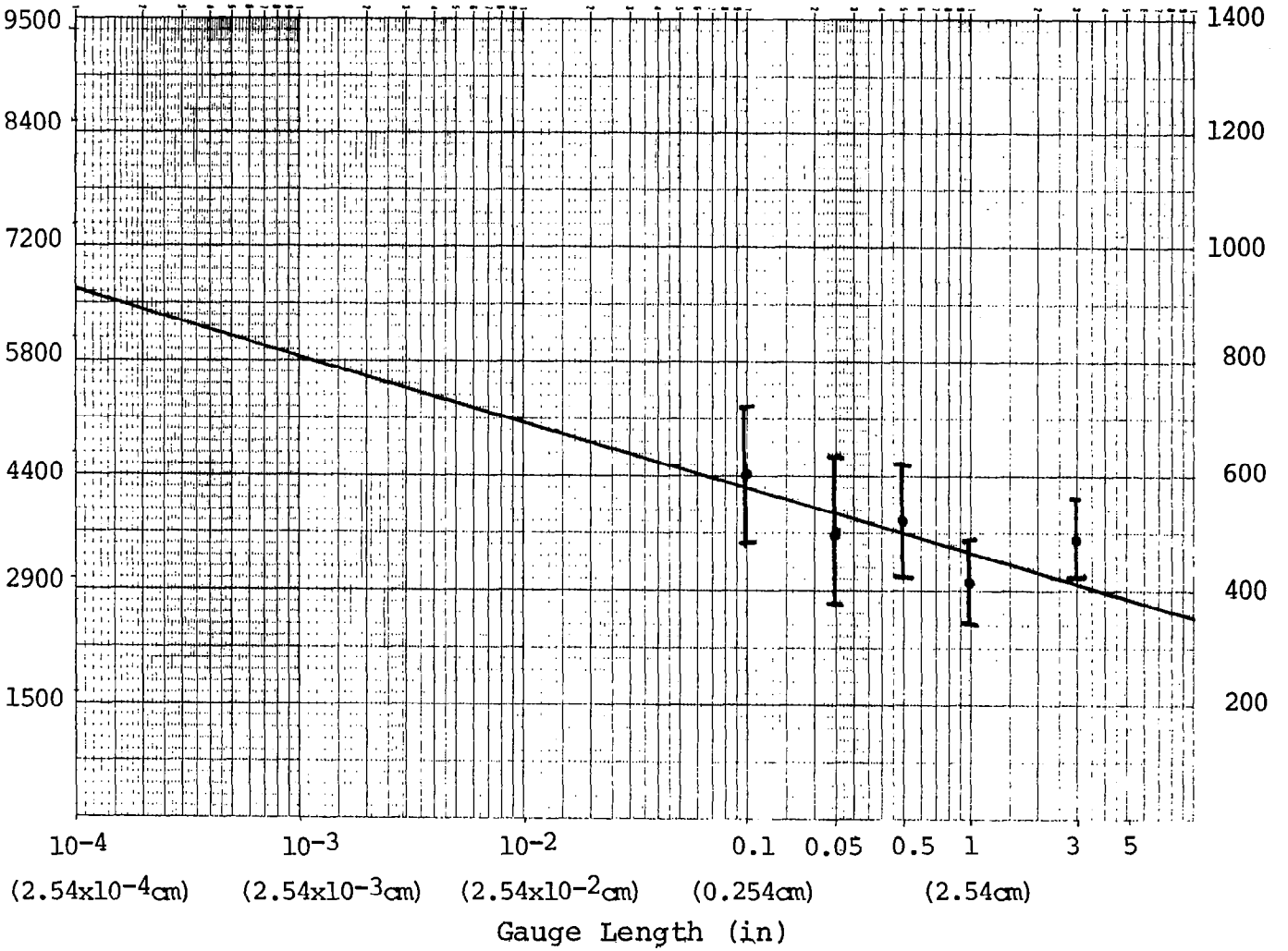

FIGURE F-9. C-6K/SR LOT #9732

APPENDIX G. TENSILE FIXTURE TO STUDY SINGLE FILAMENT ADHESION PROPERTIES

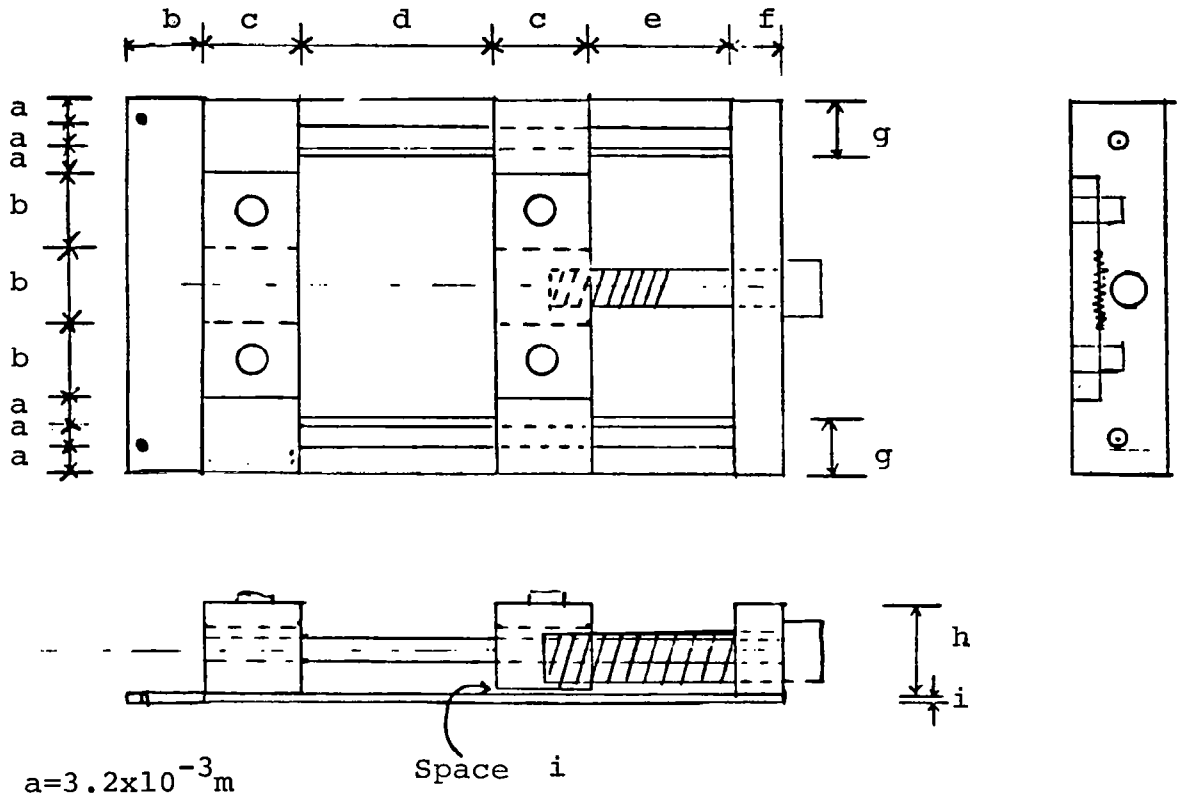

a=3.2x10^{-3}m
b=9.5x10^{-3}m
c=1.27x10^{-2}m
d=2.54x10^{-2}m
e=1.9x10^{-2}m
f=6.4x10^{-3}m
g=7.9x10^{-3}m
h=1.3x10^{-2}m
i=8x10^{-4}m

FIGURE G-1. TENSILE FIXTURE FOR LEITZ OPTICAL MICROSCOPE DRAWN TO SIZE

APPENDIX H. SINGLE FILAMENT INTERFACIAL SHEAR STRENGTH DETERMINATION PROGRAM

The purpose of this program is to apply a Weibull Distribution statistical analysis of the critical aspect ratio of the fibers where Weibull parameters as well as the average shear strength and the variance of the shear strength are determined.

```
10 !*** INTERFACIAL SHEAR STRENGTH PROGRAM -- CRITICAL LENGTH DETERMINA
TION  ***
20 DIM D(500),L(500),R(350)
30 ON KEY# 1,"ENTER" GOTO 170
40 ON KEY# 2,"STORE" GOTO 600
50 ON KEY# 3,"DISPLAY" GOTO 760
60 ON KEY# 4,"EDIT" GOTO 940
70 ON KEY# 5,"CALC" GOTO 1200
80 ! ON KEY# 6,"HISTO" GOTO
90 ! ON KEY# 7,"WEIBULL" GOTO
100 ! ON KEY# 8,"NORMAL" GOTO
110 !
120 CLEAR @ KEY LABEL
130 DISP "INTERFACIAL SHEAR STRENGTH DETERMINATION!"
140 DISP "CRITICAL LENGTH MEASUREMENT."
150 DISP "SELECT OPTION"
160 GOTO 160
170 ! ****   DATA ENTRY   ****
180 CLEAR @ DISP "ENTER DATA FROM KEYBOARD (K) OR TAPE (T)?"
190 INPUT Y$
200 IF Y$="K" THEN 250
210 IF Y$="T" THEN 500
220 GOTO 180
230 !
240 !
250 ! ***   ENTER DATA FROM KEYBOARD   ***
260 !
270 CLEAR @ DISP "ENTER SAMPLE NAME?"
280 INPUT A$
290 DISP "MEAN VALUE OF FIBER CRITICAL LENGTH (MICRON) IS:";@ INPUT W1
320 DISP "TENSILE STRENGTH (PSI) OF FIBER AT";W1;" GAGE LENGTH IS:";@ IN
PUT S
350 DISP "THE TOTAL NUMBER OF SPECIMEN TESTED:";@ INPUT N1
380 DISP "THE TOTAL NUMBER OF BREAKS:";@ INPUT N
410 DISP "ENTER FIBER DIAMETER AND CRITICAL LENGTH (MICRON)"
420 FOR I=1 TO N
430 DISP "D(";I;"), L(";I;")="
450 INPUT D(I),L(I)
460 NEXT I
470 GOTO 120
480 !
490 ! ****   DATA  ENTRY   ****
500 !
505 DISP "INSERT DATA FILE TAPE! (WAIT FOR THE NEXT COMMAND!"
506 BEEP
507 WAIT 3000
510 DISP "ENTER FILE NAME:";@ INPUT A$
520 ASSIGN# 1 TO UFC$(A$)
530 READ# 1 ; A$,W1,S,N1,N,D(),L()
570 ASSIGN# 1 TO *
580 GOTO 120
590 !
600 ! ***  STORE DATA ON TAPE  ***
610 !
620 DISP "INSERT DATA FILE TAPE! [WAIT FOR THE NEXT COMMAND!]"
621 BEEP
622 WAIT 3000
630 CLEAR @ DISP "ENTER FILE NAME";@ INPUT A$
```

```
640 DISP "NEW OR EXISTING FILE (N/E)?"
650 INPUT Q$@ IF UPC$(Q$[1,1])="N" THEN 660 ELSE GOTO 670
660 CREATE UPC$(A$),50
670 ASSIGN# 1 TO UPC$(A$)
680 PRINT# 1 ; A$,W1,S,N1,N,D(),L()
720 ASSIGN# 1 TO *
730 DISP "DATA ON";UPC$(A$);"STORED ON TAPE" @ KEY LABEL
735 WAIT 3000
740 GOTO 120
750 !
760 !  ***   DISPLAY  DATA   ***
770 !
780 CLEAR @ DISP "DATA IN MEMORY? (Y OR N)";@ INPUT T$
790 IF T$="Y" THEN 810
800 IF T$="N" THEN 120
805 DISP "ENTER Y OR N"
806 GOTO 780
810 CLEAR @ PRINT "SAMPLE",A$
820 PRINT USING 830 ; "TENSILE STRENGTH (PSI) OF FIBER AT",W1,"GAGE LENG
TH IS:",S
830 IMAGE 34A,4D.3D,16A,D.3DE
840 PRINT USING 850 ; "TOTAL NUMBER OF SPECIMENS TESTED IS:",N1
850 IMAGE 42A,2D
860 PRINT USING 870 ; "TOTAL NUMBER OF BREAKS IS:",N
870 IMAGE 32A,3D
880 FOR I=1 TO N
890 PRINT USING 900 ; "D(",I,"), L(",I,")=",D(I),L(I)
900 IMAGE 2A,3D,5A,3D,4A,2D.2D,5D.2D
910 NEXT I
920 GOTO 120
930 !
940 ! EDIT ROUTINE *****
950 !
960 CLEAR @ DISP "ADD(A), CHANGE(C), END(E)";@ INPUT Z$
970 IF Z$="A" THEN 1000
980 IF Z$="C" THEN 1110
985 IF Z$="E" THEN 120
990 GOTO 960
1000 ! ADD ROUTINE
1010 DISP "ENTER ADDITIONAL NUMBER OF SPECIMENS TESTED:";@ INPUT M1
1020 DISP "ENTER ADDITIONAL NUMBER OF BREAKS:";@ INPUT M
1030 N1=N1+M1
1040 FOR I=N+1 TO N+M
1050 DISP "D(",I,"), L(",I,")="
1070 INPUT D(I),L(I)
1080 NEXT I
1090 N=N+M
1100 GOTO 960
1110 ! CHANGE ROUTINE
1112 DISP "CHANGE TENSILE STRENGTH (S), MEAN CRITICAL LENGTH (W), DIAMET
ER AND LENGTH (L)"
1113 INPUT D$
1114 IF D$="S" THEN 1117
1115 IF D$="L" THEN 1120
1116 IF D$="W" THEN 1181
1117 DISP "TENSILE STRENGTH=",S
1118 DISP "CHANGE TO TENSILE STRENGTH=" @ INPUT S
1119 GOTO 1180
```

```
1120 DISP "ENTER ITEM # TO CHANGE"
1130 INPUT I
1140 DISP "OLD VALUES:"
1150 DISP "D(",I,"), L(",I,")=",D(I),L(I)
1160 DISP "NEW VALUES:"
1170 DISP "D(",I,"), L(",I,")=";@ INPUT D(I),L(I)
1180 GOTO 960
1181 DISP "MEAN CRITICAL LENGTH=",W1
1182 DISP "CHANGE TO MEAN CRITICAL LENGTH=" @ INPUT W1
1183 GOTO 960
1190 !
1200 ! *** WEIBULL DISTRIBUTION PARAMETERS ***
1210 !
1220 S1,S2,S3,C,F2=0
1230 ! INITIALIZE ALPHA TO BE 10
1240 A=10
1250 ! INITIALIZE ITERATION STEP TO BE 1
1260 X=1
1270 ! ASPECT RATIO DETERMINATION
1280 FOR I=1 TO N
1290 R(I)=L(I)/D(I)
1295 NEXT I
1299 CLEAR
1300 DISP "STORE DATA FOR HISTOGRAM/WEIBULL PLOT ? (Y OR N)";@ INPUT Q$
1310 IF Q$="Y" THEN 1330
1320 IF Q$="N" THEN 1460
1325 GOTO 1300
1330 !
1340 ! STORE ASPECT RATIO FOR HISTO/WEIBULL/NORMAL PLOT ***
1350 !
1360 CLEAR @ DISP "ENTER FILE NAME? (END WITH H)";@ INPUT B$
1370 DISP "NEW OR EXISTING FILE (N/E)?"
1380 INPUT P$@ IF UPC$(P$[1,1])="N" THEN 1390 ELSE GOTO 1400
1390 CREATE UPC$(B$),20
1400 ASSIGN# 1 TO UPC$(B$)
1420 PRINT# 1 ; N,R()
1440 ASSIGN# 1 TO *
1450 DISP "DATA ON ";UPC$(B$);" STORED ON TAPE."
1460 DISP "DO YOU WANT A PRINT OUT? (Y/N)?" @ INPUT C$
1461 IF C$="Y" THEN 1463
1462 IF C$="N" THEN 1468
1463 PRINT USING 1464 ; "N","R"
1464 IMAGE A,8X,A
1465 FOR I=1 TO N @ PRINT USING 1466 ; I,R(I) @ NEXT I
1466 IMAGE 3D,5X,3D.3D
1468 BEEP
1469 CLEAR
1470 S1,S2,S3=0
1480 FOR I=1 TO N
1490 S1=S1+R(I)^A*LOG(R(I))
1500 S2=S2+R(I)^A
1510 S3=S3+LOG(R(I))
1520 NEXT I
1525 DISP "A=";A
1526 DISP "F2=";F2
1530 !
1540 F=S1/S2-1/A-S3/N
1545 DISP "F=";F
```

```
1550 IF ABS(F)<.000001 THEN 1680
1560 IF C>0 THEN 1600
1570 F2=F
1580 C=1
1590 GOTO 1650
1600 IF F2>0 THEN 1630
1610 IF F<0 THEN 1650
1620 GOTO 1640
1630 IF F>0 THEN 1650
1640 X=-X/10
1650 A=A-X
1660 F2=F
1670 GOTO 1470
1680 !
1690 B=(1/N*S2)^(1/A)
1700 P=1-1/A
1710 GOSUB 1960
1900 G2=G
1910 T=S/2/B*G2
1920 P=1-2/A
1921 DISP "P=",P
1930 GOSUB 1960
1940 V=S^2/4/B^2*(G-G2^2)
1941 V=SQR(V)
1945 GOTO 2310
1950 !
1960 ! GAMMA FUNCTION SUBROUTINE ***
1970 !
1980 IF P-57<=0 THEN 2020
2000 G=1.E75
2001 DISP "P>57,OVERFLOW,G SET TO 1.E75";
2002 WAIT 3000
2003 BEEP
2010 RETURN
2020 P1=P
2030 E=.000001
2040 C=0
2050 G=1
2060 IF P1-2<=0 THEN 2110
2070 IF P1-2<=0 THEN 2220
2080 P1=P1-1
2090 G=G*P1
2100 GOTO 2070
2110 IF P1-1<0 THEN 2140
2120 IF P1-1=0 THEN 2270
2130 IF P1-1>0 THEN 2220
2140 IF P1-E>0 THEN 2190
2150 Z=SGN(P1)*INT(ABS(P1)-.5)-P1
2160 IF ABS(Z)-E<=0 THEN 2280
2170 IF 1-Z-E<=0 THEN 2280
2180 IF P1-1>0 THEN 2220
2190 G=G/P1
2200 P1=P1+1
2210 GOTO 2180
2220 Z=P1-1
2230 W=Z*(-.5684729+Z*(.2548205+Z*-.0514993))
2240 W=Z*(.985854+Z*(-.8764218+Z*(.8328212+W)))
2250 G1=1+Z*(-.5771017+W)
```

```
2260 G=G*G1
2270 RETURN
2280 DISP "P IS WITHIN 1.E-6 OF BEING A -VE INTEGER"
2281 WAIT 3000
2282 BEEP
2290 RETURN
2300 !
2310 ! DATA OUTPUT ***
2320 PRINT USING 2330 ; "SAMPLE:",A$
2330 IMAGE 7A,10A
2340 PRINT USING 2350 ; "TOTAL NUMBER OF SPECIMENS=",N1
2350 IMAGE 26A,3D
2360 PRINT USING 2370 ; "TOTAL NUMBER OF BREAKS=",N
2370 IMAGE 23A,4D
2380 PRINT USING 2390 ; "WEIBULL DISTRIBUTION ALPHA=",A
2390 IMAGE 27A,3D.3D
2400 PRINT USING 2410 ; "WEIBULL DISTRIBUTION BETA=",B
2410 IMAGE 26A,4D.3D
2420 PRINT USING 2430 ; "TENSILE STRENGTH (PSI) OF FIBER AT",W1," GAGE L
ENGTH=",S
2430 IMAGE 35A,4D.3D,13A,D.3DE
2440 PRINT USING 2450 ; "INTERFACIAL SHEAR STRENGTH=",T
2450 IMAGE 27A,D.3DE
2460 PRINT USING 2470 ; "VARIANCE OF THE SHEAR STRENGTH=",V
2470 IMAGE 31A,D.3DE
2480 !
2490 END
```

APPENDIX I. WEIBULL DISTRIBUTION OF CRITICAL LENGTH A HISTOGRAM PLOT

The purpose of this program is to plot the Weibull Distribution curve and the population density curve of the critical aspect ratio of the fibers.

```
10 COM Z9
20 ! *****DATA PLOT PROGRAM***********VERSION 6.09*********
30 DIM P(2),L(2),N1(2),S2(2),X(2,350),T$[80],X$[80],Y$[80],S$[80],L1(2),
Y1(2,350),R(350)
40 DIM T1$[80]
50 ! *****INITIALIZATION************************************
60 G$="AG" @ N$="NY" @ K$="KTC" @ L1(0)=0 @ S$="" @ N=0
70 N1=0 @ Z9=1 @ DEG
80 ON KEY# 1,"ENTER" GOTO 180
90 ON KEY# 2,"SETUP" GOTO 530
100 ON KEY# 3,"HEADING" GOTO 830
110 ON KEY# 4,"    PLOT" GOTO 2130
120 ON KEY# 5,"STORE" GOTO 390
130 ON KEY# 6,"EDIT" GOTO 1460
140 ON KEY# 7," LEGEND" GOTO 1390
150 ON KEY# 8,"   RANGE" GOTO 900
160 CLEAR @ KEY LABEL
170 GOTO 170
180 !
190 ! *****DATA ENTRY************************************
200 CLEAR @ DISP "Enter Data from Keyboard(K) or Tape(T) or from Calcula
tion(C)"
210 INPUT Q$@ Q2=POS(K$,UPC$(Q$[1,1]))
220 IF Q2=0 THEN 200
230 ON Q2 GOTO 240,750,741
240 FOR I=N+1 TO 6
250 CLEAR @ DISP "Enter Data for Set ";I;" (Y/N)"
260 INPUT Q$@ Q2=POS(N$,UPC$(Q$[1,1]))
270 IF Q2=0 THEN 250
280 ON Q2 GOTO 370,290
290 DISP "Enter Data Pairs(ENDLINE ends)"
300 FOR J=1 TO 100
310 DISP "X(";I;",";J;"), Y(";I;",";J;") = ";@ INPUT Q$,R$
320 IF Q$="" THEN 350
330 X(I,J)=VAL(Q$) @ Y1(I,J)=VAL(R$)
340 NEXT J
350 N1(I)=J-1 @ N1=N1+N1(I)
360 NEXT I
370 N=I-1
380 ON Z9 GOTO 530,160
390 ! *****STORE DATA ON TAPE***
400 Z9=2
410 CLEAR @ DISP "Store on Tape(Y/N)"
420 GOSUB 3190 @ ON Q9 GOTO 160,430
430 DISP "FILE NAME";@ INPUT F$
440 DISP "New or Existing File (N/E)"
450 INPUT Q$@ IF UPC$(Q$[1,1])="N" THEN 460 ELSE GOTO 470
460 CREATE UPC$(F$),50
470 ASSIGN# 1 TO UPC$(F$)
480 PRINT# 1 ; N,N1(),X0,Y0,X1,Y1,X(,),Y1(,),L1(),P(),L(),S(),S$,T$,Y$,X
$,F1,F2,Q1,X2,X3,Y2,Y3
490 PRINT# 1 ; T1$
500 ASSIGN# 1 TO *
505 CLEAR
510 DISP "DATA SET ";UPC$(F$);" STORED ON TAPE" @ KEY LABEL
520 Z9=2 @ GOTO 170
530 ! *****DETERMINE COLOR, LINE AND SYMBOL**************
540 CLEAR
```

```
550 FOR I=1 TO N
560 DISP
570 DISP "ENTER PEN # (1-4)," @ DISP "LINETYPE # (1-8) AND              PL
OTTING SYMBOL # (1-6)"
580 DISP "FOR DATA SET";I
590 IF I=1 THEN 600 ELSE 700
600 PRINT "PEN COLOR KEY" @ PRINT "1= BLACK" @ PRINT "2  RED" @ PRINT "3
  GREEN" @ PRINT "4  BLUE"
610 PRINT @ PRINT "LINETYPE KEY" @ PRINT "1= SOLID"
620 PRINT "2  BLANK" @ PRINT "3  DOT" @ PRINT "4  S.DASH"
630 PRINT "5  L.DASH" @ PRINT "6  DASH/DOT"
640 PRINT "7  L.DASH/S.DASH" @ PRINT "8  DASH/DOT/DOT"
650 PRINT @ PRINT
660 PRINT "PLOTTING SYMBOL KEY"
670 PRINT "1= DOT" @ PRINT "2  CIRCLE" @ PRINT "3  SQUARE"
680 PRINT "4  TRIANGLE" @ PRINT "5  PLUS SIGN" @ PRINT "6  DIAMOND"
690 PRINT @ PRINT @ PRINT @ PRINT
700 INPUT P(I),L(I),S(I)
710 IF P(I)<1 OR P(I)>4 THEN 700
720 IF L(I)<1 OR L(I)>8 THEN 700
730 IF S(I)<1 OR S(I)>6 THEN 700
740 NEXT I @ ON Z9 GOTO 830,160
741 ! CALCULATION FOR WEIBULL DISTRIBUTION
742 DISP "ENTER FILE NAME WITH R() MATRIX FOR WEIBULL DISTRIBUTION" @ IN
PUT F$@ ASSIGN# 1 TO F$
743 READ# 1 ; N5,R()
744 ASSIGN# 1 TO *
745 N=1 @ N1(1)=N5
746 DISP "ENTER   VALUES" @ INPUT A,B
747 CLEAR @ DISP "CUMULATIVE PLOT (C) OR DENSITY POPULATION PLOT (D)?" @
 INPUT E$
748 IF E$="C" THEN 750
749 IF E$="D" THEN 752 ELSE 747
750 FOR I=1 TO N5 @ X(1,I)=(R(I)/B)^A @ Y1(1,I)=1-EXP(-X(1,I)) @ X(1,I)=
R(I) @ NEXT I
751 Z9=2 @ GOTO 160
752 FOR I=1 TO N5 @ X(1,I)=(R(I)/B)^A @ Y1(1,I)=A/B*(R(I)/B)^(A-1)*EXP(-
X(1,I)) @ X(1,I)=R(I)
753 NEXT I
754 Z9=2 @ GOTO 160
759 ! DATA ENTRY***************
760 DISP "ENTER FILE NAME";@ INPUT F$
770 ASSIGN# 1 TO UPC$(F$)
780 READ# 1 ; N,N1(),X0,Y0,X1,Y1,X(,),Y1(,),L1(),P(),L(),S(),S$,T$,Y$,X$
,F1,F2,Q1,X2,X3,Y2,Y3
790 READ# 1 ; T1$
800 ASSIGN# 1 TO *
810 Z9=2
820 GOTO 160
830 ! *****ENTER HEADINGS*********************************
840 CLEAR @ DISP "ENTER TITLE";@ INPUT T$
850 DISP "ENTER SUBTITLE";@ INPUT T1$
860 DISP "ENTER X axis TITLE";@ INPUT X$
870 DISP "ENTER Y axis TITLE";@ INPUT Y$
880 P(0)=1
890 ON Z9 GOTO 900,160
900 ! *****DEFINE GRAPH**********************************
910 X0,Y0=10^99 @ X1,Y1=-10^99
```

```
1010 FOR I=1 TO N
1020 FOR J=1 TO N1(I)
1030 X0=MIN(X0,X(I,J)) @ X1=MAX(X1,X(I,J))
1040 Y0=MIN(Y0,Y1(I,J)) @ Y1=MAX(Y1,Y1(I,J))
1050 NEXT J
1060 NEXT I
1070 DISP "X DATA RANGE IS ";X0;" TO ";X1
1080 DISP "Y DATA RANGE IS ";Y0;" TO ";Y1
1100 DISP "DO YOU WISH TO SET GRAPH LIMITS ";@ GOSUB 3170
1110 ON Q9+1 GOTO 1100,1160,1120
1120 DISP "ENTER Xmin,Xmax,Ymin,Ymax ";
1140 INPUT X0,X1,Y0,Y1
1150 IF X1<X0 OR Y1<Y0 THEN 1120
1160 DISP "DO YOU WISH AXES OR GRID        (A or G)";
1170 INPUT Q$@ Q1=POS(G$,Q$)
1175 DISP @ DISP "NUMERICAL LABELS:"
1177 DISP "on horizontal axis..."
1180 ON Q1+1 GOTO 1160,1190,1240
1190 DISP "Units per label, units          per tic mark";
1200 INPUT X3,X2@ X3=INT(X3/X2+.51) @ IF X3<0 THEN 1190
1205 DISP @ DISP "on vertical axis..."
1210 DISP "Units per label, units          per tic mark";
1220 INPUT Y3,Y2@ Y3=INT(Y3/Y2) @ IF Y3<0 THEN 1210
1230 GOTO 1290
1240 DISP "units per GRID LINE,units       per tic mark";
1250 INPUT X3,X2@ X3=INT(X3/X2+.51) @ IF X3<0 THEN 1240
1255 DISP @ DISP "on vertical axis..."
1260 DISP "units per GRID LINE,units       per GRID LINE";
1270 INPUT Y3,Y2@ Y3=INT(Y3/Y2+.51) @ IF Y3<0 THEN 1260
1280 ON ERROR GOSUB 3220
1290 IF Y2<1 THEN F2=2 ELSE F2=0
1300 IF Y2<.1 THEN F2=4
1310 IF X2<1 THEN F1=2 ELSE F1=0
1320 IF X2<.1 THEN F1=4
1330 DISP "INTEGER LABELS ON X-AXIS";
1340 GOSUB 3170
1350 ON Q9 GOTO 1370,1360
1360 F1=0
1370 OFF ERROR
1380 ON Z9 GOTO 1390,160
1390 ! *******ENTER LEGENDS******
1400 S$="" @ CLEAR
1410 FOR I=1 TO N
1420 DISP "Enter Legend for Group ";I
1430 INPUT I$@ S$=S$&I$ @ L1(I)=LEN(S$)
1440 NEXT I
1450 ON Z9 GOTO 390,160
1460 ! EDIT ROUTINE
1470 CLEAR @ DISP "Enter data set number"
1480 INPUT I
1490 DISP "There are";N1(I);" data pairs (X,Y) in this set"
1500 DISP @ DISP "Enter startins & endins item numbers for list (ENDLINE
 ends)"
1510 INPUT D$,E$
1520 IF D$="" THEN 2122
1530 FOR J=VAL(D$) TO MIN(VAL(E$),N1(I))
1540 DISP J;"=";X(I,J);",";Y1(I,J)
1550 NEXT J
```

```
1560 DISP "Add(A), Delete(D),Change(C), Insert(I),End(E)"
1570 INPUT Y1$
1580 IF UPC$(Y1$[1,1])="A" THEN 1640
1590 IF UPC$(Y1$[1,1])="D" THEN 1700
1600 IF UPC$(Y1$[1,1])="C" THEN 2050
1610 IF UPC$(Y1$[1,1])="I" THEN 1850
1620 IF UPC$(Y1$[1,1])="E" THEN 1500
1630 GOTO 1500
1640 ! ADD ROUTINE
1650 DISP "X(";I;",";N1(I)+1;"),Y(";I;",";N1(I)+1;") ="
1660 N1(I)=N1(I)+1
1670 INPUT X(I,N1(I)),Y1(I,N1(I))
1680 GOTO 1560
1690 !
1700 ! DELETE ROUTINE
1710 DISP "Enter item # to delete"
1720 INPUT J
1730 DISP "X(";I;",";J;"),Y(";I;",";J;") = ";X(I,J);" ";Y1(I,J)
1740 DISP "Enter D to delete"
1750 !
1760 INPUT Y1$
1770 IF UPC$(Y1$[1,1])#"D" THEN 1560
1780 N1(I)=N1(I)-1
1790 FOR J1=J TO N1(I)
1800 X(I,J1)=X(I,J1+1)
1810 !
1820 Y1(I,J1)=Y1(I,J1+1)
1830 NEXT J1
1840 DISP "Item";J;" deleted" @ GOTO 1560
1850 ! INSERT ROUTINE
1860 DISP "Insert item before item #"
1870 !
1880 INPUT J
1890 DISP "X(";I;",";J;"),Y(";I;",";J;") = "
1900 INPUT G8,G9
1910 N1(I)=N1(I)+1
1920 FOR J1=N1(I) TO J+1 STEP -1
1930 !
1940 X(I,J1)=X(I,J1-1)
1950 Y1(I,J1)=Y1(I,J1-1)
1960 NEXT J1
1970 X(I,J)=G8
1980 Y1(I,J)=G9
1990 !
2000 GOTO 1560
2010 !
2020 !
2030 !
2040 !
2050 ! CHANGE ROUTINE
2060 DISP "Enter Item # to Change"
2070 INPUT J
2080 DISP "Old Values:" @ DISP
2090 DISP X(I,J);",";Y1(I,J)
2100 DISP @ DISP "Enter New Values"
2110 INPUT X(I,J),Y1(I,J)@ DISP @ DISP
2120 GOTO 1560
2122 CLEAR @ PRINT USING "9/" ; @ PRINT "Press RANGE User Key before
```

```
 PLOT" @ KEY LABEL @ GOTO 170
2130 ! *****GRAPH*****************************************
2140 DISP "PLOT ON:"
2150 DISP "   1. HP SCREEN"
2160 DISP "   2. PLOTTER" @ DISP "   3. POSTER"
2170 INPUT Z
2180 IF Z=1 THEN 2270
2190 IF Z=2 THEN 2230
2200 IF Z=3 THEN 2230
2210 GOTO 2140
2220 Z9=2
2230 PLOTTER IS 705
2240 IF Z=3 THEN 2280
2250 LIMIT 0,250,15,195
2260 GOTO 2280
2270 PLOTTER IS 1
2280 LOCATE 26,120,20,80
2290 SCALE X0,X1,Y0,Y1
2300 FXD F1,F2 @ CSIZE 4,.6,0 @ LINETYPE 1 @ GCLEAR @ PEN 1
2310 ON Q1 GOTO 2320,2340
2320 LAXES -X2,Y2,X0,Y0,X3,Y3
2330 GOTO 2350
2340 LGRID -X2,Y2,X0,Y0,X3,Y3 @ FRAME
2350 PEN P(0) @ MOVE X0+(X1-X0)/2,Y1+(Y1-Y0)*3/20
2360 LORG 4 @ CSIZE 2*Z+2,.7,0
2370 LABEL T$
2380 CSIZE 2*Z+1,.7
2390 LABEL T1$
2400 SETGU
2410 MOVE 70,3
2420 LORG 4
2430 LABEL X$
2440 MOVE 8,45
2450 LDIR 90 @ LABEL Y$
2460 LDIR 0
2470 SETUU
2650 ! *****PLOT DATA*************************************
2660 FOR I=1 TO N
2670 PEN P(I)
2680 MOVE X(I,1),Y1(I,1)
2690 GOSUB 2890
2700 MOVE X(I,1),Y1(I,1)
2710 FOR J=2 TO N1(I)
2720 LINETYPE L(I)
2730 DRAW X(I,J),Y1(I,J)
2740 GOSUB 2890
2750 MOVE X(I,J),Y1(I,J)
2760 NEXT J
2770 GOSUB 2800
2780 NEXT I @ PEN 0
2782 IF Z=1 THEN CLEAR @ DISP USING "7/" ; @ DISP "Press KEY LABEL when
ready" @ WAIT 2000
2784 IF Z=1 THEN CLEAR @ GRAPH @ GOTO 170
2790 GOTO 160
2800 ! *****DRAW KEY*************************************
2810 SETGU @ LINETYPE L(I)
2820 MOVE 110,96-3*(I-1)
2830 IDRAW 5,0
```

```
2840 GOSUB 2890 @ SETGU
2850 MOVE 117,96-3*(I-1)
2860 LORG 2 @ CSIZE 3,.6 @ LDIR 0
2870 LABEL S$[L1(I-1)+1,L1(I)]
2880 SETUU @ RETURN
2890 ! *****PLOT SYMBOLS**********************************
2900 SETGU @ LINETYPE 1
2910 ON S(I) GOTO 2920,2940,2990,3040,3080,3130
2920 ! *****DOT*****************
2930 RPLOT 0,0 @ SETUU @ RETURN
2940 ! *****CIRCLE**************
2950 IMOVE .15,0
2960 FOR A=0 TO 360 STEP 30
2970 PDIR A @ RPLOT .8,0
2980 NEXT A @ SETUU @ RETURN
2990 ! *****SQUARE**************
3000 IMOVE -1,-1
3010 IDRAW 2,0 @ IDRAW 0,2
3020 IDRAW -2,0 @ IDRAW 0,-2
3030 SETUU @ RETURN
3040 ! *****TRIANGLE*************
3050 IMOVE 0,1
3060 IDRAW 1,-2 @ IDRAW -2,0
3070 IDRAW 1,2 @ SETUU @ RETURN
3080 ! *****PLUS SIGN************
3090 IDRAW 0,1 @ IDRAW 0,-2
3100 IMOVE 0,1
3110 IDRAW 1,0 @ IDRAW -2,0
3120 SETUU @ RETURN
3130 ! *****DIAMOND*************
3140 IMOVE 0,1 @ IDRAW 1,-1
3150 IDRAW -1,-1 @ IDRAW -1,1
3160 IDRAW 1,1 @ SETUU @ RETURN
3170 ! *****YES OR NO*************************************
3180 DISP "(Y/N)"
3190 INPUT Q$@ Q9=POS(N$,Q$)
3200 IF Q9=0 THEN 3180
3210 RETURN
3220 ! *****CHECK FOR DIVISION BY************ZERO*******
3230 IF ERRN=8 THEN F1,F2=0
3240 RETURN
```

APPENDIX J. INSTRUMENTED IMPACT TESTER

The ETI-Dynatup drop dart instrumented impact tester monitors and records the entire impact event, from initial impact and acceleration from rest to plastic bending to fracture initiation and propagation to failure. Also, the drop dart system permits dynamic tests to be made at impact energies and velocities not available with other testing machines.

The drop dart impact test consists of a drop tower and instrumentation package - a microprocessor. The drop tower is a gravity driven impact machine equipped with remote controls for release of the hammer and tup assembly, and a motorized lift mechanism for easy return of the hammer to a predetermined drop position. An automatic rebound brake is furnished as standard.

The hammer and tup assembly is designed so that the weight of the hammer can be varied and the tups can be interchanged. The base plate of the drop tower permits interchangeability of anvil supports to accommodate different specimen size and geometries.

A typical output is shown in Figure J-1. P_I and P_F are the loads correspond to the initial damage of the composite and the maximum load required for punch through. The corresponding energy absorbed at each stage is E_I and E_F. The total energy absorbed during the whole event is E_T. In this report, P_F and E_T are used to characterize the impact toughness of the laminates.

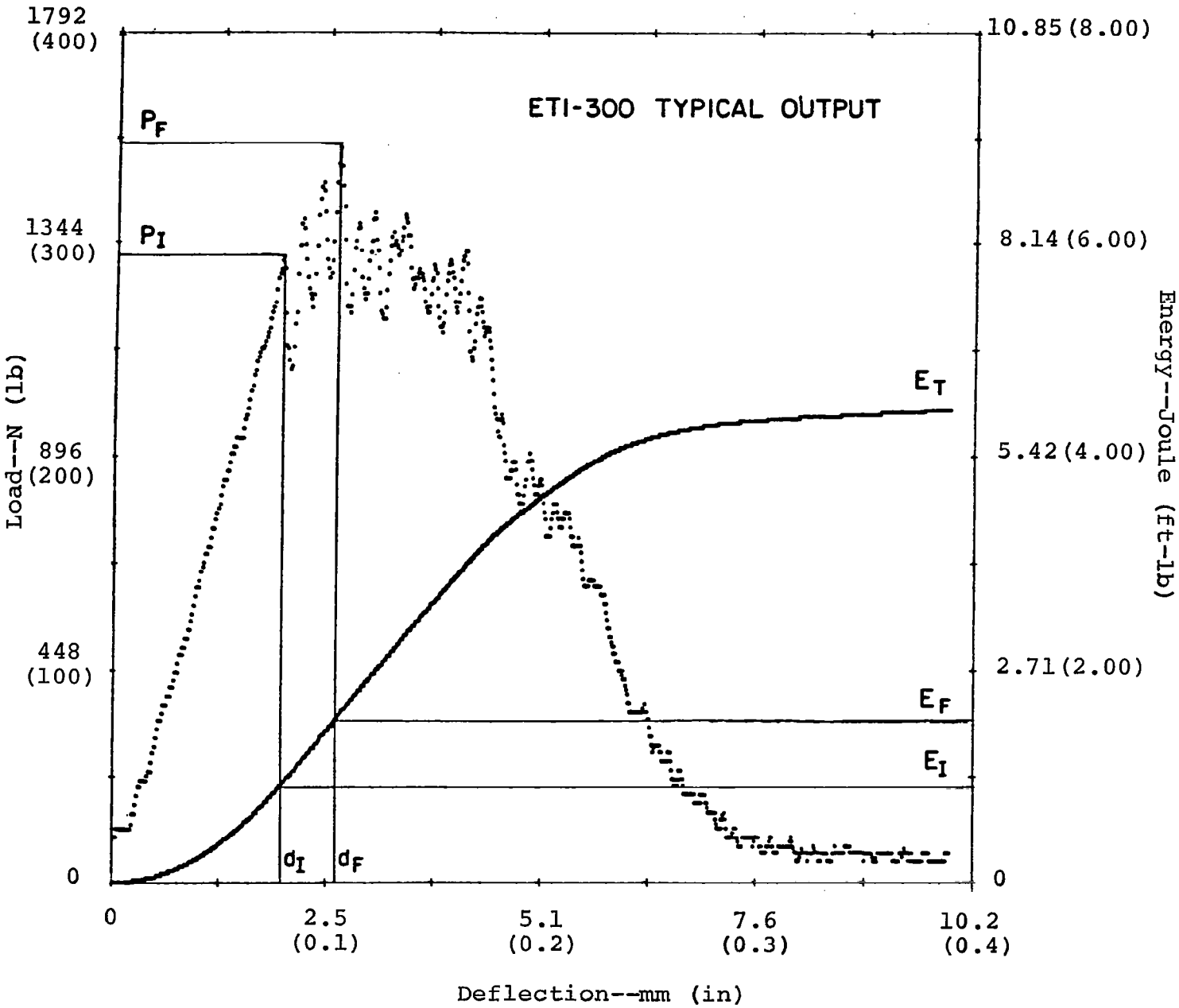

FIGURE J-1. TYPICAL OUTPUT OF AN ETI-DYNATUP INSTRUMENTED IMPACT TESTER

1. Report No.	2. Government Accession No.	3. Recipient's Catalog No.
NASA CR- 3607		

4. Title and Subtitle	5. Report Date
EFFECTS OF FIBER/MATRIX INTERACTIONS ON THE PROPERTIES OF GRAPHITE/EPOXY COMPOSITES	SEPTEMBER 1982
	6. Performing Organization Code

7. Author(s)	8. Performing Organization Report No.
Paul E. McMahon Lincoln Ying	
	10. Work Unit No.

9. Performing Organization Name and Address	11. Contract or Grant No.
Celanese Corporation Celanese Research Company 86 Morris Ave., Summit, NJ 07901	NAS1-15749 Task No. 3

12. Sponsoring Agency Name and Address	13. Type of Report and Period Covered
National Aeronautics and Space Administration Washington, DC 20546	Contractor Report SEP 80 - DEC 81
	14. Sponsoring Agency Code

15. Supplementary Notes

Langley Technical Monitors: S. S. Tompkins and J. B. Nelson
Final Report, Task Assignment No. 3.

16. Abstract

A state-of-the art literature review of the interactions between fibers and resin within graphite epoxy composite materials was performed. Emphasis centered on: adhesion theory; wetting characteristics of carbon fiber; load transfer mechanisms; methods to evaluate and measure interfacial bond strengths; environmental influence at the interface; and the effect of the interface/interphase on composite performance, with particular attention to impact toughness.

In conjunction with the literature review, efforts were made to design experiments to study the wetting behavior of carbon fibers with various finish variants and their effect on adhesion joint strength. The properties of composites with various fiber finishes were measured and compared to the base-line properties of a control. It was shown that by tailoring the interphase properties, a 30% increase in impact toughness was achieved without loss of mechanical properties at both room and elevated temperatures.

17. Key Words (Suggested by Author(s))	18. Distribution Statement
graphite fibers, graphite fiber/epoxy composite, interphase, interface, impact toughness, adhesion, wetting, load transfer mechanisms, adhesion test methods, fracture mechanisms	Unclassified-Unlimited Subject Category - 24

19. Security Classif. (of this report)	20. Security Classif. (of this page)	21. No. of Pages	22. Price*
UNCLASSIFIED	UNCLASSIFIED	160	A08

* For sale by the National Technical Information Service, Springfield, Virginia 22161

NASA-Langley, 1982

NASA-C-168 (Rev. 10-75)